NASA/TM–2000–206892, Vol. 8

SeaWiFS Postlaunch Technical Report Series

Stanford B. Hooker and Elaine R. Firestone, Editors

Volume 8, The SeaBOARR–99 Field Campaign

Stanford B. Hooker and Gordana Lazin

January 2000

NASA/TM–2000–206892, Vol. 8

SeaWiFS Postlaunch Technical Report Series

Stanford B. Hooker, Editor
NASA Goddard Space Flight Center, Greenbelt, Maryland

Elaine R. Firestone, Senior Technical Editor
SAIC General Sciences Corporation, Beltsville, Maryland

Volume 8, The SeaBOARR–99 Field Campaign

Stanford B. Hooker
NASA Goddard Space Flight Center
Greenbelt, Maryland

Gordana Lazin
Satlantic, Inc.
Halifax, Canada

National Aeronautics and
Space Administration

Goddard Space Flight Center
Greenbelt, Maryland 20771

January 2000

ISSN 1522–8789

Available from:

NASA Center for AeroSpace Information
7121 Standard Drive
Hanover, MD 21076–1320
Price Code: A17

National Technical Information Service
5285 Port Royal Road
Springfield, VA 22161
Price Code: A10

ABSTRACT

This report documents the scientific activities during the second Sea-viewing Wide Field-of-view Sensor (SeaWiFS) Bio-Optical Algorithm Round-Robin (SeaBOARR-99) field campaign, which took place from 2 May to 7 June 1999 on board the Royal Research Ship *James Clark Ross* during the eighth Atlantic Meridional Transect cruise (AMT-8). The ultimate objective of the SeaBOARR activity is to evaluate the effect of different measurement protocols on bio-optical algorithms using data from a variety of field campaigns. The SeaBOARR-99 field campaign was concerned with collecting a high quality data set of simultaneous in-water and above-water radiometric measurements. The deployment goals documented in this report were to: a) use four different surface glint correction methods to compute water-leaving radiances, $L_W(\lambda)$, from above-water data; b) use two different in-water profiling systems and three different methods to compute $L_W(\lambda)$ from in-water data; c) use instruments with a common calibration history to minimize intercalibration uncertainties; d) monitor the calibration stability of the instruments in the field with the original SeaWiFS Quality Monitor (SQM) and a commercial, second-generation device called the SQM-II, thereby allowing a distinction between differences in methods from changes in instrument performance; and e) compare the $L_W(\lambda)$ values estimated from the above-water and in-water measurements. In addition to describing the instruments deployed and the data collected, a preliminary analysis of part of the SeaBOARR-99 data set is presented (using only the data collected during clear sky, calm sea, and Case-1 waters).

1. INTRODUCTION

The Atlantic Meridional Transect (AMT) Program exploits the passage of the Royal Research Ship *James Clark Ross* (JCR) as it transits the North and South Atlantic Oceans between Grimsby (UK) and Stanley (Falkland Islands) with a port call in Montevideo (Uruguay). In September, the JCR sails from the UK, and the following April it makes the return trip. The AMT Program collects scientific data from approximately 50°N to 50°S with a primary objective to investigate physical and biological processes, as well as to measure the meso- to basin-scale bio-optical properties of the Atlantic Ocean. The vicarious calibration and algorithm validation of remotely sensed observations of ocean color is an inherent objective of these studies: first, by relating *in situ* measurements of water-leaving radiance to satellite measurements, and second, by measuring the bio-optically active constituents of the water (Aiken et al. 1998).

The objectives of the Sea-viewing Wide Field-of-view Sensor (SeaWiFS) Project are to obtain valid ocean color data of the world ocean for a five-year period, to process the data in conjunction with ancillary data to meaningful biological parameters, and to make the data readily available to researchers (Hooker and Esaias 1993). The success of the SeaWiFS mission will be determined by the quality of the ocean color data set and its availability. The Calibration and Validation Element (CVE) is responsible for the former which involves characterizing and calibrating the SeaWiFS system; supporting the development and validation of algorithms for bio-optical properties and atmospheric correction; analyzing trends and anomalies in the derived products and sensor performance; selecting ancillary data sets that are used in data processing (e.g., winds, ozone, and atmospheric pressure); and verifying the processing code (McClain et al. 1992). The culmination of properly executing these responsibilities is achieving a radiometric accuracy to within 5% absolute and 1% relative, water-leaving radiances to within 5% absolute, and chlorophyll *a* concentration to within 35% over a range of 0.05–50.0 mg m^{-3} (Hooker et al. 1992).

The initial SeaWiFS validation results (Hooker and McClain 2000) have provided an immediate and quantitative demonstration of the strengths of the SeaWiFS calibration and validation plan:

1. The SeaWiFS instrument has been stable over the first two years of operation with the gradual changes in some wavelengths being accurately quantified using the solar and lunar calibration data;
2. The vicarious calibration approach using in-water data results in consistent global L_W values; and
3. The remote sensing products meet the aforementioned accuracy goals over a limited, but diverse, set of open ocean validation sites.

Although the emphasis on in-water validation data has been largely successful, there are disadvantages in the approach which are not present in above-water methods, but they in turn pose new problems that are not present in the in-water techniques. The CVE has been incrementally engaging in above-water measurements with the objective of extracting the largest amount of validation data from both types of measurements.

From 2 May to 7 June 1999, scientists and technicians from the National Aeronautics and Space Administration

(NASA) Goddard Space Flight Center (GSFC) and Satlantic, Inc. (Halifax, Canada) deployed on the JCR after it stopped in Montevideo for a crew change. The purpose of the deployment was to make in- and above-water radiometric measurements in support of two activities:

a) Continue an ongoing time series of bio-optical measurements that are used by the SeaWiFS Project and AMT Program for algorithm validation and bio-optical research; and

b) Collect a high quality data set of simultaneous in- and above-water radiometric measurements along with a suite of bio-optical parameters for intercomparing both techniques.

The deployment was a continuation of the first SeaWiFS Bio-Optical Algorithm Round-Robin (SeaBOARR-98) experiment which took place from 5–17 July 1998 (Hooker et al. 1999), and was called SeaBOARR-99. The ultimate objective is to evaluate the effect of the different measurement protocols on bio-optical algorithms from a variety of field campaigns. This report details the second field campaign in that long-term commitment.

Spectral water-leaving radiance, $L_W(\lambda)$, is the central physical quantity for bio-optical studies in the upper ocean. Whether determined from below- or above-surface measurements, $L_W(\lambda)$ must be accurately measured. The SeaWiFS Project goal of $L_W(\lambda)$ uncertainties of 5% or less is thought to be routinely achievable for in-water measurements in Case-1 waters (Hooker and Maritorena 2000), but the uncertainty associated with above-water measurements has not been well quantified. The main difficulty with above-water methods is associated with correcting the observations for the effect of surface waves which introduce significant fluctuations into the glint and reflected skylight components of the surface radiance field. The problem is made more difficult by the presence of clouds which increase the fluctuations and associated uncertainties.

Although the SeaBOARR-98 data set provided a rigorous intercomparison of in- and above-water techniques, the field campaign took place at a tower in the northern Adriatic Sea, so the majority of the data was in Case-2 water (Hooker et al. 1999). The tower deployment was also of limited duration, approximately 10 days in the field with 3 days of useful data, so an extensive set of observations was not possible. The SeaBOARR-99 field campaign was designed to overcome both of these shortcomings. By using the AMT transect, an extensive opportunity for data collection was ensured, the majority of which would be in Case-1 water. Using a ship also allowed for the possibility of collecting data while the vessel was underway, which represents an important possible advantage for above-water measurements over the current in-water techniques which require the vessel to stop.

At present, there are several methods for surface glint correction that were developed for different conditions in which remote measurements are made, i.e., clear or cloudy sky, and Case-1 or Case-2 water: Austin (1974); Morel (1980); Carder and Steward (1985); Bukata et al. (1988); Mueller and Austin (1995), the so-called SeaWiFS Ocean Optics Protocols (SOOP); Lee et al. (1996); and Lazin (1998). Hereafter, Morel (1980), Carder and Steward (1985) and as further explained in Lee et al. (1996), the Mueller and Austin (1995) SOOP, and Lazin (1998) are referred to as M80, C85, S95, and L98, respectively.

The in-water analysis techniques currently in use are based primarily on the Smith and Baker (1984) method, hereafter referred to as S84. Variations are derived from what measurement procedures (and platforms) are used to acquire the data, and how the in-water data is propagated to the surface. Two alternative techniques were implemented in the ProSoft† software which is freely available for processing bio-optical data collected with Satlantic, Inc.‡ (Halifax, Canada) instruments. The two alternative ProSoft methods rely on a surface buoy to measure the in-water radiance field close to the sea surface and are categorized according to when the options were added to ProSoft, which occurred in 1994 and 1997, so the two are referred to hereafter as P94 and P97, respectively.

The SeaBOARR-99 goals documented here were to:

1. Use two above-water measurement systems and four surface glint correction methods (M80, C85, S95, and L98) to compute $L_W(\lambda)$ from above-water data;
2. Use two in-water profiling systems and three in-water analysis methods (S84, P94, and P97) to compute $L_W(\lambda)$ from in-water data;
3. Use radiometers with a common calibration history to minimize intercalibration uncertainties;
4. Monitor the calibration stability of the instruments in the field with the original SeaWiFS Quality Monitor (SQM) plus a second-generation version called the SQM-II to separate differences in methodologies from changes in instrument performance;
5. Collect data on station with both types of systems and collect underway data with the above-water systems; and
6. Compare the results to the $L_W(\lambda)$ values estimated from the above-water and in-water measurements.

With the exception of the underway sampling (which is not possible on a tower), these objectives were essentially

† ProSoft is a bio-optical data analysis and visualization program from the Department of Oceanography at Dalhousie University (Halifax, Canada); it is written using MatLab™ software from Mathworks, Inc. (Natick, Massachusetts), and is available at `ftp.satlantic.com/pub/optics/dalhousie`.

‡ Identification of commercial equipment to adequately specify or document the experimental problem does not imply recommendation or endorsement, nor does it imply that the equipment identified is necessarily the best available for the purpose.

the same as the ones for SeaBOARR-98, although the mixture of equipment involved was somewhat different. The primary differences were the addition of instruments with better spectral resolution, and a slightly different diversity of measurement wavelengths.

2. INSTRUMENTATION

Although the primary reason for selecting the JCR for SeaBOARR-99 was the ongoing use of the ship by a rigorous group of optical oceanographers, the other reasons were its ability to accommodate a wide variety of instruments [see Robins et al. (1996) for a summary of the vessel's capabilities], its stability (very good optical measurements have always been possible on the JCR), and the AMT transect is predominately in Case-1 water. The latter was deemed particularly important, because the SeaBOARR-98 field campaign was executed at a coastal site dominated by Case-2 water, and most of the techniques to be evaluated were developed primarily for Case-1 sampling.

For SeaBOARR-99, the total number of optical systems deployed on the JCR was as follows:

a) The Low-Cost NASA Environmental Sampling System (LoCNESS) with the Three-Headed Optical Recorder (THOR) option and a surface reference,

b) The SeaWiFS Free-Falling Advanced Light Level Sensors (SeaFALLS) with the SeaWiFS Buoyant Optical Surface Sensor (SeaBOSS) as a reference,

c) The SeaWiFS Surface Acquisition System (SeaSAS),

d) The SeaWiFS Underway Surface Acquisition System (SUnSAS),

e) The SeaWiFS Shadow Band (SeaSHADE) radiometer system,

f) The Dalhousie University Buoyant Optical Surface Sensor (DalBOSS), and

g) An SQM and an SQM-II, which were set up in the Underway Instrumentation and Control (UIC) room.

Detailed descriptions of each measurement system are presented in Sects. 2.1–2.7, respectively, so only a brief description is given here. LoCNESS and SeaFALLS made in-water measurements, SeaSAS and SUnSAS made above-water measurements, and DalBOSS made both types of measurements. SeaSHADE provided reference measurements for the SeaSAS and SUnSAS platforms.

The SQM-II and all of the radiometers used with the optical measurement systems, were manufactured by Satlantic, Inc. This commonality in equipment was not accidental; the SeaBOARR science team decided this was the easiest way to ensure redundancy and intercalibration. Another reason for relying on one manufacturer was it greatly simplified calibration monitoring with the SQM and SQM-II, because all the radiometers had identical outer dimensions, which meant neither SQM had to be repeatedly reconfigured.

LoCNESS, SeaSAS, SUnSAS, and SeaSHADE all use 7-channel ocean color radiance series 200 (OCR-200) sensors, as well as 7-channel ocean color irradiance series 200 (OCI-200) sensors. Both radiometers use 16-bit analog-to-digital (A/D) convertors and are capable of detecting light over a four-decade range. SeaFALLS, SeaBOSS, and DalBOSS are equipped with both 13-channel OCI and OCR series 1000 radiometers (OCI-1000 and OCR-1000, respectively), which employ 24-bit A/D convertors and gain switching and are usually capable of detecting light over a seven-decade range [the gain switching option was disabled in preparation for SeaBOARR-99, because recent analyses (Hooker and Maritorena 2000) have shown these systems are not performing at the level expected and the gain switching circuit is considered the most likely explanation for performance degradation].

To facilitate tracking of the radiometric instruments during the SQM and SQM-II sessions, each radiometer was assigned a three-character code constructed from a letter identifying the type of measurement and a two-digit serial number. A summary of the instruments, along with their primary physical measurements (in terms of vertical sampling), their spectral resolution (7 or 13 channels), and their sensor codes are given in Table 1.

Table 1. A summary of the radiometers used during SeaBOARR-99 along with their primary physical measurement (in terms of their vertical sampling), their spectral resolution (λ_7 means 7 channels and λ_{13} means 13 channels), and their sensor codes.

System	*Sensor*	*Measure*	*Code*
SeaSAS	OCR-200	$L_i(0^+, \lambda_7)$	T69
	OCR-200	$L_T(0^+, \lambda_7)$	T75
	DIR-10	ϑ, ϕ	D01
SUnSAS	OCR-200	$L_i(0^+, \lambda_7)$	T68
	OCR-200	$L_T(0^+, \lambda_7)$	T28
	OCR-200	$L_p(0^+, \lambda_7)$	T28
SeaSHADE	OCI-200	$E_d(0^+, \lambda_7)$	M35
	OCI-200	$E_i(0^+, \lambda_7)$	M95
LoCNESS	OCR-200	$L_u(z, \lambda_7)$	R36
	OCI-200	$E_d(z, \lambda_7)$	I50
	OCI-200	$E_u(z, \lambda_7)$	I48
	OCI-200	$E_d(0^+, \lambda_7)$	M30
SeaFALLS	OCR-200	$L_u(z, \lambda_{13})$	Q16
	OCI-200	$E_d(z, \lambda_{13})$	H23
SeaBOSS	OCI-200	$E_d(0^+, \lambda_{13})$	N46
DalBOSS	OCR-1000	$L_u(z_0, \lambda_{13})$	Q33
	OCI-1000	$E_d(0^+, \lambda_{13})$	N48

A benefit of assembling (nearly) identical equipment from the participating investigators was the wavelengths and bandwidths (10 nm) for the different instruments were

Table 2. Channel numbers and center wavelengths (in nanometers) for the 7-channel radiometers used with the SeaBOARR-99 radiometric sampling systems. The sensor systems are given with their individual sensor codes, which are formed from a one-letter designator for the type of sensor, plus a two-digit serial number (S/N). The M35 and M95 radiometers are the SeaSHADE irradiance sensors. All of the channels have 10 nm bandwidths.

Channel	*LoCNESS*			*SeaSAS*		*SUnSAS*		*References*		
Number	R36	I48	I50	T69	T75	T28	T68	M30	M35	M95
1	411.6	411.4	411.3	412.6	412.3	412.7	412.3	411.9	412.2	412.3
2	442.7	442.7	442.5	442.4	443.1	443.1	442.8	443.0	443.0	442.3
3	489.9	490.0	489.3	491.3	489.9	489.5	490.1	489.9	489.6	489.5
4	510.3	509.3	509.1	510.3	510.1	510.1	510.3	511.0	511.0	510.6
5	554.2	554.3	554.8	554.1	555.0	554.8	555.7	555.5	554.2	554.4
6	665.3	665.9	666.0	781.5	780.6	780.6	780.1	665.2	780.6	781.0
7	683.8	682.4	682.9	866.5	865.1	865.4	864.3	683.7	865.1	865.3

very similar. A summary of the 7- and 13-channel radiometer wavelengths and their sensor codes is given in Tables 2 and 3, respectively. This made it much easier to make substitutions in the event of failures. For example, early in the cruise, the SeaSHADE references malfunctioned, so the LoCNESS reference was routed to the SeaSAS and SUnSAS systems with only a partial loss in data collection (the diffuse irradiance data was lost).

Table 3. Channel numbers and center wavelengths (in nanometers) for the 13-channel radiometers used with the SeaBOARR-99 radiometric sampling systems. The sensor systems are given with their individual sensor codes. All of the channels have 10 nm bandwidths. The N46 radiometer is the SeaBOSS sensor, and the Q33 and N48 radiometers are the DalBOSS sensors.

Channel	*SeaFALLS*		*References*		
Number	Q16	H23	N46	Q33	N48
1	565.0	564.3	565.0	406.5	405.1
2	411.8	411.1	411.7	412.2	412.4
3	665.8	665.9	665.9	435.3	435.6
4	443.0	442.9	443.2	443.4	442.9
5	470.3	470.4	469.9	455.9	456.1
6	489.3	489.2	489.9	489.9	489.3
7	510.4	511.0	510.3	510.4	510.4
8	531.9	531.5	531.7	531.6	531.5
9	554.8	555.3	554.4	554.6	554.5
10	590.3	590.2	590.3	590.3	590.4
11	519.8	519.0	520.1	665.1	664.8
12	683.1	683.6	683.4	670.0	670.0
13	434.0	434.5	434.7	700.6	700.6

The LoCNESS profiler measures spectral upwelled radiance and irradiance plus downwelled irradiance as a function of depth, $L_u(z,\lambda)$, $E_u(z,\lambda)$, and $E_d(z,\lambda)$, respectively. A separate reference sensor measures the total solar irradiance (the direct plus the indirect, or diffuse, components) just above the sea surface, $E_d(0^+,\lambda)$. Internal tilt sensors quantify the vertical orientation (φ) of the profiler as it falls through the water column. The free-fall aspects of the LoCNESS design are derived from the SeaFALLS profiler which is based on a Satlantic SeaWiFS Profiling Multichannel Radiometer (SPMR).

In the SeaFALLS design, 13-channel OCR-1000 and OCI-1000 sensors are connected in line with power and telemetry modules (24-bit A/D convertors for the light sensors) to form a 1.24 m long cylinder. The OCR-1000 is oriented as the *nose* to measure $L_u(z,\lambda)$, and the OCI-1000 as the *tail* to measure $E_d(z,\lambda)$. The addition of weight to the nose and buoyant (foam) fins to a tail bracket produces a rocket-shaped package that falls through the water column with minimum tilts (originally less than 5°, but the use of larger fins and additional weight improved the stability to less than 2°). The power and telemetery cable extends through the field of view of the irradiance sensor, but the small diameter of the cable (7 mm) minimizes any negative effects on the measured light field. The addition of a conductivity and temperature (CT) probe, plus a miniature fluorometer (with a counterbalancing dummy on the opposite side of the profiler), provides a good description of basic water column properties.

The SeaSAS instruments measure the spectral indirect (or sky) radiance reaching the sea surface, $L_i(0^+,\lambda)$, and the (total) radiance right above the sea surface, $L_T(0^+,\lambda)$. The latter is composed of three terms: the radiance leaving the sea surface from below (the so-called water-leaving radiance), the direct sunlight reflecting off the surface (the so-called sun glint), and the indirect skylight reflecting off the surface (the so-called sky glint). SUnSAS makes the same measurements as SeaSAS, $L_i(0^+,\lambda)$ and $L_T(0^+,\lambda)$, but the surface-viewing radiometer looks through a square aperture that can be blocked with a calibrated gray or white plaque, so it can also measure the radiance of the plaque, $L_p(0^+,\lambda)$.

SeaSHADE is composed of two separate sensors. One is used to measure the total or global solar irradiance just above the sea surface, $E_d(0^+,\lambda)$, and the other is equipped

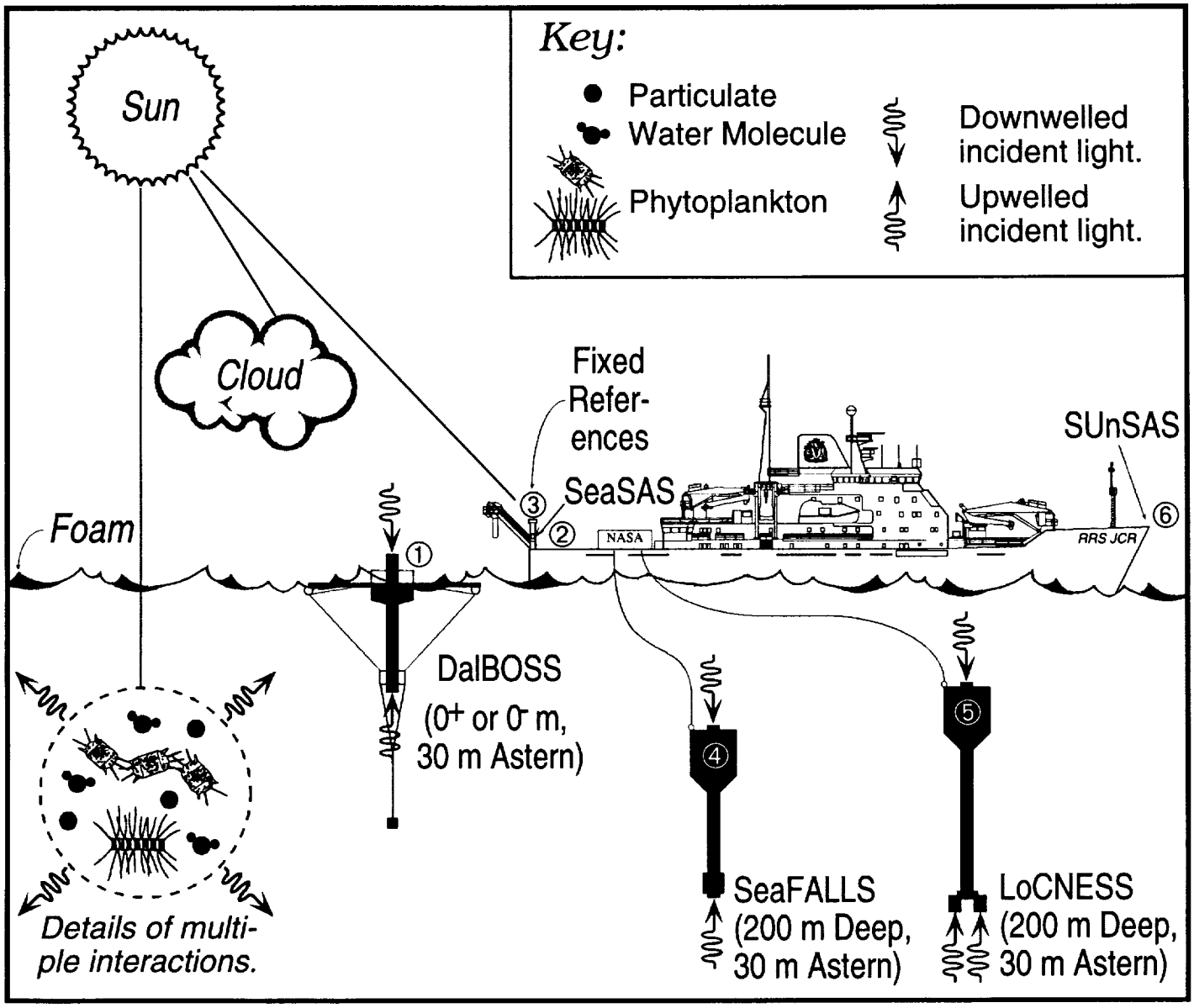

Fig. 1. The JCR showing the deployment locations of the instruments used during SeaBOARR-99 (circles with numbers): 1) DalBOSS, which was deployed as a drifting buoy within a stabilization frame; 2) SeaSAS, which was deployed on the starboard trawl post; 3) SeaSAHADE, SeaBOSS, and the LoCNESS reference, which were deployed on masts mounted to both trawl posts; 4) SeaFALLS; and 5) LoCNESS, which were deployed as free-falling profilers from the stern; and 6) SUnSAS, which was mounted on the bow rail.

with a motorized shadow band that periodically occults the irradiance sensors so the indirect (or diffuse) solar irradiance, $E_i(0^+, \lambda)$, can be measured. SeaSHADE provided all of the reference data for both SeaSAS and SUnSAS during SeaBOARR-99. The other major difference between the two systems is in the design of their frames: the SUnSAS frame is compact with several limitations in its sampling orientations, whereas the SeaSAS frame is large with very few restrictions in its viewing or pointing aspects.

The basic data sampling activity involved collecting data from all of the instruments as simultaneously as possible, so hand-held radios were used to coordinate the beginning and ending of sampling intervals. The sea and sky states were recorded with a charge-coupled device (CCD) digital camera. Although it would have been preferable to have all of the instruments sampling the smallest patch of water possible, space limitations and illumination constraints on the ship did not permit this; there was also a desire to collect underway data, so the SUnSAS system was mounted on the bow to prevent contamination of the data by the vessel's wake (Fig. 1).

Besides the above-water and in-water optical measure-

ments, a variety of other data were collected to help characterize the optical properties of the JCR transect:

1. Seawater temperature (T) and salinity (S) both vertically and along track;
2. Pigment analyses using the high performance liquid chromatography (HPLC) technique;
3. Seawater fluorescence and beam transmission both vertically and along track;
4. Meteorological observations including cloud cover, plus wind speed and direction; and
5. Wave height and swell direction.

In addition to paying close attention to the optimal viewing capabilities of each instrument system, some instruments were equipped with sensors that measured their viewing angles. SeaSAS, for example, had an external module that measured the vertical (two-axis) tilts and horizontal (compass) pointing of the radiometers (the so-called DIR-10 unit). A second DIR-10 was not available for SUnSAS (although the frame was built to accommodate one), so the output of the SeaSAS DIR-10 was routed to the SUnSAS acquisition computer. LoCNESS, SeaFALLS, SeaBOSS, and DalBOSS were all equipped with internal sensors that measured the vertical (two-axis) tilts of the radiometers. A generalized coordinate system for these pointing systems is given in Fig. 2 (this is the same coordinate system used during SeaBOARR-98).

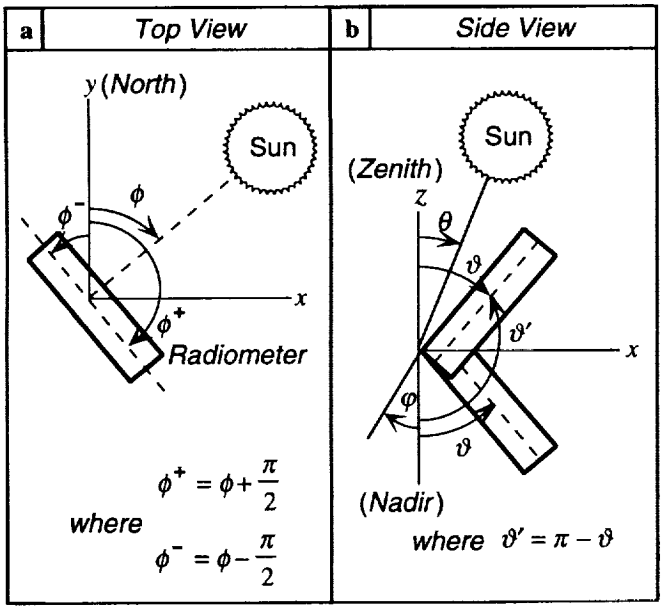

Fig. 2. The coordinate systems used for instrument pointing: a) looking down from above (the z-axis is out of the page), and b) looking from the side (the y-axis is out of the page). The ϕ coordinate is the solar azimuth angle, θ is the solar zenith angle, and ϑ is the radiometer pointing angle with respect to the vertical axis, z. The perturbations (or tilts) in vertical alignment, which can change the pointing angles, are given by φ.

Note that ϕ is measured with respect to an arbitrary reference, in this case due north, and ϑ is measured with respect to nadir (the direction pointing straight down to the sea surface). The angle ϑ' corresponds to the angle ϑ measured with respect to the zenith (the direction pointing straight up from the sea surface).

2.1 SeaFALLS and SeaBOSS

The big advantage of the SeaFALLS system, in terms of sampling strategies, is it can be deployed quickly by only two people, so the ship can be stopped when light conditions are optimal. SeaFALLS is deployed from the stern of the vessel, and whenever possible, the ship maintains a headway speed of approximately 0.5 kts. The profiling instrument is carefully lowered into the water and slowly released at the surface until it has drifted clear of any possible shadowing effect. When the profiler reaches the desired distance from the stern (usually 30–50 m), it is ready for deployment and can be *dropped* or released. Once released, the rocket-shaped profiler quickly orients itself vertically and starts to descend (the first few meters of data usually have large tilts and are ignored). The cable is almost neutrally buoyant and has a low coefficient of drag, so the profiler falls freely through the water column and measures $E_d(z,\lambda)$, $L_u(z,\lambda)$, fluorescence, plus T-S on the way down. The desired depth is usually the 1% light level, but deeper casts to completely sample some other aspect of the upper water column are frequently made. A schematic of what SeaFALLS measures is given in Fig. 3.

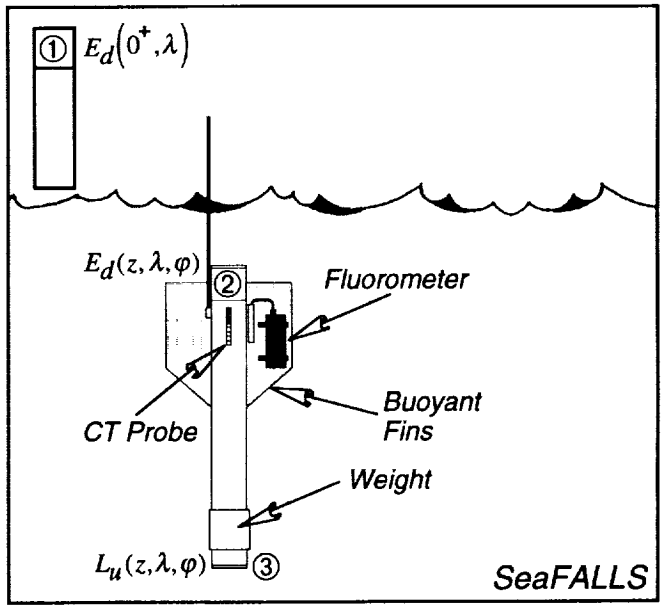

Fig. 3. A schematic of the SeaFALLS profiler.

The most important aspect for collecting good data with SeaFALLS is to prevent the telemetry cable from ever coming under tension, because even brief periods of tension on the cable can adversely affect the vertical orientation (tilt) and velocity of the profiler. To ensure this does

not occur, the operator always leaves a few coils of cable at the surface. A tangle-free and continuous feed of cable into the water is also needed, so all of the cable (approximately 300 m) is laid out or *flaked* on deck prior to each deployment in such a manner as to minimize any entanglements. The profiler descends at approximately 1 $\mathrm{m\,s^{-1}}$ so a relatively deep cast can be acquired very quickly (less than 3 min for a 150 m cast)

In the original design concept (Waters et al. 1990), SeaFALLS was deployed with the SeaWiFS Square Underwater Reference Frame (SeaSURF). SeaSURF is based on a Satlantic SeaWiFS Multichannel Surface Reference (SMSR) and measured the incident solar irradiance at a fixed depth just below the sea surface, $E_d(z_0, \lambda)$, and is floated away from the boat using a buoyant frame. A comprehensive analysis by Hooker and Maritorena (2000) showed this practice was inferior to measuring the incident solar irradiance on a mast mounted on the boat (at least on the JCR), so this technique has been abandoned. The SeaFALLS reference data comes from SeaBOSS which measures $E_d(0^+, \lambda)$ and can be deployed as a drifting buoy or on a mast. The Hooker and Maritorena (2000) study showed the latter produced the best data, so SeaBOSS was deployed on a mast during SeaBOARR-99.

The RS-485 signals from SeaFALLS and SeaBOSS were combined in a Satlantic deck box and converted to RS-232 communications for computer logging. The deck box also provided the (computer-controlled) power for all the sensors and was designed to avoid instrument damage due to improper power-up sequences over varying cable lengths. The RS-232 data were logged on a Macintosh PowerBook computer using software developed at the University of Miami Rosenstiel School for Marine and Atmospheric Science (RSMAS) and the SeaWiFS Project.

The software time stamps the two data streams (in-water and above-water measurements) and writes them to disk simultaneously. The data is stored as American Standard Code for Information Interchange (ASCII), tab-delimited (spreadsheet) files. The software controls the logging and display of the data streams as a function of the data collection activity being undertaken: dark data (caps on the radiometers), down cast, SQM calibration monitoring, etc. The selection of the execution mode automatically sets the file name, so all the operator has to do is push buttons to initiate and terminate data aquisition. All of the telemetry channels can be displayed in real time, and the operator can select from a variety of plotting options to visualize the data being collected.

2.2 LoCNESS

The first LoCNESS profiler was built from the modular, low-cost components used with the original SeaWiFS Optical Profiling System (SeaOPS) on AMT cruises (Robins et al. 1996): a DATA-100 (with 16-bit A/D convertors) for power and telemetry, and 7-channel OCR-200 and OCI-200 sensors. In the LoCNESS configuration, the DATA-100 and the two light sensors are connected in line using extension brackets, with the OCR-200 at the nose, and the OCI-200 at the tail (like SeaFALLS). The design proved so successful, an entirely separate profiler was built from new components. The LoCNESS profiler can also be built with the THOR option, which was the configuration used for SeaBOARR-99 and several other AMT cruises (Aiken et al. 1998). In the THOR configuration, an adapter plate is used on the nose to permit the mounting of the usual $L_u(z, \lambda)$ sensor plus an additional $E_u(z, \lambda)$ sensor. The THOR profiler is longer than the two-headed version, because the DATA-100 includes another A/D module. The two nose sensors do not disturb the stability of the profiler during descent. In fact, THOR has the smallest and most stable tilts of all the profilers, because of its length (1.78 m) and the large surface area of the fins. This stability, and the fact that three components of the light field are measured during each profile, makes it one of the most versatile profilers in use today.

An in-air irradiance sensor (M30) measured the incident solar irradiance just above the sea surface, $E_d(0^+, \lambda)$. The irradiance sensor was packaged with a DATA-100 module that converted the analog output of the OCI-200 radiometer to RS-485 serial communications. The sensor package was mounted on a mast on the port trawl post. The height and location of the mast ensured none of the ship's superstructure shadowed the sensor under almost all illumination conditions. A summary of the data collected with the LoCNESS profiler and its reference is presented in Appendix B; a schematic of the instruments used with the profiler is given in Fig. 4, and a comparison of the SeaFALLS and LoCNESS is shown in Fig. 5.

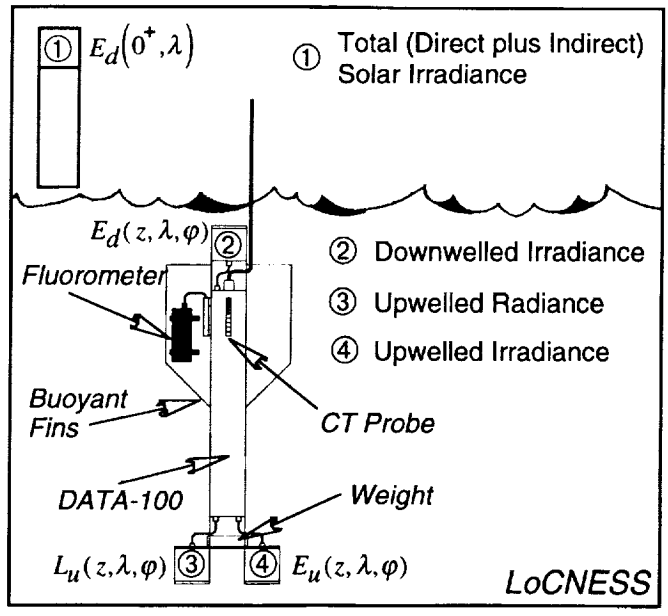

Fig. 4. A schematic of the LoCNESS profiler.

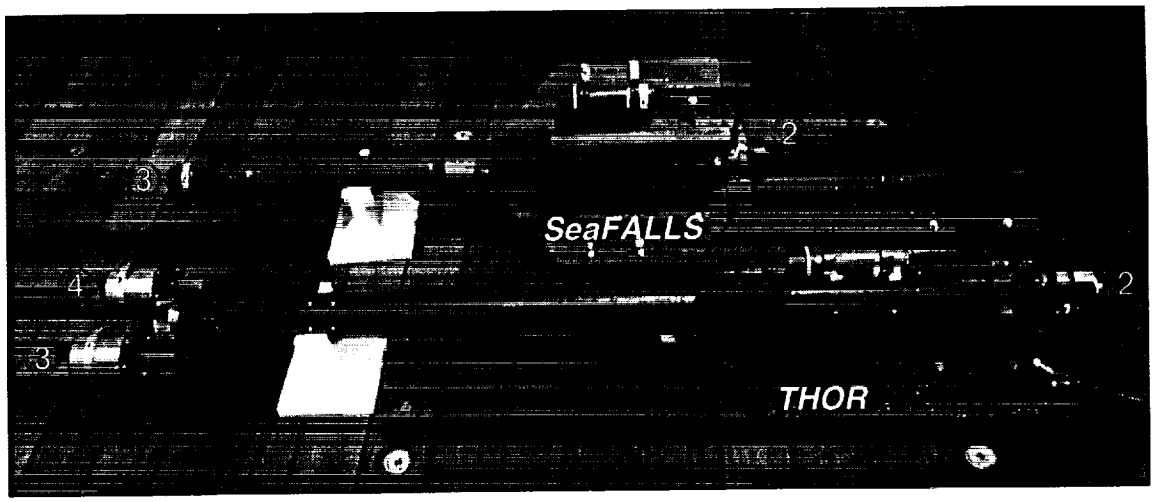

Fig. 5. A side-by-side comparison of the free-falling profilers discussed in this report: THOR (front) and SeaFALLS (back). THOR is 1.78 m long and SeaFALLS is 1.24 m long. The numbered bullets on the sensors correspond to the same bullets in Figs. 3 and 4.

The power-telemetry and data acquisition for LoCNESS and its reference was very similar to that used for SeaFALLS and SeaBOSS.

2.3 SeaSAS

SeaSAS was equipped with four radiometers. One radiance sensor (T68) measured the indirect (or sky) radiance, $L_i(0^+)$; a second radiance sensor (T28) measured the total radiance right above the sea surface, $L_T(0^+)$; and the two in-air irradiance sensors from SeaSHADE measured the total solar irradiance just above the sea surface (M35), $E_d(0^+, \lambda)$, plus the indirect (or diffuse) irradiance just above the sea surface (M95), $E_i(0^+, \lambda)$. In addition to the radiometers, SeaSAS was equipped with a DIR-10 which measured the pointing geometry and stability (vertically and horizontally) of the SeaSAS frame.

The SeaSAS frame is a unique device consisting of a pedastal and two rails with sensor mounting plates connected to a gear box which is free to rotate in the horizontal (azimuthal) plane. The gear box allows the two rails to move in a scissor-like fashion (i.e., when one is moved up a certain amount, the other moves down by the same amount); thus, if one rail is positioned 40° up from the vertical, the other rail will be 40° down from the vertical. A DATA-100 was mounted on the rail pointed skyward, so it could digitize the $L_i(0^+)$ and the DIR-10 signals. The other rail was pointed seaward and contained the $L_T(0^+)$ sensor fitted to a second DATA-100 in an integral package.

One of the design objectives of the SeaSAS frame was to make the sea and sky radiance measurements with only one radiometer. Although this has the disadvantage of increasing the amount of time to make a complete set of measurements, it has the advantage of eliminating any intercalibration differences between the sensors. It also means a smaller (and, therefore, less costly) amount of equipment is needed to make the measurements. The SeaSAS frame can be readily moved in between the two viewing orientations, so the only other requirement is to have execution modes in the software that distinguish between these data collection scenarios. A generalized schematic of what SeaSAS measured is presented in Fig. 6.

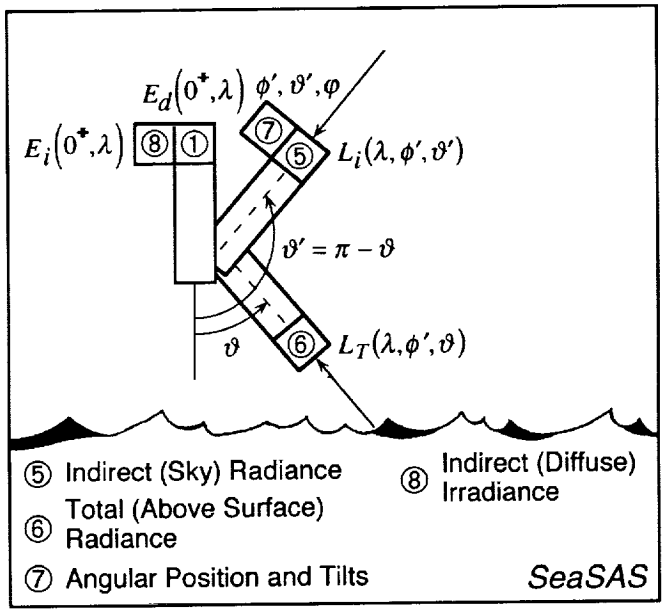

Fig. 6. A schematic of the SeaSAS instruments.

As with the in-water profilers, the SeaSAS light sensors sent their data to DATA-100 units which sent the digitized data back to the deck box that was providing power for the equipment. The RS-485 signals from the two DATA-100 units were combined in the deck box and converted to RS-232 communications for computer logging. The RS-232 data were logged on a Macintosh PowerBook computer using a variant of the software developed

for the profiling instruments. The software time stamped the two data streams (in-water and above-water measurements) and wrote them to disk simultaneously. The data was stored as ASCII, tab-delimited (spreadsheet) files.

The software controls the logging and display of the data as a function of the acquisition activity: dark data (caps on the radiometers), sea and sky viewing, sea-only viewing, sky-only viewing, SQM calibration monitoring, etc. As with the LoCNESS software, the selection of the execution mode automatically sets the file name, so all the operator has to do is push buttons to initiate and terminate data aquisition. This makes it very easy for one operator to control the acquisition of several data streams. All of the telemetry channels are displayed in real time, and the operator can select from a variety of plotting options to visualize the data being collected. The user can also choose to collect data over a 3 min interval (3 min at 6 Hz produces 1,080 data samples, which is a sufficient amount for standard time series spectral analysis). This feature was used repeatedly during SeaBOARR-98 to synchronize the different acquisition systems.

For SeaBOARR-99, the SeaSAS system was deployed on the starboard trawl post as shown in Fig. 7. A summary of the data collected with the SeaSAS instruments is given in Appendix C.

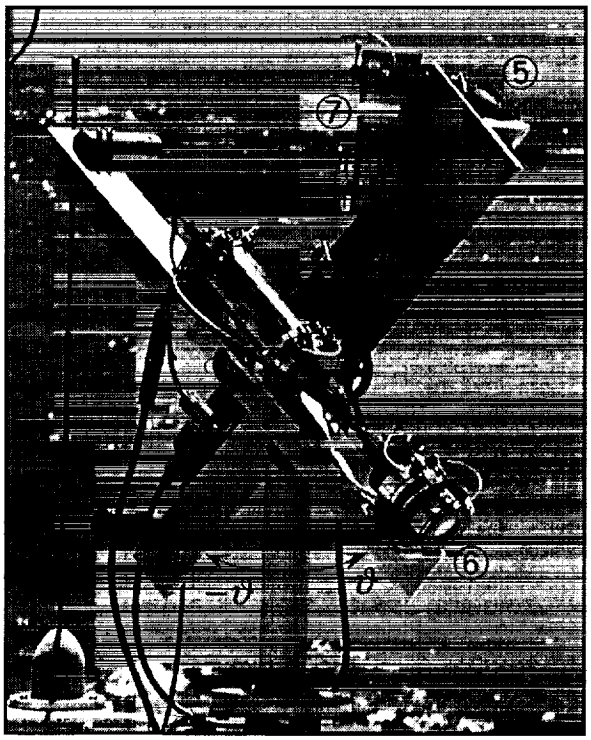

Fig. 7. The SeaSAS frame with the rails oriented at approximately 40° with respect to nadir and zenith ($\vartheta \approx 40°$). The numbered bullets correspond to the sensors in Fig. 6. When not in use, the two rails can be locked together in the $\vartheta = 90°$ position which prevents large accelerations during adverse environmental conditions.

2.4 SUnSAS

The SUnSAS system is similar in design to SeaSAS, but it is more compact and can be used with a reflectance standard. For SeaBOARR-99, the light sensors were mounted on movable plates which were mechanically secured at the desired viewing angle (using aluminum wedges cut at the appropriate angle). The largest mounting plate was designed to accommodate the light sensor that measured the total radiance just above the sea surface (T75). A square aperture was situated in the field of view of this sensor, so a plaque (usually gray, but sometimes white during diffuse illumination conditions) could be inserted before (or after) each surface-viewing sequence. This permitted the sequential measurement of $L_T(\lambda)$ and $L_p(\lambda)$ with the same radiometer. The $L_i(\lambda)$ sensor (T69) was fitted to a smaller plate that was always pointed skyward. The two SeaSHADE in-air irradiance sensors M35 and M95 provided $E_d(0^+, \lambda)$ and $E_i(0^+, \lambda)$ data, respectively.

A generalized schematic of what SUnSAS measured is shown in Fig. 8. The two SeaSHADE irradiance sensors were mounted on the top of the starboard, stern trawl post. A side view of SUnSAS deployed on the bow of the JCR is shown in Fig. 9. The latter shows the plaque frame with the square aperture centered in the field of view of the L_T sensor (the plaque is not shown). A summary of the data collected with SUnSAS is presented in Appendix F.

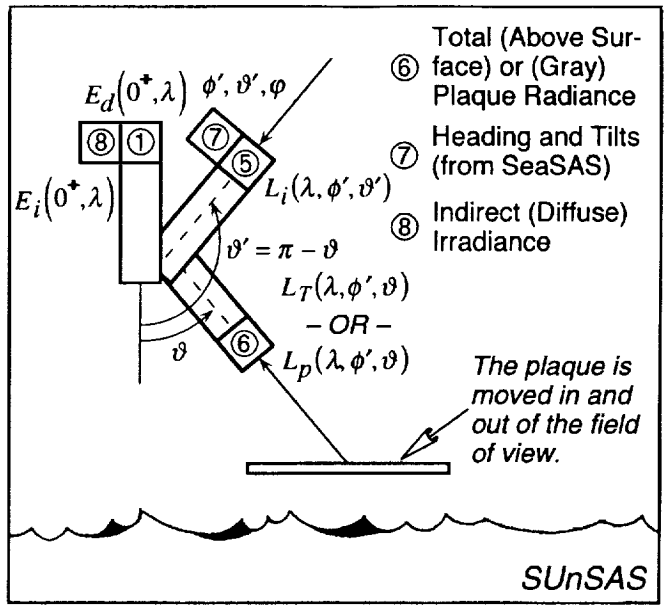

Fig. 8. A schematic of the SUnSAS system.

The gray plaque used in this campaign was a 25 cm (10 in) gray Spectralon™ plaque from Labsphere, Inc. (North Sutton, New Hampshire), with a nominal 10% reflectance (SRT–10–100). This reflectance value permits radiometers with typical above-water saturation values to make this measurement without saturating (approximately $6\,\mu W\,cm^{-2}\,nm^{-1}\,sr^{-1}$). Unlike the 99% reflectance of pure

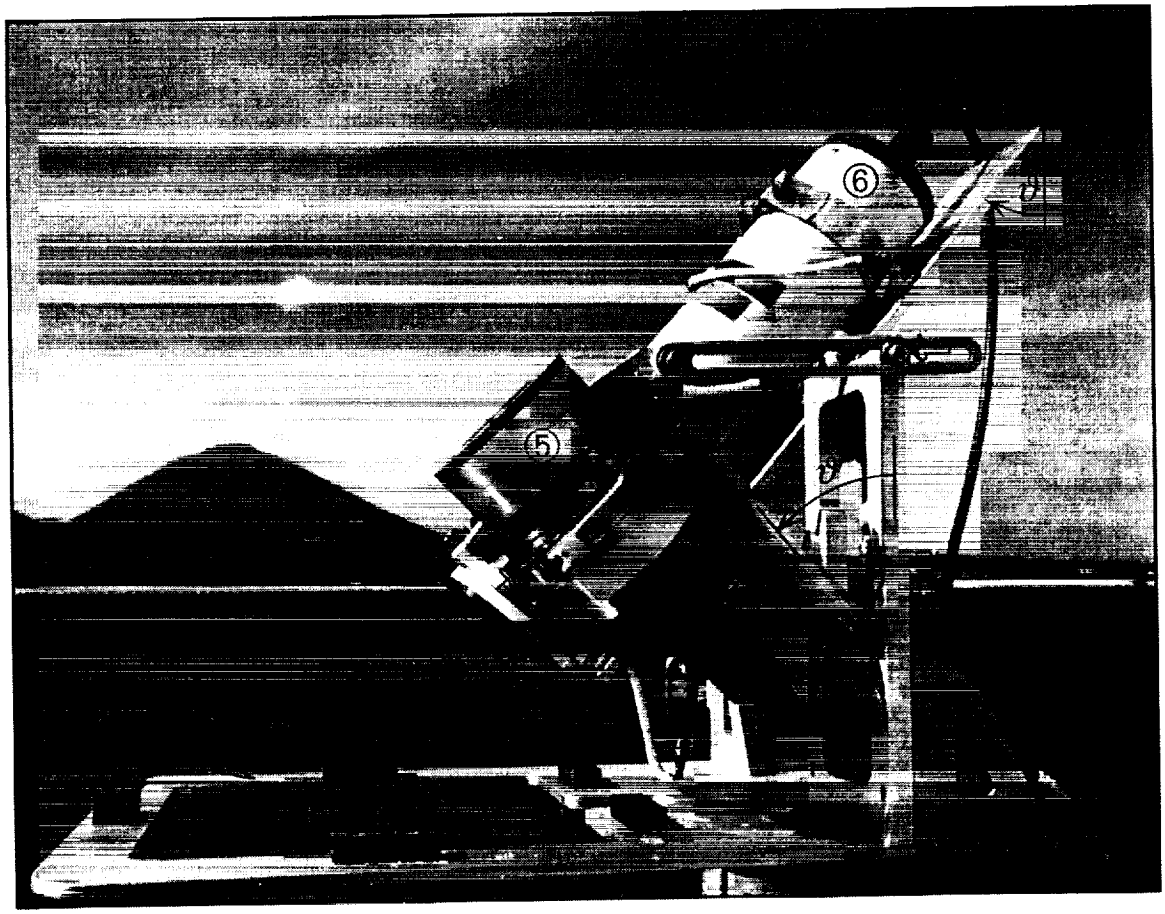

Fig. 9. The SUnSAS frame on the bow of the JCR. The numbered bullets on or near the sensors correspond to the same bullets in Fig. 8. The long white cylinder is the DATA-100 which is integral with the L_T (and L_p) sensor. The L_i sensor is attached to a movable plate that can be secured at the desired viewing angle. A similar mechanical system is used with the DATA-100.

(white) Spectralon plaques (SRT–99–100), which are usually used for radiometric calibration, gray plaques are much less lambertian, because of the added impurities of the black doping material. Variations in viewing and illumination geometries, as are naturally found in the field, are likely to add significant variance in this measurement. According to the Labsphere product catalog, for example, a 20% plaque will have a 2% higher reflectance at 45° (compared to 8°) and +5% at 61° for $\lambda = 600\,\mathrm{nm}$ (for a 99% plaque these values are −0.6% at 45°, and −0.5% at 61°).

The use of a 99% plaque and sky-viewing radiometers (the latter have typical saturation values of approximately $60\,\mu\mathrm{W\,cm^{-2}\,nm^{-1}\,sr^{-1}}$) would reduce the uncertainty in measurements, because of the significant non-lambertian reflectivity of gray plaques. This idea was not tested during SeaBOARR-99; instead, both a gray and white plaque were used during diffuse illumination conditions, so a comparison between the two could be made.

The homogeneity of a plaque should be checked at a minimum of four spots on the plaque surface, and variations greater than 2% between the spots should eliminate the use of the plaque for any validation work. A directional/directional (i.e., 0°/45°) plaque calibration, instead of the standard directional/hemispherical calibration was used for this campaign, because this was closer to the actual field geometry (25–45° illumination/50° viewing).

Although Spectralon is very hydrophobic, it readily absorbs grease and oil which are very difficult to remove and can cause significant variance in calibrations. Special precautions must be taken to avoid touching the diffusive material and to avoid long exposure to marine aerosols. During this campaign, the plaques were kept in a padded, airtight enclosure when not in use and only exposed during the measurement sequences. Both plaques always wrapped in acid-free paper during transport and storage before and after each measurement session.

Like SeaSAS, the radiometers used with SUnSAS were connected in a modular fashion. The two radiance sensors were connected to the same DATA-100. The T75 sensor was integral to the DATA-100, and the T69 sensor was cabled into an extra port. With this arrangement, the two sensors took and reported data (via RS-485 serial communications) simultaneously. The irradiance sensors were

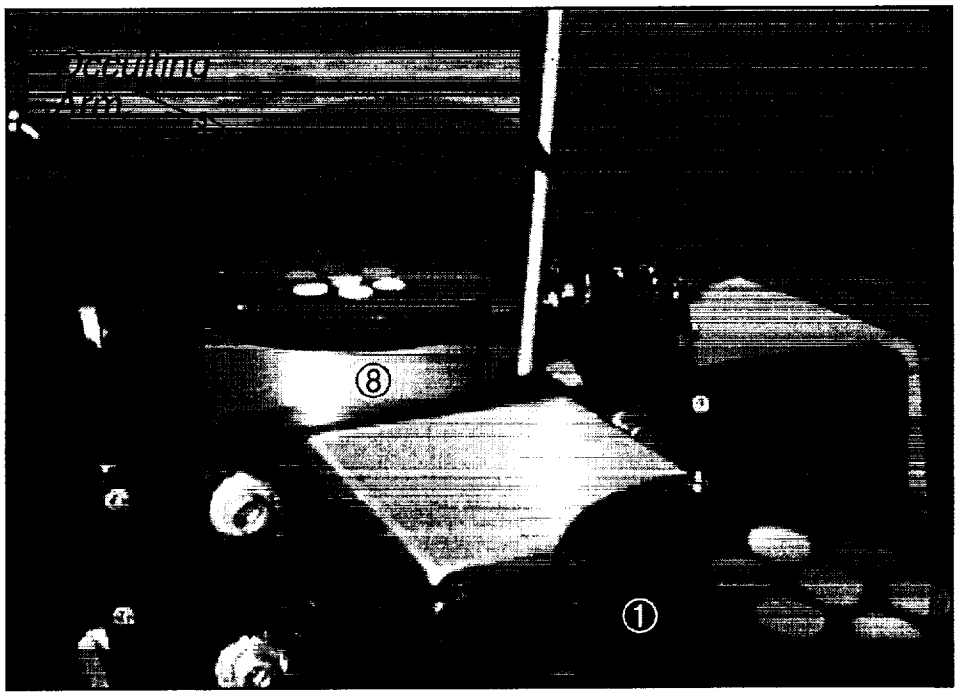

Fig. 10. SeaSHADE deployed during SeaBOARR-99. The numbered bullets on the sensors correspond to the same bullets in Figs. 6 and 8.

also connected to one DATA-100. The M35 sensor was integral to the DATA-100, and the M95 sensor was cabled into an extra port. Again, this arrangement allowed the two sensors to take and report data (via RS-485 serial communications) simultaneously.

2.5 SeaSHADE

The SeaSHADE system deployed during SeaBOARR-99 consisted of two irradiance sensors: M35 measured the total (direct plus indirect or diffuse) irradiance at the surface, $E_d(0^+, \lambda)$, and M95 measured primarily the diffuse component, $E_i(0^+, \lambda)$, but the mechanism used for occulting the sensor resulted in both types of measurements being made at different times during a measurement interval. The diffuse measurement was made possible by moving a hemispherical arm through 180° over the top of the irradiance sensor. The width of the arm and the speed of the motion was chosen to ensure each sensor is occulted for approximately 2 s. Since the Satlantic instruments sample at 6 Hz, this means there were 12 occulted samples from each channel during one complete transect of the arm from +90° to −90° with respect to zenith. When the arm was at one terminus or the other, no channels were occulted and the arm did not protrude above the surface of the irradiance sensor, so the total irradiance was measured. The SeaSHADE instrument was delivered only a few days before the start of the field campaign, so the M35 instrument was deployed as a redundant sensor to ensure irradiance data could be collected in the event of a malfunction in the occulting mechanism mounted on M95.

The shadow band module consists of a control box and mounting bracket that accepts OCI-200 or OCI-1000 irradiance sensors. The selected sensor is fitted into the bracket and a quick-release mounting clamp secures the sensor in the proper orientation. The control box has connections for power-telemetry plus a separate RS-232 connector for communicating with the microcontroller controlling the motion of the occulting arm. For SeaBOARR-99, the MVD-013 unit containing M35 was modified to supply power for the control box and the M95 sensor, digitize the signals from both units, and to send the data back to the deck box use RS-485 communications. This arrangement guaranteed that when both sensors were measuring the total irradiance, the data was digitized at the same time.

The controller operates the motor driver circuitry maintaining the speed and position of the occulting arm. The controller also allows for determining the value of the analog voltage output. The motor driver operates as a chopper-stabilized amplifier with full-, half-, and micro-step capabilities. For the SeaSHADE implementation, the arm was operated in micro-step mode only, in order to minimize arm oscillations and the amount of power used. An optical encoder is mounted on the motor shaft and was intended to allow the controller to detect stalls and to allow the arm to be moved to a *home* position by locking against a hard stop. Unfortunately, the programming for these applications was not fully developed in time for SeaBOARR-99. The speed of the arm is adjustable, but the selection set before the field campaign was completely satisfactory, so this was not changed. A picture of the SeaSHADE system is shown in Fig. 10.

Fig. 11. DalBOSS deployed during SeaBOARR-99. The numbered bullet on the sensor corresponds to the same bullets in Fig. 12. Note the splash plate right above the flotation collar.

2.6 DalBOSS

DalBOSS is a variant of the SeaBOSS design: an in-air OCI-1000 sensor (N48) measures $E_d(0^+, \lambda)$, but an additional OCR-1000 sensor (Q33) is fitted to the bottom of the sensor package. This downward-looking sensor measures the upwelled radiance right below the sea surface, $L_u(z_0, \lambda)$. For SeaBOSS and DalBOSS, the sensor package is fitted inside a removable buoyant collar, so it can be deployed on a mast or as a tethered buoy. When deployed as the latter, the irradiance sensor protrudes a small distance above the flotation collar, so one of the difficulties is keeping the irradiance sensor dry during each deployment session.

During the AMT-5 cruise, several experiments were conducted with SeaBOSS to determine how best to cheaply and effectively float an in-air sensor away from a ship while keeping it dry and minimizing tilts while it was deployed. Experiments were also conducted with SeaSURF, which is composed of an in-water irradiance sensor, $E_d(z_0, \lambda)$, suspended below a tethered, square floating frame. Rigging SeaSURF with elastic stabilizing chords greatly minimized the tilts associated with the ambient wave field, so it was decided to combine the two flotation systems with SeaBOSS. After several trials, an acceptable arrangement was engineered wherein two sets of elastic stabilizing cords fitted between the frame and the body of the irradiance housing: one at the top of the flotation collar and one at the bottom of the sensor cylinder. The elastic cords significantly dampened the wave motion and kept the sensor package more oriented towards the vertical. It was also noted that the flotation collar can be moved down the cylinder (toward the base) to expose a retaining plate that normally keeps the flotation collar from working up the cylinder. If this is done, the retaining plate acts like a splash plate, and helps keep water off the irradiance diffusers.

During SeaBOARR-99, DalBOSS was deployed in the AMT-5 SeaBOSS configuration (Fig. 11). A schematic of the radiometric measurements is shown in Fig. 12. A summary of the data collected with the DalBOSS system is presented in Appendix G.

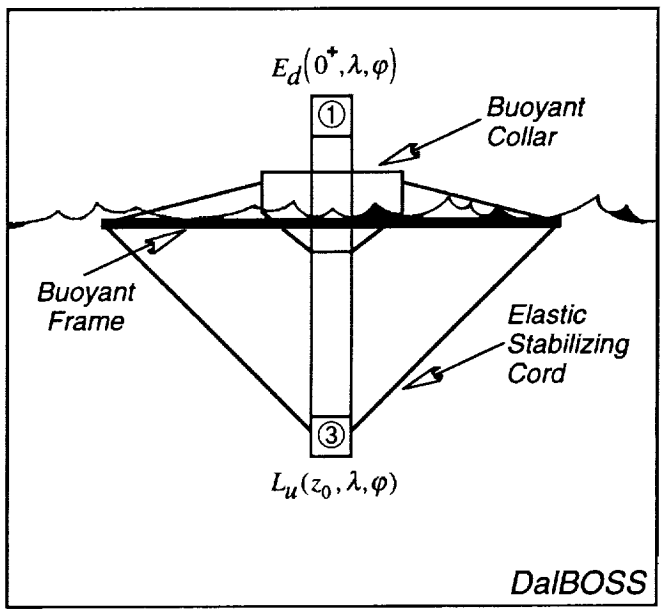

Fig. 12. A schematic of the DalBOSS system.

The RS-485 signals from the SMSR unit were combined in a Satlantic deck box and converted to RS-232 communications for computer logging. The deck box also provided the (computer-controlled) power for the sensors. The RS-232 data were logged on a Macintosh PowerBook computer using the aforementioned software developed by RSMAS and the SeaWiFS Project. The two data streams (in-water and above-water measurements) were time stamped and written to disk simultaneously. The software controlled the logging and display of the data streams as a function of the data collection activity being undertaken: dark data (caps on the radiometers), down cast, constant depth soak, up cast, etc. All of the telemetry channels were displayed in real time, and the operator could select from a variety of plotting options to visualize the data as it was being collected.

2.7 SQM and SQM-II

The SQM is a compact light source developed by NASA and the National Institute of Standards and Technology (NIST) for monitoring the radiometric stability of radiometers used to measure the *in situ* optical properties of seawater while they are being deployed in the field. The engineering design and characteristics of the SQM are described by Johnson et al. (1998), so only a brief description is given here. A separate rack of electronic equipment, composed principally of two computer-controlled power supplies and a multiplexed, digital voltmeter (DVM), are an essential part of producing the stable light field. The SQM does not have, nor does it require, an absolute calibration, but it has design objectives of better than 2% stability during field deployments.

The SQM has two sets of miniature lamps with eight lamps in each set; both lamp sets are arranged symmetrically on a ring and operate in series, so if one lamp fails, the entire set goes off. The lamps in one set are rated for 1.05 A (4.2 V) and are operated at 1.00 A, and the lamps in the other set are rated for 2.00 A (5.0 V) and are operated at 2.0 A; the lamp sets are hereafter referred to as the 1 A and 2 A lamps, respectively. The lamps are operated at approximately their full amperage rating to maximize the emitted flux.

A low, medium, and high intensity flux level is provided when the 1 A, 2 A, and both lamp sets are used, respectively. Each lamp set was *aged* for approximately 100 hours before deploying the SQM to the field. The interior light chamber has bead-blasted aluminum walls, so the diffuse component of the reflectance is significant. The lamps illuminate a circular, blue plastic diffuser protected by safety glass and sealed from the environment by o-rings. The diffuser is resilient to ultraviolet yellowing, but can age nonetheless. The exit aperture is 20 cm in diameter and has a spatial uniformity of 98% or more over the interior 15 cm circle.

A faceplate or *shadow collar* provides a mounting assembly, so the device under test (DUT), usually a radiance or irradiance sensor, can be positioned in the shadow collar. The DUT has a D-shaped collar fitted to it at a set distance, 3.81 cm (1.5 in), from the front of the DUT. This distance was chosen based on the most restrictive clearance requirement of the radiometers used in the different AMT deployment rigs. The D-shaped collar ensures the DUT can be mounted to the SQM at a reproducible location and orientation with respect to the exit aperture each time the DUT is used. The former minimizes uncertainties (principally with irradiance sensors) due to distance differences between measurement sessions, while the latter minimizes uncertainties (principally with radiance sensors) due to inhomogeneities in the exit aperture light field. In either case, the D-shaped collar keeps these sources of uncertainties below the 1% level.

The SQM faceplate can be changed to accept a variety of instruments from different manufacturers. Radiometers above a certain size, approximately 15 cm, would be difficult to accommodate, but the entire mounting assembly can be changed to allow for reasonable viewing by radiometers that are seemingly difficult to handle. To date, three radiometer designs have been used with the SQM, and there were no problems in producing the needed faceplates, D-shaped collars, or support hardware to accommodate these units; nor was there any indication of data degradation as a function of the needed modifications.

The SQM light field can change because of a variety of effects; for example, the presence of the DUT, the aging of the lamps, a deterioration in the plastic diffuser, a change in the transmittance of the glass cover, a drift in the control electronics, a repositioning of a mechanical alignment component, etc. To account for these changes, three photodiodes, whose temperatures are kept constant with a precision thermoelectric cooler (± 0.01 K), measure the exit aperture light level: the first has a responsivity in the blue part of the spectrum, the second in the red part of the spectrum, and the third has a broad-band or *white* response. All three internal monitors view the center portion of the exit aperture. The back of the SQM is cooled by a fan to prevent a build up in temperature beyond what the thermoelectric cooler can accommodate. The SQM has an internal heater to help maintain temperature stability in colder climates and to shorten the time needed for warming up the SQM.

Another SQM quality control procedure is provided by three special DUTs called *fiducials*: a white one, a black one, and a black one with a glass face (the glass is the same as that used with the field radiometers). A fiducial has the same size and shape of a radiometer, but is nonoperational. The reflective surface of a fiducial is carefully maintained, both during its use and when it is not being used. Consequently, the reflective surface degrades very slowly, so over the time period of a field expedition, it remains basically constant. A field radiometer, by comparison, has a reflective surface that is changing episodically from the wear and tear of daily use. This change in reflectivity alters the

loading of the radiometer on the SQM and is a source of variance for the monitors inside the SQM that are viewing the exit aperture, or the radiometer itself when it is viewing the exit aperture. The time series of a fiducial, as measured by the internal monitors, gives an independent measure of the temporal stability of the emitted light field.

The SQM has been used to track changes in instruments between calibrations and on four cruises lasting approximately 5–6 weeks each (Hooker and Maritorena 2000). Until SeaBOARR-99, most SQM sessions were conducted with only the 1 A lamps and they were operated at 95% of their current rating. Although the latter was a controversial decision and the topic of conflicting recommendations during the design phase of the SQM, there has been no observable degradation in the performance of the lamps as a result of this—indeed, they have survived long shipment routes (US to UK to Falkland Islands and back, plus the US to South Africa to the UK and back) on repeated occasions, as well as, the high vibration environment of a ship. For SeaBOARR-99, both lamp sets were used and both were operated at their full current rating (to maximize the emitted flux and to collect data with the 1 A lamps at maximum current).

Satlantic, Inc., developed the SQM-II as a commercial version of the SQM and based the design on the original. The main difference with the new unit is the high degree of integration. The entire system consists of two components, a deck box that provides DC power to the SQM-II, and the SQM-II itself. The latter contains the lamp rings (which use the same lamps as the original SQM), heating and cooling subsystems, control circuitry, the system computer, plus display and data storage.

The SQM-II system is designed to be self-contained and does not require a computer to operate. Only two cables are required to complete system assembly (an AC power cord for the deck box and a DC power cord to link the deck box to the SQM-II). Although this integration reduces system complexity, it comes with increased vulnerability: a failure in any one of the subsystems can render the entire system inoperable with no opportunity for simply swapping in a new (external) subassembly, like a power supply or DVM. As has always been done with the original SQM, Satlantic recommends running the SQM-II on an uninterruptable power supply (UPS), and this was done during SeaBOARR-99 (this prevents a sudden outage of the lamps in the event of a power failure, which is very stressful to the filaments). A picture of the SQM and SQM-II in the UIC on the JCR with the DalBOSS instrument kinematically mounted to the front is shown in (Fig. 13). A summary of the data collected with the SQM-II is presented in Appendix H.

User input to start and monitor the system is via a simple 4-button keypad which has a 4×20 fluorescent display at the rear of the device for displaying command options. Commands can be entered using the menus on the display or remotely from a personal computer (PC). A computer can also be connected to the system to log data during a calibration evaluation and radiometric testing (CERT) session, or the data can be stored internally on a flash card and downloaded later.

The differences between the two SQM units are not restricted to their control architecture. The SQM-II has many improvements that use of the original unit has shown to be desirable under different circumstances:

1. The bulbs are mounted at the front, facing away from the exit aperture, which increases the average path length of the light emitted by each bulb, and it makes it easier to service the lamps (individually or as a subassembly);
2. The light chamber is lined with white Spectralon, so the emitted flux is higher, and the aperture uniformity is greater; and
3. At 490 nm, the SQM-II is about seven times more intense than the SQM (the apparent blackbody temperature of the SQM-II is 3,100 K, whereas, the SQM is about 2,400 K).

Although the greater flux of the SQM-II is a desirable attribute for the blue part of the spectrum, the higher output in the red saturates many sensors. This is mitigated by the use of a blue filter in the exit aperture (as is used with the SQM), but it points to a difficult problem associated with any light source: the flux level must be tuned to match the saturation levels of the radiometers. In the case of the SQM architecture, the variety of suitable lamps is limited, so the interior reflective surfaces and the exit aperture diffuser(s) are the only variables that can be changed.

3. METHODS

The number of hours for scientific sampling during the cruises has steadily increased from 48 hours (AMT-1 and AMT-2) to the current total of 144 hours. The additional sampling time has usually made it possible to have two stations during daylight hours: the primary (late morning) station involved deploying a conductivity, temperature, and depth (CTD) system to provide water for biological and chemical sampling along with a complete set of optical measurements; the secondary (early afternoon) station was usually restricted to optical instruments that could be deployed rapidly (free-fall profilers deployed by hand and above-water systems). If time was available, and if the situation warranted it (i.e., the area being sampled was scientifically of a wider interest to the other scientists on board), the afternoon station included a CTD deployment. At the outset, the strategy for AMT-8 was to plan for two optical stations per day, subject to the normal passage constraints on vessel speed and way point scheduling.

The primary station commenced at approximately 1030 (ship's time) and the principal objective was to acquire in- and above-water optical measurements at the SeaWiFS wavelengths along with concurrent data on phytoplankton

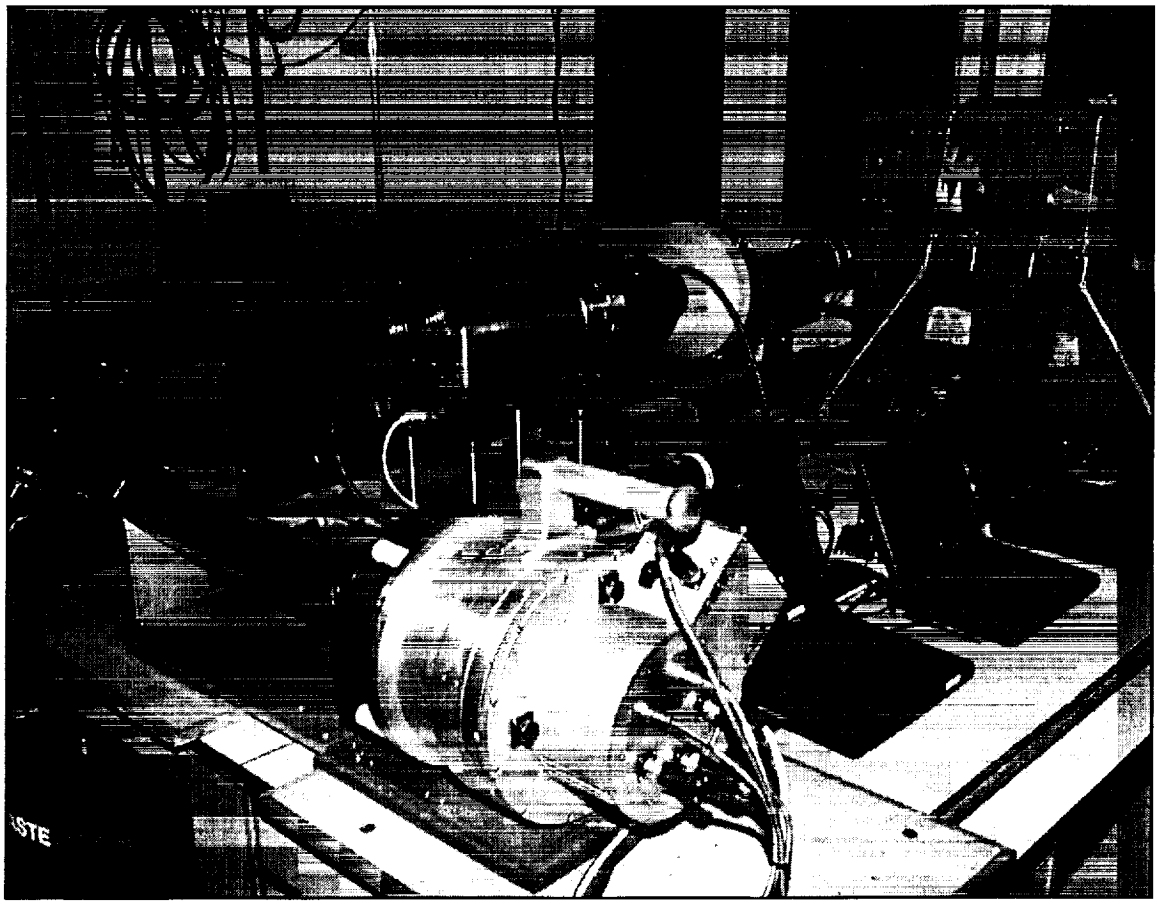

Fig. 13. The SQM and SQM-II in the UIC with SeaFALLS mounted to the former and DalBOSS to the latter. The large case with handles to the right contains the control electronics for the SQM.

pigments and species, zooplankton, hydrographic properties, and water for primary productivity, biogases, and nutrients. To collect the needed samples, four main instrument systems were deployed into the water simultaneously: zooplankton nets, CTD rosette, and up to two in-water optical systems (two free-fall profilers or one profiler plus DalBOSS). The high quality of the ship's crew allowed for the safe deployment of all four main instrument systems simultaneously and was the primary reason why station time could be kept to the shortest time possible without negatively effecting data collection opportunities or putting any one system at an unreasonable risk. The other reason for time efficiency was the CTD (provided by the SeaWiFS Project) was equipped with 12×30 L water bottles and gave sufficient water for everyone requiring it.

The second station in the afternoon was always timed to exploit the most favorable sky conditions and SeaWiFS overpass. In general, this worked well, and many of the afternoon stations were in excellent cloud-free conditions or at least in periods of stable illumination. As in the case for the morning in-water optics casts, the afternoon casts were usually to at least the 1% light level. All above-water optical data was collected in 3 min sequences, and since the in-water profilers descended at approximately $1\,m\,s^{-1}$, individual data collection events were less than 3 min. With both types of sampling lasting 3 min or less, it was very easy to keep the data streams synchronized, i.e., the in-water data was collected simultaneously with the above-water data (barring any mishaps that interrupted the synchronization of the starts). The in- and above-water optical systems were sufficiently easy to use that station time could be kept to as little as 30 min if the light field was not changing.

3.1 Experimental Protocols

The sampling protocols used were a direct consequence of the 3 min acquisition sequencing and the mixture of investigative objectives. For the purposes of defining and then categorizing the various activities involved, a *cast* was defined as an independent sampling opportunity for deriving water-leaving radiance:

a) A 3 min acquisition sequence of the sky and sea (or plaque) surface, or

b) A vertical profile of the water column (typically 1–3 min).

In most cases, the various instruments acquired data simultaneously, which was coordinated with hand-held marine radios. This was an important requirement, because the people operating the SAS instruments were approximately 100 m away from one another. An *experiment* was defined as a separate series of casts collected to investigate a specific scientific objective or hypothesis.

In the case of the above-water systems (SUnSAS and SeaSAS), the sensors measuring sea surface radiance were pointed to the sea surface at 40° from nadir, and the associated radiance sensors measuring sky radiance were oriented in the same plane at 40° from zenith. Both systems were mounted on a rotating platform with unobstructed fields of view to allow at least 240° of rotation (SUnSAS was mounted on the bow and had about a 180° unobstructed azimuthal field of view). The azimuthal orientation of each SAS platform was chosen to achieve optimal viewing geometry (Mueller and Austin 1995). To minimize direct sun glint, the system was oriented at least 90° away from the solar plane, or in the direction of minimum direct sun glint (visually determined). Adjustments were made before every cast to compensate for changes in ship heading and solar azimuth.

When the above-water systems were used together, they always collected data simultaneously (which was synchronized with the use of handheld radios). During each sequence, the following parameters were recorded by the system operator:

i) Azimuthal orientation relative to the ship's bow (in degrees),

ii) Sky conditions around the sun (cloud coverage),

iii) Sky conditions in the region of the sky observed by the sky-viewing sensor (cloud coverage),

iv) Sea surface conditions in the region observed by the sea-viewing sensor (amount of sun glint and foam), and

v) General sky and sea conditions.

SeaSAS was always operated in a sea- and sky-viewing mode, whereas SUnSAS was usually alternated between the sea- and sky-viewing mode, and the plaque- and sky-viewing mode.

When the in-water systems were used together, every attempt was made to collect their data plus the data from at least one above-water system simultaneously. Differences in how the profilers moved in the ambient currents, however, sometimes frustrated this objective. The two profilers have very different fin surface areas, which frequently causes one or the other (and at times both) to be swept in close to the ship over the course of a profile. If this happened, the effected instrument(s) were brought to the surface, positioned in the ship's wake, and then a burst of propeller wash was used to push the profiler clear of the ship (usually to a minimum distance of 30 m). Every effort was made to make sure the in-water instruments were 30–50 m away from the ship before a cast was started.

During each in-water cast, the sky conditions around the sun (cloud coverage) were recorded along with any interruptions to the general observation. All casts were timed to provide 1–3 min of stable sky conditions, but fast-moving clouds were occasionally misjudged or clouds simply formed unexpectedly around the solar disk, which resulted in periods of illumination instability. Sea and sky pictures were always taken with a digital camera during each station. These pictures were usually taken in the middle of the station time, or at a time that best represented the average sky conditions.

Because the in-water instruments fall freely through the water column, there are very few parameters that can be varied by the operator, so the experimental set for the in-water instruments was restricted to intercomparisons between a) LoCNESS and SeaFALLS station casts, and b) the above- and in-water station casts. Many more parameters could be varied for the above-water instruments, and seven kinds of intercomparison data sets were collected during SeaBOARR-99:

1. SeaSAS and SUnSAS station data;
2. SeaSAS and SUnSAS underway data;
3. Above- and in-water station data;
4. Underway data (usually SUnSAS) taken right before or after a station with the station data;
5. One above-water system at a fixed viewing angle (usually SUnSAS) and the other with a variable azimuth angle (usually SeaSAS);
6. One above-water system at a fixed viewing angle (usually SUnSAS) and the other with a variable nadir- and zenith-viewing angle (usually SeaSAS); and
7. SeaSAS and SUnSAS with variable (but coincident) nadir- and zenith-viewing angles.

A concerted effort was made to conduct these experiments under varying, but stable, environmental conditions, and at different sun zenith angles. The length and breadth of the cruise ensured a good diversity of illumination levels, surface roughness, and chlorophyll concentrations, but the recurring schedule of satellite overpasses and the need to set a daily work schedule for several of the AMT-8 cruise objectives (particularly the SQM data collection which was greatly expanded for this cruise, because two SQMs were being used) made the diversity in solar zenith angles more difficult to achieve. Fortunately, the large range in latitudes crossed (approximately 90°) ensured a certain range in solar zenith angles.

In addition to the *macro* experiments (above), several *mini* experiments were conducted to investigate the following:

a) Comparing measurements obtained from a white Spectralon plaque (T25322) and a gray Spectralon plaque (T24328) during diffuse (overcast) illumination conditions (when the L_p sensors would not saturate while looking at a white plaque);

b) Positioning the sun with respect to the ship, so both SeaSAS and SUnSAS could be viewing the same azimuth position with respect to the sun;

c) Positioning the sun with respect to the ship, so SeaSAS and SUnSAS could be viewing azimuth positions 180° apart with respect to the sun;

d) Replacing the L_p sensor on SUnSAS with the L_i sensor on SeaSAS on a sunny day, and then using a white Spectralon plaque (T25322) in addition to the gray plaque (T24328); and

e) Viewing unperturbed water behind the ship, and then viewing the turbulence caused by the ship's propeller to obtain a clear comparison of a unperturbed and foamy surface.

3.2 Optical Methods

Three different in-water and four different above-water methods for determining $L_W(\lambda)$ were intercompared during SeaBOARR-99: S84, P94, and P97 for the former; and M80, C85, S95, and L98 for the latter. These were the same methods used during SeaBOARR-98 and are well described by Hooker et al. (1999), so only a brief summary is presented here:

S84 The subsurface profile of $L_u(z,\lambda)$ is used to estimate the spectral diffuse attenuation coefficient, $K_u(\lambda)$, and the subsurface signal is propagated to the sea surface using $K_u(\lambda)$; the upwelled radiance is then transmitted across the sea surface to produce $L_W(\lambda)$.

P94 The subsurface upwelling radiance measured at $z =$ 70 cm is propagated to the sea surface using $K_u(\lambda)$ estimated from simultaneous profiles of $L_u(z,\lambda)$ (following the techniques in S84), and then across the sea surface to produce $L_W(\lambda)$.

P97 $K_u(\lambda)$ is estimated using a combination of the Morel (1988) and Austin and Petzold (1981) algorithms. The ratio of $L_u(443)$ to $L_u(550)$ is used to estimate $K_u(490)$ and $K_u(520)$ as described by Austin and Petzold (1981). The computed $K_u(490)$ and $K_u(520)$ values are used to compute the chlorophyll concentration, C, by inverting the algorithm for $K_u(\lambda)$ as detailed by Morel (1988). Once C is computed, $K_u(\lambda)$ for the other wavelengths can be computed using the Morel (1988) model. The subsurface upwelling radiance at $z = 70$ cm is propagated to the sea surface using the estimated $K_u(\lambda)$, and then across the sea surface to produce the $L_W(\lambda)$ values.

M80 Sky glint correction is based on the assumption that $L_W(\lambda)$ in a near-infrared (NIR) band, $L_W(\lambda_r)$, is equal to zero (Gordon 1981). Consequently, the above-water radiance measured at λ_r is entirely due to surface reflection. The infrared estimates of sky glint are then extended over the whole spectrum by using the measured wavelength dependence of the incident sky radiance. Estimated sky glint is subtracted from the total signal in order to recover $L_W(\lambda)$.

C85 This method uses data averaged over 10 s intervals, so each L_T spectrum incorporates the contribution of temporal sun glint which have to be removed by a correction algorithm. The above-water measurements are corrected for sky glint assuming specular reflection of sky radiance at the sea surface. The residual reflection of downwelling radiation from the wave facets is computed assuming the residual signal in the NIR region is entirely due to surface reflection, i.e., $L_W(\lambda_r) = 0$. Measurements of a horizontally oriented gray reflectance plaque are used to compute the plaque downwelling total irradiance, $E_p(\lambda)$.

S95 The total surface radiance is corrected for sky glint using sky radiance measurements in the direction appropriate for the specular reflection from the sea surface into the sensor. The $L_i(\lambda)$ measurements can be made either by looking at a horizontal *first surface* mirror (a mirror with no layers other than the reflective surface) at the same nadir and azimuth angles used for the $L_T(\lambda)$ observations, or by pointing the radiometer into the sky at a zenith angle equal to the nadir angle of the $L_T(\lambda)$ observations.

L98 Sky glint correction for this method is also based on the assumption that $L_W(\lambda_r) = 0$, so the signal received in the λ_r part of the spectrum is entirely due to surface reflection. The L98 method uses the wavelength dependence of diffuse sky irradiance to extend the estimate of sky glint at λ_r over the whole spectrum. Estimated sky glint is subtracted from the total signal in order to recover $L_W(\lambda)$. The advantage of this method is that it incorporates the effect of clouds and variable sky conditions. The technical advantage is that $E_d(0^+,\lambda)$ and $E_i(0^+,\lambda)$ can be measured with the same instrument: an upward-viewing radiometer where the diffuse component can be determined by cyclically blocking the sun disc to the radiometer, so $E_d(0^+,\lambda)$ and $E_i(0^+,\lambda)$ can be continuously monitored during remote sensing observations.

A summary of the in- and above-water methods, along with their physical assumptions and input variables, is presented in Tables 4 and 5, respectively.

Based on the consensus reached at the Normalized Remote Sensing Reflectance (NRSR) Workshop [see the summary in Hooker et al. (1999) for a meeting summary], all of the above-water methods used in the SeaBOARR-99 field campaign used a viewing angle of 40° with respect to the vertical except when specific experiments were executed to

Table 4. A summary of the three in-water methods for calculating $L_W(\lambda)$. Note that the final calculation for $L_W(\lambda)$ is the same in each method, and that the primary differences in the methods are in how $K_u(\lambda)$ is derived as an input variable (the refractive index of seawater, $n_w(\lambda)$, is assumed to be 0.544).

Method	*Assumptions*	*Input Variables*	$L_W(\lambda)$ *Calculation*
S84	$z_0 - \Delta z \le z < z_0 + \Delta z$ $\Delta z \approx 4$ to 10 m	$K_u(z,\lambda)$ from $L_u(z,\lambda)$ $L_u(0^-,\lambda) = L_u(z_0,\lambda)\exp\left[z_0 K_u(z_0,\lambda)\right]$	$L_W(\lambda) = 0.544\,L_u(0^-,\lambda)$
P94	$z_0 - \Delta z \le z < z_0 + \Delta z$ $\Delta z \approx 4$ to 10 m	$K_u(z,\lambda)$ from $L_u(z,\lambda)$ $L_u(0^-,\lambda) = L_u(0.7,\lambda)\exp\left[0.7\,K_u(\lambda)\right]$	$L_W(\lambda) = 0.544\,L_u(0^-,\lambda)$
P97	$K_u(490,520)$ from $L_u(443,550)$ and C from $K_u(490,520)$	$\chi(\lambda)$ and $e(\lambda)$ using Morel (1988) $K_u(\lambda) = K_w(\lambda) + \chi_c(\lambda)C^{e(\lambda)}$ $L_u(0^-,\lambda) = L_u(0.7,\lambda)\exp\left[0.7\,K_u(\lambda)\right]$	$L_W(\lambda) = 0.544\,L_u(0^-,\lambda)$

Table 5. A summary of the four surface glint correction methods applied to the above-water radiance measurements. The assumptions of each method and the input measurements required by the method are given in the second and third columns, respectively. The algorithms for calculating $L_W(\lambda)$ are shown in the fifth column. All of the methods require ideal sky conditions (cloud free or uniformly overcast), except L98, which can be used under a variable sky. The assumption for S95 is that $\rho(\lambda,\phi)$ can be approximated by a flat sea surface. Note that M80, S95, and L98 require the removal of temporal sun glint from the high frequency $L_T(\lambda)$ spectra, whereas C85 uses averaged (10 s) $L_T(\lambda)$ spectra. In addition, note that for all of the SeaBOARR-99 data, $\lambda_r = 780$ nm.

Method	*Assumptions*	*Input Variables*	$L_W(\lambda)$ *Calculation*
M80	$L_W(\lambda_r) = 0$ and Ideal Sky	$L_T(\lambda)$ and $L_i(\lambda)$	$L_W(\lambda) = L_T(\lambda,\phi',\vartheta) - L_i(\lambda,\phi',\vartheta')\left[\frac{L_T(\lambda_r,\phi',\vartheta)}{L_i(\lambda_r,\phi',\vartheta')}\right]$
C85	$L_W(\lambda_r) = 0$ and Ideal Sky	$L_T(\lambda)$, $L_i(\lambda)$, and $L_p(\lambda)$	$L_W(\lambda) = L_T(\lambda,\phi',\vartheta) - \rho(\lambda,\phi)L_i(\lambda,\phi',\vartheta') - \Delta L$ where $\Delta L = \left[L_T(\lambda_r) - \rho(\lambda,\phi)L_i(\lambda_r,\phi',\vartheta')\right]E_p(\lambda)/E_p(\lambda_r)$ and $E_p(\lambda) = \pi L_p(\lambda,\phi',\vartheta)/\rho_p(\lambda,\phi',\vartheta)$
S95	$\rho(\lambda,\phi)$ and Ideal Sky†	$L_T(\lambda)$ and $L_i(\lambda)$	$L_W(\lambda) = L_T(\lambda,\phi',\vartheta) - \rho(\lambda,\phi)L_i(\lambda,\phi',\vartheta')$
L98	$L_W(\lambda_r) = 0$	$L_T(\lambda)$ and $E_i(\lambda)$	$L_W(\lambda) = L_T(\lambda,\phi',\vartheta) - \left[\frac{L_T(\lambda_r)}{E_i(\lambda_r)}\right]E_i(\lambda)$

† The SOOP indicates S95 can "probably" be used under variable cloud conditions.

vary the viewing angle. Every effort was made to adhere to the agreed upon sampling criteria, but the most important requirement was to collect data during stable environmental conditions, i.e., clear sky, calm sea, low wind speed, etc., with stable illumination being the most important criteria.

3.3 SQM and SQM-II Protocols

To monitor the stability (in the field) of the in- and above-water radiometers used during SeaBOARR-99, and to quantify the performance of the SQM-II during its field commissioning, the procedures given in Hooker and Aiken (1998) were followed where applicable. A CERT session was defined and a sequence of procedures was implemented for each one:

1. The number of hours on each lamp set were tracked by recording the starting number of hours on each lamp set.
2. One fiducial was selected for powering and warming up each SQM (glass S/N 001 and white S/N 005 for the SQM and SQM-II, respectively). The first data collected during a CERT session were the dark voltages for each SQM system, which was achieved by putting the chosen fiducial in each SQM and collecting internal dark voltages for 3 min.

3. Once each SQM was powered up at the selected lamp level, it was allowed to warm up for at least 1 h, during which internal monitor voltages were recorded. The warm-up period was considered completed when the internal monitors were constant to within less than 0.1%. The radiometric stability usually coincided with a thermal equilibrium as denoted by the internal thermistors.
4. After the warm-up period, the individual radiometric sensors were tested sequentially and then each fiducial was measured. First, the previous DUT was removed and replaced with a fiducial (glass for the SQM and white for the SQM-II). Second, dark voltages for the radiometer and internal monitor data for the chosen fiducial were simultaneously collected for 3 min. Third, the fiducial was removed and replaced with the radiometer. Finally, internal monitor and radiometer data were recorded for 3 min. Each data collection event (3 min) is referred to here as a data acquisition sequence (DAS) and represents approximately 1,080 radiometer samples and 450 internal monitor samples.
5. Before the SQMs were shut down, the fiducials that were not used during the CERT sessions were measured. These measurements, plus the fiducial data acquired in between radiometer dark and light measurements, are the primary sources for tracking the stability of the SQM and SQM-II emitted flux. After the lamps were powered down, the ending number of hours on each lamp set were recorded.

It is important to note the warm-up process only involved the SQM and SQM-II, and it was done only once before the individual DUTs were measured; the DUTs were not warmed up per se, although, they were kept in the same room as the SQM and SQM-II, so they were at room temperature.

4. PRELIMINARY RESULTS

A summary of the environmental characteristics during the SeaBOARR-99 stations is given in Table 6. Although one of the data collection objectives was to collect as much data as possible following the restrictions agreed to at the NRSR meeting, the opportunities for data collection were dictated by the weather, and the primary objective was simply to collect the best data possible under the conditions at the time. Nonetheless, most of the acquisition events were within the workshop restrictions.

In this preliminary analysis, only the data collected during clear sky, calm sea, and Case-1 water are considered. The first data investigated are the water-leaving radiances derived from the LoCNESS and SeaFALLS in-water instruments, $L_W^L(\lambda)$ and $L_W^S(\lambda)$, respectively. Figure 14 shows these data from a time period when the two instruments were deployed simultaneously.

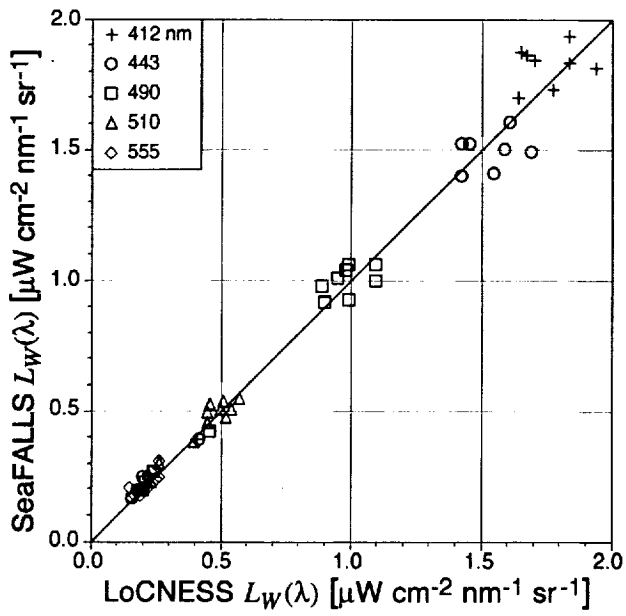

Fig. 14. A comparison of the water-leaving radiances derived from the LoCNESS and SeaFALLS in-water instruments.

The root mean square difference (RMSD) was computed for each in-water wavelength as:

$$\psi(\lambda) = 100\left[\sum \frac{1}{N}\left[\frac{L_W^S(\lambda) - L_W^L(\lambda)}{L_W^L(\lambda)}\right]^2\right]^{\frac{1}{2}}, \quad (1)$$

where N is the number of measurements. The average of the $\psi(\lambda)$ values, $\overline{\psi}_\lambda$, for the wavelengths shown in Fig. 14, is 8.1%. The data is well distributed about the 1:1 line, so the level of agreement as determined by the slope of the reduced major axis linear regression (Ricker 1973, and Press and Teukolsky 1992) line (m) and the coefficient of determination (R^2) is very good with a difference of approximately 0.3% ($m = 1.003$ and $R^2 = 0.990$).

Percent differences, $\delta(\lambda)$, are used for the above-water analyses and are formed by using one of the variables as a reference. The reference point is not necessarily truth, but it is the closest value to truth or it is the most suitable value for normalization. If X is the variable under consideration, then the percent difference of any point i with respect to the reference observation j is as follows:

$$\delta^i(\lambda) = 100\,\frac{X^i(\lambda) - X^j(\lambda)}{X^j(\lambda)}. \quad (2)$$

The mean percent differences, $\overline{\delta}_\lambda$, are the average of the total number of nonreference observations, N, for each wavelength. The total mean percent difference, $\overline{\delta}$, is the average of the individual mean percent differences at each wavelength:

$$\overline{\delta} = \frac{1}{M}\sum_{i=1}^{M} \overline{\delta}_{\lambda_i}. \quad (3)$$

Table 6. A summary of the environmental characteristics encountered during the SeaBOARR-99 stations for the Sequential Day of the Year (SDY) with all times reported in GMT (SDY 123 is 3 May). The sea state codes are as follows: 0) calm, 1) moderately rough, and 2) rough with whitecaps. Wind speed is given in units of $m\,s^{-1}$, wind and wave direction in true degrees, wave height in meters, and total chlorophyll *a* concentration in $mg\,m^{-3}$.

Station		*Position*		*Station*		*Wind*		*Sea*	*Wave*		*Chl.*	*Cloud*	*General*
SDY	*No.*	*Lon.*	*Lat.*	*Beg.*	*End*	*Speed*	*Dir.*	*State*	*Ht.*	*Dir.*	*Conc.*	*Cover*	*Sky Conditions*
123	9	−51.672	−35.078	1415	1440	9	245	2			0.142	4/10	Sunny, light cirrus, hazy.
124	10	−47.018	−32.963	1405	1420	9	215	2			0.045	9/10	Overcast w/brightening.
125	12	−42.268	−30.735	1555	1717	7	32	1			0.087	10/10	Overcast w/brightening.
126	13	−38.318	−28.852	1404	1428	12	25	2			0.073	10/10	Overcast w/brightening.
127	14	−34.252	−26.894	1312	1331	16	126	2	3.5	360	0.075	5/8	Moving clouds, brightening.
128	15	−29.560	−24.553	1513	1540	6	31	1			0.027	5/10	Cumulus, cirrus.
129	16	−25.817	−22.228	1402	1507	4	100	1			0.029		Sunny, scattered clouds.
130	17	−23.221	−19.212	1139	1221	7	114	1	1.5	70	0.037	2/8	Sunny, moving cumulus.
	18	−23.058	−18.995	1413	1500	6	117	1			0.066	2/10	Sunny, moving cumulus.
				1500	1605	5	131	1					Sunny, moving cumulus.
131	19	−20.532	−16.047	1215	1230	5	105	1	1.5	60	0.030	2/8	Sunny, cumulus.
	20	−20.402	−15.852	1417	1500	6	128	1			0.026	2/10	Sunny, cumulus.
				1500	1545	5	129	1				4/10	Sunny, cumulus.
132	21	−18.126	−13.171	1055	1134	6	134	2	1.5	70	0.039	3/8	Sunny, moving cumulus.
	22	−17.912	−12.890	1338	1415	4	189	2	1.0	70	0.057	3/8	Sunny, moving cumulus.
133	23	−15.400	−9.861	1042	1111	7	132	2	1.0	80	0.086	3/8	Sunny, moving cumulus.
	24	−15.212	−9.607	1306	1330	5	177	1			0.082	3/10	Sunny, moving cumulus.
				1345	1415	5	136	1				2/10	Sunny, moving cumulus.
138	25	−14.517	−7.642	1443	1445	9	262	2			0.072	5/10	Sunny, cumulus.
139	26	−15.530	−4.119	1039	1116	10	20	2	2.5	135	0.161	4/8	Sunny, gray cumulus.
	27	−15.613	−3.872	1320	1335	10	315	2			0.184	5/10	Sunny, cirrus, cumulus.
140	28	−16.711	−0.076	1037	1112	5	150	1	1.0	135	0.139	6/10	Variable, clouds.
	29	−16.800	0.232	1311	1353	4	155	1			0.110	3/10	Sunny, hazy, cirrus.
141	30	−17.883	3.899	1037	1139	3	101	0	0.5	130	0.152	3/10	Haze, cirrus, cumulus.
	31	−18.012	4.313	1403	1439	2	73	0	0.1	180	0.113	3/10	Haze, cirrus, cumulus.
142	32	−18.988	7.620	1038	1127	4	35	0	0.2	330	0.168		Sunny, hazy, thin cumulus.
	33	−19.053	7.847	1250	1345	2	293	0	0.1	Var.	0.136		Sunny, hazy, thin cumulus.
143	34	−20.152	11.563	1042	1048	5	260	1	0.1	Var.	0.237	3/10	Sunny, hazy, thin cumulus.
	35	−20.260	11.917	1352	1425	3	303	2			0.145	8/8	Sunny, hazy, thin cumulus.
144	36	−21.003	15.000	1053	1130	9	76	2	1.5	15	0.414		Sunny, hazy, uniform sky.
				1231	1350	8	15	2					Sunny, hazy, uniform sky.
145	37	−21.003	18.802	1035	1120	8	46	2	1.5	15	0.814	7/8	Overcast w/brightening.
	38	−21.000	19.308	1410	1453	9	338	2			0.412		Overcast w/brightening.
146	39	−21.015	22.917	1044	1117	5	52	0	0.5	15	0.117	4/8	Sunny, scattered clouds.
	40	−21.065	23.278	1338	1403	3	158	0			0.145	2/10	Clear w/scattered cumulus.
147	41	−21.807	23.278	1045	1115	3	144	0	0.2	355	0.079	1/10	Clear w/scattered cumulus.
	42	−21.870	27.052	1315	1445	2	148	0	0.0	355	0.094	3/8	Sunny, dense cirrus.
148	43	−21.563	30.467	1033	1115	5	25	0	0.5	355	0.048	8/8	Overcast w/brightening.
	44	−21.498	30.956	1409	1432	3	60	0	0.1	10	0.037	7/8	Overcast w/brightening.
149	45	−20.788	34.367	1050	1118	8	14	2	0.5	330	0.054	5/8	Sunny, moving cumulus.
	46	−20.692	34.550	1305	1333	8	133	2	1.0	330	0.052	3/8	Sunny, moving cumulus.
150	47	−20.012	38.178	1034	1106	9	37	2	1.5	320	0.036	5/8	Sunny, scattered cumulus.
	48	−20.003	38.642	1405	1441	8	335	2	1.5	320	0.079	6/8	Overcast then clearing.
151	49	−20.012	41.850	1042	1123	11	17	2	1.5	20	0.124	6/8	Overcast then clearing.
	50	−20.008	42.263	1304	1321	9	48	2	1.5	10	0.137	6/8	Sunny, cumulus.
152	51	−19.978	45.943	1014	1101	5	219	0	0.1	20		1/8	Sunny, cirrus.
	52	−20.002	46.378	1333	1358	9	40	2	0.8	230		6/8	Sunny, nonuniform cirrus.

Table 6. (cont.) A summary of the environmental characteristics encountered during the SeaBOARR-99 stations for the SDY with all times reported in GMT (SDY 156 is 5 June). The sea state codes are as follows: 0) calm, 1) moderately rough, and 2) rough with whitecaps. Wind speed is given in units of $m\,s^{-1}$, wind and wave direction in true degrees, wave height in meters, and total chlorophyll *a* concentration in $mg\,m^{-3}$.

Station		Position		Station		Wind		Sea	Wave		Chl.	Cloud	General
SDY	No.	Lon.	Lat.	Beg.	End	Speed	Dir.	State	Ht.	Dir.	Conc.	Cover	Sky Conditions
153	54	−15.663	47.453	1039	1118	9	21	2	1.0	260		8/8	Overcast w/brightening.
	55	−14.772	47.540	1524	1553	10	23	2			0.852		Overcast w/brightening.
154	56	−9.665	48.148	1051	1120	10	134	2	1.5	260	0.514	4/8	Clear, scattered cumulus.
	57	−9.408	48.213	1249	1400	9	103	2	1.5	260	2.400	3/8	Clear, scattered cumulus.
	58	−9.235	48.253	1506	1544	8	14	2	1.5	260	2.028	4/8	Sunny, cirrus.
155	59	−9.250	48.982	1052	1123	15	168	2	1.5	265	0.932	8/8	Overcast w/thick cirrus.
	60	−9.178	48.983	1254	1336	13	324	2	1.5	270	0.942	8/8	Overcast w/brightening.
	61	−8.865	49.032	1509	1520	12	113	2			0.647		Overcast.
156	62	−4.458	49.702	0935	1035	14	181	2	1.5	220	1.950	8/8	Overcast, sunny, overcast.

Note: The total chlorophyll concentrations for stations 57 and 62 are averages; the ranges of concentrations seen at these stations were 1.9–2.9 and 1.5–2.4 $mg\,m^{-3}$, respectively.

Figure 15 shows the results of two azimuthal pointing experiments during calm sea and wind conditions plus stable (clear sky) solar illumination. The data are from the same day, but two different time periods (morning and afternoon), so they are normalized with respect to the 90° sample, that is, the percent difference is formed by subtracting the $L_W(\lambda)$ value at 90° from the other $L_W(\lambda)$ values and then dividing by the $L_W(\lambda)$ 90° value and multiplying by 100 [using S95 for calculating $L_W(\lambda)$].

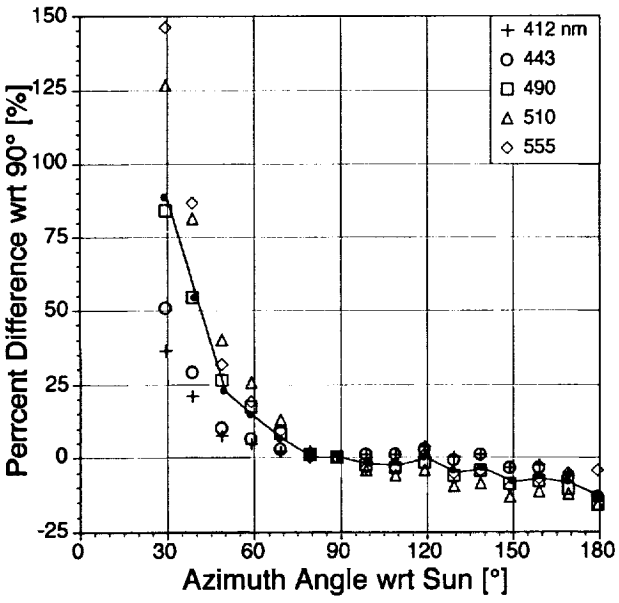

Fig. 15. The results of two azimuthal pointing experiments during calm sea and wind conditions plus stable (clear sky) solar illumination. The mean percent difference ($\overline{\delta}$) is given by the solid line (and solid circles). The 90° azimuth angle corresponds to a radiometer pointed perpendicular with respect to the sun plane.

The importance of pointing a surface-viewing radiometer perpendicular to the sun plane (i.e., maintaining at least a 90° azimuthal angle with respect to the plane defined by the sun and the radiometer) is well demonstrated in the Fig. 15 data: there is a rapid increase in $L_W(\lambda)$ as the radiometer is moved closer to the sun plane and exposed to an increasing amount of glint ($\overline{\delta}$ is less than 5% only between 80 and 90°); when the radiometer is moved farther away from the sun, however, $L_W(\lambda)$ does not change appreciably until the azimuthal angle reaches 150° ($\overline{\delta}$ is less than 5% between 90 and 140°).

Several experiments were conducted to estimate the sensitivity of above-water measurements to vessel speed. One such experiment was executed on SDY 146 (26 May) after the afternoon station and during clear sky conditions. The first speed level sampled was 7 kts, which was followed by 5, 9, and 11 kts. The entire experiment took 44 min to execute, so this analysis uses remote sensing reflectance (R_{rs}) rather than water-leaving radiance, because the former includes a normalization for changes in the incident solar irradiance. The reference values for the percent difference calculations were the $R_{rs}(\lambda)$ values determined at the station right before the underway data sampling was started.

The results for the speed sensitivity data are shown in Fig. 16. Although the spectral range of variance for all of the different underway experiments is approximately ±9%, much of the data are well distributed around zero except for the data corresponding to 7 and, to a lesser extent, 11 kts. The data at 9 kts is distinctive, because the range of the observations with respect to the station values is the greatest. An increase in variance with ship speed is one of the expected results of the underway experiments, because a higher ship speed produces less platform stability which increases measurement variance. Note that three sample sets were collected for each vessel speed except 11 kts. For

the latter, the last two sample sets were collected under deteriorating sky conditions and were not included in the analysis.

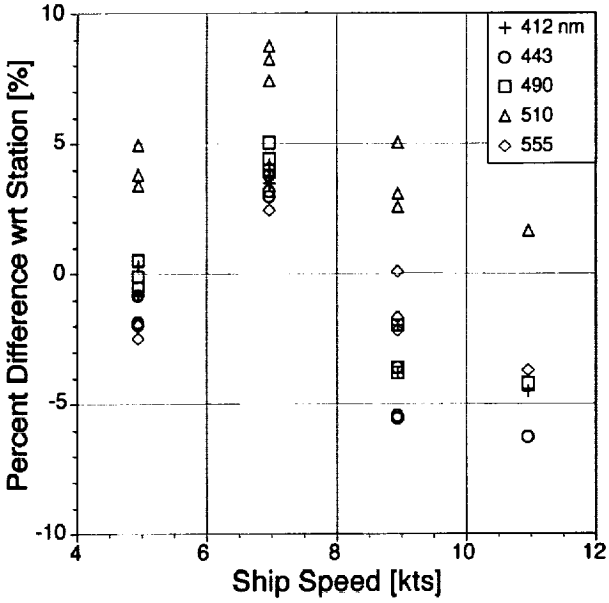

Fig. 16. The percent difference in $R_{rs}(\lambda)$ with respect to the station value and as a function of the speed of the vessel.

The $\overline{\delta}$ values for the speed sensitivity measurements are given in Table 7. The (averaged) data from 5 and 9 kts are within 2% of the station values; whereas, the data from 7 and 11 kts are within 5%. The poor agreement at 11 kts is not unexpected, because it was the last experiment executed and the temporal difference with respect to the station sampling was maximum (plus only one sample set was acquired, so the range of variance is not the same as for the other sample sets). The larger uncertainty in agreement at 7 kts is perplexing, however, because the data for this experiment were collected closest to the station sampling, and the data taken before and after produced reasonable results (agreement to within 2%).

Table 7. A summary of the sensitivity of making above-water measurements while underway.

Ship Speed	$\overline{\delta}$ [%]
5 kts	0.00
7	4.61
9	−1.83
11	−3.47
Average	−0.17
Absolute Average	2.48

Preliminary SQM and SQM-II analyses have been completed for the 16-bit SeaBOARR-99 radiometers (OCR-200 and OCI-200 sensors) using the 1 A data and the blue SQM internal detector (the SQM-II has one internal detector in the blue). The temporal performance of a radiometer is determined by calculating the percent deviation of the radiometer (during a particular SQM session) from the mean of all of the normalized signals, where the normalized signals incorporate the internal SQM detector to account for changes in the emitted flux of the SQM (Hooker and Aiken 1998). Although AMT-8 was not the first time the SQM-II was used in the field, it was one of the longest deployments and the only one when the original SQM was deployed at the same time, so it represents an important opportunity to intercompare the two instruments.

Figure 17 presents a summary of sensor stability as measured by the two SQMs organized according to their measurement types: sea and sky radiance (Fig. 17a), solar irradiance reference (Fig. 17b), and in-water radiance and irradiance (Fig. 17c). The data shows the radiometers were usually stable to within 1%, but there were exceptions. As already noted in previous SQM deployments (Hooker and Maritorena 2000), the largest uncertainties were in the blue channels and irradiance sensors were less stable than radiance sensors.

An overall summary of sensor stability is presented in Table 8; once again, the average stability of the radiometers are categorized according to their deployment and data collection types. The average stability as measured by the SQM and SQM-II for a) radiance sensors was 0.41 and 0.58, respectively; b) irradiance sensors was 0.74 and 0.62, respectively; and all sensors was 0.57 and 0.60, respectively.

Table 8. A summary of the stability (in percent) of the (16-bit) radiometers used during SeaBOARR-99.

Sensor Type	*SQM*	*SQM-II*
In-Air Radiance	0.67	0.72
In-Air Irradiance	0.66	0.58
In-Water Radiance	0.15	0.43
In-Water Irradiance	0.81	0.66
Radiance Average	0.41	0.58
Irradiance Average	0.74	0.62
Total Average	0.57	0.60

5. DISCUSSION

To provide a quick look at the data collected during SeaBOARR-99, only a small subsample of the data collected during the entire activity was analyzed, and the *in situ* data was restricted to the best environmental conditions. The latter is an important restriction, because it means the results may not be indicative of a wider or more realistic set of conditions. The preliminary results from this effort indicate the following:

1. The SQM-II performed comparably to the SQM and was capable of monitoring calibration stability to within 1%, so differences within the individual experiments above the 1% level are not the artifact of sensor intercalibration problems;

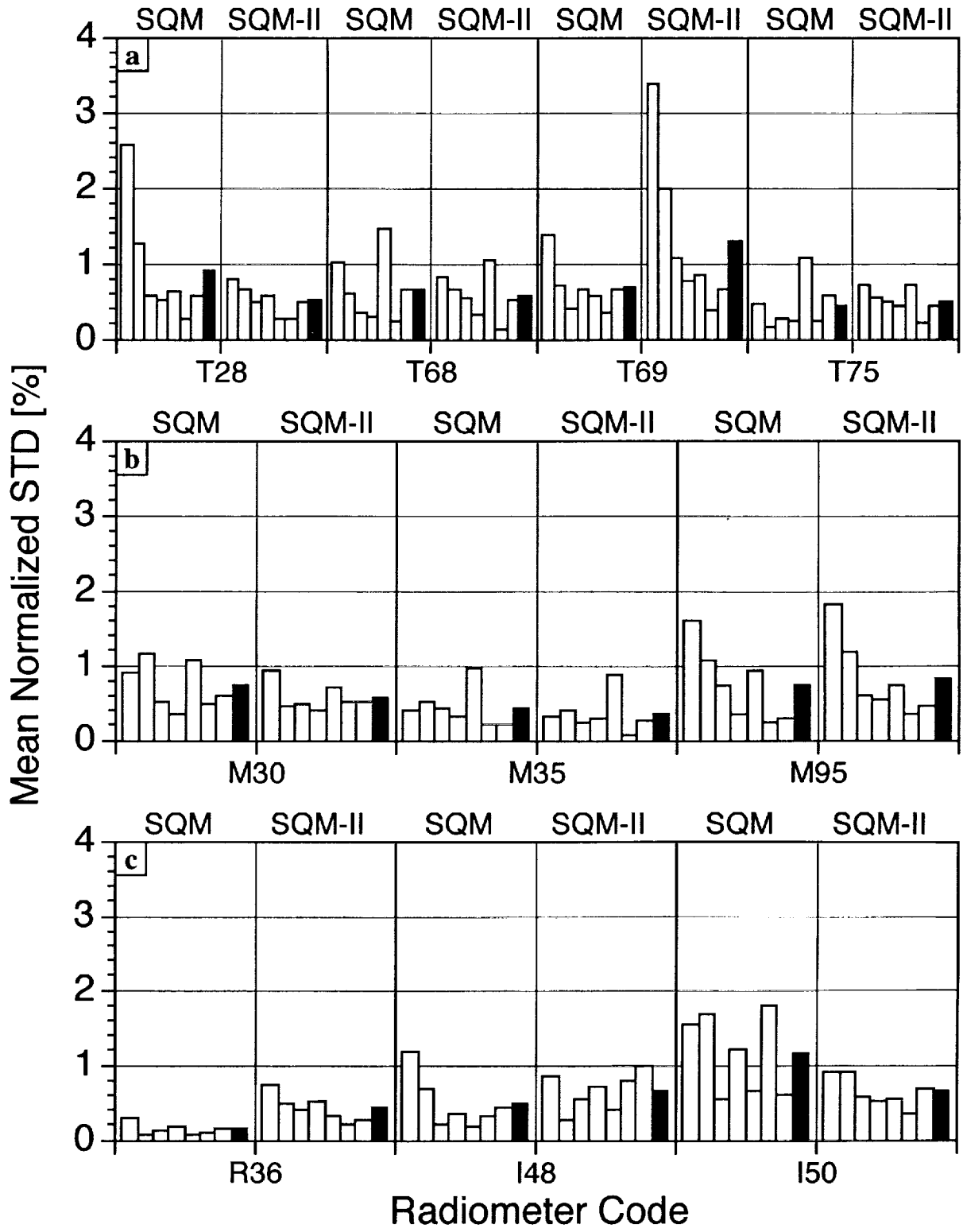

Fig. 17. The stability of some of the SeaBOARR-99 radiometers as measured by the SQM and SQM-II: **a)** the in-air sea and sky sensors, **b)** the in-air references, and **c)** the in-water radiometers. The white bars give the individual channels (channels 1–7 from left to right), and the (right-most) black bars give the spectral averages (of all seven channels).

2. The in-water instruments showed an overall agreement at the 0.3% level (based on linear regression analysis);
3. The azimuthal pointing experiments indicate less than a 5% difference in $L_W(\lambda)$ estimation if the azimuthal angle with respect to the sun plane is 80–140°; and
4. Experiments with above-water sampling while the ship was underway show a vessel speed of 11 kts or less contributes an average uncertainty of approximately 2.5% (estimated using the absolute value of the individual speed uncertainties given in Table 7 rather than the ensemble average).

Demonstrating the capabilities of the SQM-II is an important accomplishment, because it is a commercial version of the original SQM that can be purchased by anyone interested in quantifying the calibration stability of radiometers in the field. If the SeaWiFS Project radiometric objectives are to be respected, this is an essential part of any vicarious calibration or algorithm validation data set (Hooker and McClain 2000), because it allows for a complete quantification of an instrument's uncertainty budget (Hooker and Maritorena 2000).

If substantiated by further analyses, the estimate of underway sampling uncertainty with an above-water system is an important and encouraging result. Above-water systems are more efficient than in-water systems, in terms of their ability to collect the largest number of independent samples of water-leaving radiance in a particular time period, and if they can also collect valid data while the ship is underway, they will be even more attractive to use.

Acknowledgments

SeaBOARR-99 could not have been executed at the high level that was achieved without the competent contributions of the AMT-8 Principal Scientist, Nigel Rees, and the JCR officers and crew. Many other individuals have contributed to the success of various components of the SeaWiFS Field Team activities within the AMT Program, including J. Brown, S. Maritorena, and C. Dempsey; their dedicated contributions are gratefully acknowledged. The stewardship of the AMT Program and the collection of the optical data has been a high priority for J. Aiken; his diligence and commitment has been essential to the high quality and quantity of the optical data collected. The final preparation of the manuscript benefitted from the editorial and logistical assistance of E. Firestone.

Appendices

Appendix A

SeaBOARR-99 Science Team

The science team members are presented alphabetically.

Anthony Creamer
NASA/SAIC GSC/Code 970.2
Bldg. 28, Room W120
Greenbelt, Maryland 20771–0001
USA
Voice: 301–286–3057
Fax: 301–286–0268
Net: tony@seawifs.gsfc.nasa.gov

Stanford Hooker
NASA/GSFC/Code 970.2
Bldg. 28, Room W126
Greenbelt, Maryland 20771–0001
USA
Voice: 301–286–9503
Fax: 301–286–0268
Net: stan@ardbeg.gsfc.nasa.gov

Gordana Lazin
Satlantic, Inc.
Pier 9, Richmond Terminals
3295 Barrington Street
Halifax, Nova Scotia B3K 5X8
CANADA
Voice: 01–902–492–4780
Fax: 01–902–492–4781
Net: gogo@satlantic.com

Guy Westbrook
Plymouth Marine Laboratory
Prospect Place
Plymouth PL1 3DH
UNITED KINGDOM
Voice: 44–1–752–633–406
Fax: 44–1–752–633–101
Net: a.westbrook@pml.ac.uk

Appendix B

The SeaFALLS, SeaBOSS, and DalBOSS Deployment Log

The SeaFALLS, SeaBOSS, and DalBOSS Deployment Log is summarized in Table B1.

Appendix C

The LoCNESS Deployment Log

The LoCNESS Deployment Log is summarized in Table C1.

Appendix D

The SeaSAS Deployment Log

The SeaSAS Deployment Log is summarized in Table D1.

Appendix E

The SUnSAS Deployment Log

The SUnSAS Deployment Log is summarized in Table E1.

Appendix F

The SQM and SQM-II Deployment Log

The SQM and SQM-II Deployment Log is summarized in Table F1.

Table B1. A summary of the SeaFALLS (SF), SeaBOSS (SB), and DalBOSS (DB) Deployment Log for the SDY during SeaBOARR-99 with all times reported in GMT (SDY 123 is 3 May and SDY 156 is 5 June).

Cast		*Position*		*Darks*			*Cast*		*CCD*	*Depth*	*Sky Conditions*
No.	*SDY*	*Longitude*	*Latitude*	*SB*	*DB*	*SF*	*Beg.*	*End*	*Pic.*	[m]	*Around the Sun*
1	123	−51.6712	−35.0827	0818		0818	1413	1415	0922	100	Clear.
2	123	−51.6726	−35.0839				1419	1422	1443	100	Clear.
3	123	−51.6737	−35.0847				1425	1427		100	Clear.
4	123	−51.6752	−35.0857				1432	1434		105	Clear.
5	124	−47.0163	−32.9636	1314		1314	1405	1408		145	Overcast with some brightening.
6	124	−47.0171	−32.9635				1417	1420		135	Overcast with some brightening.
7	126	−38.3187	−28.8508	1311		1311	1404	1406		115	Overcast with some brightening.
8	126	−38.3190	−28.8508				1413	1415		135	Overcast with some brightening.
9	126	−38.3200	−28.8510				1425	1427		145	More overcast, some brightening.
10	127	−34.2516	−26.8959	1301		1301	1312	1315		100	Overcast with some brightening.
11	127	−34.2515	−26.8957				1320	1322		135	Overcast with some brightening.
12	127	−34.2513	−26.8960				1328	1331		135	Overcast with some brightening.
13	128	−29.5651	−24.5547	1413		1413	1513	1516		145	Partly cloudy, cirrus in front of sun.
14	128	−29.5669	−24.5540				1522	1524		150	Partly cloudy, cirrus in front of sun.
15	128	−29.5686	−24.5537				1530	1533	1537	140	Partly cloudy, cirrus in front of sun.
16	129	−25.8173	−22.2286	1330		1330	1402	1406		160	Clear.
17	129	−25.8184	−22.2276				1411	1414		160	Clear.
18	129	−25.8200	−22.2268				1420	1422		140	Clear.
19	129	−25.8227	−22.2256				1428	1431		125	Clear.
20	129	−25.8248	−22.2248				1435	1438		135	Clear.
21	129	−25.8270	−22.2244				1444	1447		170	Clear with thin cirrus.
22	129	−25.8285	−22.2245				1453	1455	1458	140	Clear.
23	129	−25.8295	−22.2247				1501	1503		125	Clear.
24	130	−23.2208	−19.2105	1123		1123	1139	1142		175	Clear.
25	130	−23.2211	−19.2096				1149	1152		175	Clear.
26	130	−23.2216	−19.2090				1202	1206		200	Clear.
27	130	−23.2233	−19.2060				1214	1216	1219	100	Clear.
28	130	−23.0392	−18.9922	1346	1346	1346	1414	1417		180	Clear.
29	130	−23.0438	−18.9909				1436	1438		110	Clear.
30	130	−23.0469	−18.9903				1450	1453		170	Clear.
31	130	−23.0484	−18.9900				1459	1502		175	Clear.
32	130	−23.0508	−18.9891				1513	1516		150	Clear.
33[1]	130	−23.0543	−18.9885				1535	1538	1539	150	Clear.
34[1]	130	−23.0569	−18.9876				1551	1554		170	Clear.
35[1]	130	−23.0590	−18.9872				1602	1605		155	Clear, cloudy at end of cast.
36	131	−20.5361	−16.0447	1149		1149	1215	1218		175	Clear.
37	131	−20.5371	−16.0444				1224	1226		145	Cloudy, sun at end of cast.
38	131	−20.3917	−15.8631		1355	1355	1417	1419		120	Cloudy, sun at end of cast.
39	131	−20.3925	−15.8621				1423	1426		165	Clear.
40	131	−20.3933	−15.8614				1431	1434	1436	175	Clear.
41[1]	131	−20.3960	−15.8576				1500	1503		180	Clear.
42[1]	131	−20.3996	−15.8539				1527	1530		180	Clear.
43[1]	131	−20.4010	−15.8527				1538	1541		180	Clear.
44[1]	132	−18.1270	−13.1682	1005	1005	1005	1056	1059		160	Clear.
45[1]	132	−18.1283	−13.1661				1105	1108	1110	145	Clear.
46[1]	132	−18.1337	−13.1615				1124	1127		145	Clear.
47	132	−17.9123	−12.8890			1149	1338	1341		150	Clear.
48	132	−17.9147	−12.8882				1347	1350		175	Clear.
49	132	−17.9223	−12.8847				1409	1412		150	Clear.
50[1]	133	−15.4025	−9.8587	0954	0954	0954	1042	1045		155	Clear, cloud at end of cast.
51[1]	133	−15.4042	−9.8585				1053	1056	1058	175	Clear, cloud edge at end of cast.
52[1]	133	−15.4063	−9.8575				1104	1106		125	Clear.
53	133	−15.2141	−9.6051			1245	1307	1309		130	Clear.
54	133	−15.2173	−9.6036				1315	1318	1322	150	Clear.
55	133	−15.2198	−9.6031				1324	1326		155	Clear, small cloud in middle of cast.

Table B1. (cont.) A summary of the SeaFALLS (SF), SeaBOSS (SB), and DalBOSS (DB) Deployment Log for the SDY during SeaBOARR-99 with all times reported in GMT (SDY 123 is 3 May and SDY 156 is 5 June).

Cast No.	SDY	Position Longitude	Latitude	Darks SB	DB	SF	Cast Beg.	End	CCD Pic.	Depth [m]	Sky Conditions Around the Sun
56	138	−14.5106	−7.6389	1315		1315	1443	1445		105	Clear with thin cumulus.
57	140	−16.7110	−0.0751	1007		1007	1038	1041		140	Thin high cumulus; cloud in middle.
58	140	−16.7098	−0.0741				1048	1050		125	Thin high cumulus.
59	140	−16.7087	−0.0735				1056	1059	1118	110	Thin high cumulus; cloud in middle.
60[1]	140	−16.7994	0.2319		1247	1247	1312	1314	1319	125	Thin high cirrus.
61[1]	140	−16.7998	0.2348				1322	1325		125	Thin high cirrus.
62	140	−16.8020	0.2420				1344	1347		115	Thin high cirrus.
63[1]	141	−17.8834	3.8994	0946	0946	0946	1038	1040		130	Thin high cirrus.
64[1]	141	−17.8833	3.9000				1047	1049		130	Thin high cirrus.
65[1]	141	−17.8835	3.9006				1055	1058	1105	130	Thin high cirrus.
66[1]	141	−17.8839	3.9022				1108	1110		110	Cloudy, brightening in middle.
67[1]	141	−17.8839	3.9026				1115	1117		125	Thin high cirrus.
68[1]	141	−17.8838	3.9028				1121	1124		125	Thin high cirrus.
69	142	−18.9876	7.6207	0947		0947	1038	1040		105	Clear with high haze.
70	142	−18.9871	7.6209				1043	1045		105	Clear with high haze.
71	142	−18.9869	7.6210				1050	1052	1054	110	Clear with high haze.
72	142	−18.9862	7.6211				1057	1100		160	Clear with high haze.
73	142	−18.9856	7.6216				1104	1106		105	Clear with high haze.
74	142	−18.9853	7.6220				1110	1113		135	Clear with high haze.
75	142	−18.9852	7.6222				1118	1121		125	Clear with high haze.
76[1]	143	−20.1479	11.5644	0959	0959	0959	1042	1044		100	Clear with high haze.
77[1]	143	−20.2589	11.9183	1251		1251	1352	1354		125	Clear with high haze; cloud at end.
78[1]	143	−20.2592	11.9177				1405	1407		100	Cloud edges throughout cast.
79[1]	143	−20.2595	11.9177				1410	1412	1415	130	Clear with high haze.
80[1]	143	−20.2598	11.9171				1418	1420		130	Clear with high haze.
81	144	−20.9998	15.1507		1254	1254	1314	1316	1254	110	Clear with high haze.
82	144	−20.9997	15.1509				1320	1322		115	Clear with high haze.
83	144	−20.9995	15.1510				1326	1327		100	Clear with high haze.
84[1]	146	−21.0071	22.9115	0956	0956	0956	1044	1046		125	Clear with thin cirrus.
85[1]	146	−21.0074	22.9123				1058	1058	1103	130	Clear with thin cirrus.
86[1]	146	−21.0079	22.9123				1106	1108		110	Clear with thin cirrus.
87[1]	146	−21.0081	22.9129				1114	1117		150	Clear with thin cirrus.
88[1]	147	−21.8056	26.6933	0931	0931	0931	1046	1049		155	Clear.
89[1]	147	−21.8046	26.6939				1053	1056	1058	150	Clear, cloud edge at end of cast.
90[1]	147	−21.8031	26.6943				1104	1107		150	Clear.
91[1]	147	−21.8020	26.6951				1112	1116		210	Clear.
92[1]	148	−21.5607	30.4769		0955	0955	1034	1047		150	Overcast with slow brightening.
93[1]	148	−21.5608	30.4776				1046	1049	1051	160	Overcast with brightening.
94[1]	148	−21.5601	30.4804				1101	1103		155	Overcast.
95[1]	148	−21.5602	30.4820				1108	1111		155	Overcast.
96	149	−20.7876	34.3650	1010		1010	1050	1053	1055	165	Clear.
97	149	−20.7874	34.3635				1101	1104		160	Clear, cloud edge in middle of cast.
98	149	−20.7883	34.3630				1112	1114		100	Clear, cloud in middle of cast.
99	150	−20.0144	38.1779	1010		1010	1035	1037	1039	120	Clear.
100	151	−20.0000	42.0021	1011		1011	1045	1048	1051	125	Overcast.
101	151	−19.9996	42.0033				1053	1056		130	Overcast with slow brightening.
102	151	−19.9963	42.0075				1121	1123		100	Clear then cloudy.
103	151	−20.0079	42.2642			1228	1304	1307	1309	150	Clear, small cloud at end of cast.
104	151	−20.0064	42.2664				1315	1318		145	Clear.
105[1]	152	−19.9783	45.9438	0934	0934	0934	1015	1017		110	Clear with thin cirrus.
106[1]	152	−19.9788	45.9440				1024	1026	1025	125	Clear with thin cirrus.
107[1]	152	−19.9798	45.9445				1032	1034		130	Clear with thin cirrus.
108[1]	152	−19.9802	45.9453				1039	1041		140	Clear with thin cirrus.
109[1]	152	−19.9812	45.9459				1045	1048		130	Clear with thin cirrus.
110	153	−14.7764	47.5429	1443		1443	1524	1525		75	Cloudy, bright at end of cast.

Table B1. (cont.) A summary of the SeaFALLS (SF), SeaBOSS (SB), and DalBOSS (DB) Deployment Log for the SDY during SeaBOARR-99 with all times reported in GMT (SDY 123 is 3 May and SDY 156 is 5 June).

Cast		*Position*		*Darks*			*Cast*		*CCD*	*Depth*	*Sky Conditions*
No.	*SDY*	*Longitude*	*Latitude*	*SB*	*DB*	*SF*	*Beg.*	*End*	*Pic.*	[m]	*Around the Sun*
111	153	−14.7785	47.5429				1535	1537		100	Cloudy.
112	153	−14.7799	47.5427				1541	1543		110	Cloudy.
113	154	−9.6649	48.1488	1053		1053	1107	1109		130	Clear.
114	154	−9.6650	48.1488				1113	1115		85	Clear, cloud at end of cast.
115	154	−9.4229	48.2121			1319	1325	1326		75	Clear, cloud at end of cast.
116	154	−9.4265	48.2122				1334	1335		50	Clear, cloud at end of cast.
117	154	−9.4275	48.2122				1336	1337		55	Clear.
118[1]	154	−9.4288	48.2121		1327		1339	1340		75	Clear.
119[1]	154	−9.4303	48.2123				1343	1344		75	Clear.
120	154	−9.4340	48.2114				1354	1355		65	Clear.
121	154	−9.4347	48.2113				1357	1358		75	Clear.
122	154	−9.2356	48.2542	1451		1451	1506	1508		65	Clear with thin cirrus.
123	154	−9.2366	48.2546				1510	1511		60	Clear with thin cirrus.
124	154	−9.2376	48.2552				1514	1515		55	Clear with thin cirrus.
125	154	−9.2382	48.2553				1517	1518	1519	65	Clear with thin cirrus.
126	154	−9.2391	48.2555				1521	1522		60	Clear with thin cirrus.
127	154	−9.2398	48.2556				1524	1525		55	Clear with thin cirrus.
128	154	−9.2417	48.2564				1532	1534		65	Clear with thin cirrus.
129	154	−9.2429	48.2569				1536	1537		70	Clear with thin cirrus.
130	154	−9.2446	48.2576				1540	1541		65	Clear with thin cirrus, cloud at end.
131[2]	155	−8.8705	49.0310	1453		1453	1509	1512	1506	70	Overcast with slow darkening.
132[2]	155	−8.8712	49.0310				1512	1515		65	Overcast with slow brightening.
133[2]	155	−8.8723	49.0311				1517	1520		65	Overcast, slow darkening, light rain.
134	156	−4.4468	49.7004	0922		0922	0935	0936		55	Overcast.
135	156	−4.4449	49.6994				0939	0940		55	Overcast.
136	156	−4.4433	49.6990				0942	0943	0945	60	Overcast.
137	156	−4.4344	49.6973				1004	1004		60	Clear.
138	156	−4.4330	49.6967				1008	1009		65	Clear.
139	156	−4.4303	49.6955				1016	1017		35	Clear, cloud at end of cast.
140	156	−4.4285	49.6950				1022	1023		55	Overcast.
141	156	−4.4258	49.6939				1030	1031		60	Overcast.

[1] Indicates simultaneous measurements with DalBOSS–all other casts are for SeaBOSS and SeaFALLS only.
[2] Indicates sampling in a coccolithophore bloom.

Table C1. The SeaBOARR-99 LoCNESS Log with all times reported in GMT.

Cast		*Position*		*Darks*		*Cast*		*CCD*	*Depth*	*Sky Conditions*
No.	*SDY*	*Longitude*	*Latitude*	*Ref.*	*Pro.*	*Beg.*	*End*	*Pic.*	[m]	*Around the Sun*
1	125	−42.2701	−30.7339	1512	1512	1553	1555		135	Mostly cloudy with brightening.
2	125	−42.2723	−30.7336			1613	1615		140	Overcast cloudy with brightening.
3	125	−42.2859	−30.7289			1714	1716		130	Overcast with some brightening.
4	128	−29.5651	−24.5547	1410	1410	1513	1516		160	Partly cloudy, cirrus in front of sun.
5	128	−29.5669	−24.5540			1522	1524		160	Partly cloudy, cirrus in front of sun.
6	128	−29.5686	−24.5537			1530	1533	1537	145	Partly cloudy, cirrus in front of sun.
7	129	−25.8268	−22.2244	1434	1434	1444	1446		150	Clear.
8	129	−25.8285	−22.2245			1453	1455	1458	160	Clear.
9	129	−25.8295	−22.2247			1501	1503		160	Clear.
10	130	−23.0392	−18.9922	1346	1346	1414	1417		170	Clear.
11	130	−23.0411	−18.9916			1418	1431		165	Clear.
12	130	−23.0439	−18.9909			1436	1439		160	Clear.
13	131	−20.5361	−16.0447	1159	1159	1215	1218		180	Clear.
14	131	−20.5371	−16.0444			1224	1226		160	Cloudy, sun at end of cast.
15	131	−20.3917	−15.8631		1355	1417	1419		120	Cloudy, sun at end of cast.
16	131	−20.3925	−15.8621			1423	1426		160	Clear.
17	131	−20.3933	−15.8614			1431	1434	1436	180	Clear.

Table C1. (cont.) The SeaBOARR-99 LoCNESS Log with all times reported in GMT.

Cast		*Position*		*Darks*		*Cast*		*CCD*	*Depth*	*Sky Conditions*
No.	*SDY*	*Longitude*	*Latitude*	*Ref.*	*Pro.*	*Beg.*	*End*	*Pic.*	[m]	*Around the Sun*
18	132	−17.9123	−12.8890	1305	1305	1338	1341		125	Clear.
19	132	−17.9147	−12.8882			1347	1350	1352	155	Clear.
20	132	−17.9221	−12.8848			1409	1411		100	Clear.
21	133	−15.2141	−9.6051	1249	1249	1307	1309		110	Clear.
22	133	−15.2173	−9.6036			1315	1318	1322	155	Clear.
23	133	−15.2198	−9.6031			1324	1326		140	Clear, small cloud in middle of cast.
24	138	−14.5101	−7.6387	1315	1315	1442	1444		100	Clear with thin cumulus.
25	139	−15.5310	−4.1196	1012	1012	1040	1042		130	Clear with high haze.
26	139	−15.5310	−4.1209			1051	1053		115	Clear with high haze; cloud at start.
27	139	−15.5309	−4.1210			1058	1101	1102	180	Clear with high haze.
28	139	−15.6181	−3.8713	1245	1245	1321	1322		105	Cirrus.
29	139	−15.6197	−3.8727			1327	1329		105	Cirrus.
30	139	−15.6211	−3.8738			1332	1334		105	Cirrus.
31	140	−16.7110	−0.0751	0954	0954	1038	1041		110	Thin high cumulus; cloud in middle.
32	140	−16.7098	−0.0741			1048	1050		120	Thin high cumulus.
33	140	−16.7087	−0.0735			1056	1059	1118	105	Thin high cumulus; cloud in middle.
34	140	−16.8019	0.2418		1336	1344	1346	1319	100	Thin high cirrus.
35	141	−18.0118	4.3128	1340	1340	1403	1405		125	Thin high cirrus.
36	141	−18.0128	4.3125			1413	1415		125	Thin high cirrus.
37	141	−18.0137	4.3121			1420	1423		140	Thin high cirrus.
38	141	−18.0147	4.3117			1428	1430	1433	125	Thin high cirrus.
39	142	−19.0523	7.8401	1205	1205	1251	1253		120	Clear with high haze.
40	142	−19.0508	7.8414			1258	1300		110	Clear with high haze.
41	142	−19.0492	7.8422			1305	1307	1308	115	Clear with high haze.
42	142	−19.0460	7.8440			1318	1320		115	Clear with high haze.
43	142	−19.0435	7.8445			1327	1329		125	Clear with high haze.
44	142	−19.0416	7.8450			1335	1337		130	Clear with high haze.
45[3]	144	−20.9987	15.1502	1001	1001	1053	1053		140	Clear with high haze.
46[3]	144	−20.9983	15.1503			1108	1110	1109	125	Clear with high haze.
47[3]	144	−20.9979	15.1502			1115	1117		125	Clear with high haze.
48[3]	144	−20.9997	15.1502		1223	1231	1234		130	Clear with high haze.
49[3]	144	−20.9996	15.1514			1239	1241		130	Clear with high haze.
50[3]	144	−20.9996	15.1514			1246	1248		125	Clear with high haze.
51[3]	144	−20.9992	15.1511			1253	1255	1254	130	Clear with high haze.
52[3]	144	−20.9998	15.1507			1314	1316		115	Clear with high haze.
53[3]	144	−20.9997	15.1509			1320	1322		110	Clear with high haze.
54[3]	144	−20.9995	15.1510			1326	1327		100	Clear with high haze.
55[3]	144	−20.9998	15.1511			1337	1339		100	Clear with high haze.
56[3]	144	−21.0003	15.1511			1343	1345		105	Clear with high haze.
57[3]	145	−20.9995	18.8022	0945	0945	1036	1038		100	Cloudy.
58[3]	145	−20.9991	18.8027			1043	1045	1051	100	Cloudy.
59[3]	145	−20.9982	18.8038			1059	1101		100	Clear then cloudy.
60[3]	145	−20.9971	18.8064			1117	1118		70	Clear then cloudy.
61[3]	145	−20.9971	19.3092			1407	1409		125	Cloudy with a little brightening.
62[3]	145	−20.9956	19.3105			1422	1424	1427	95	Clear then cloudy.
63[3]	145	−20.9943	19.3123			1428	1430		125	Cloudy with some brightening.
64[3]	145	−20.9939	19.3132			1436	1438		125	Cloudy with a little brightening.
65[3]	145	−20.9918	19.3154			1450	1451		100	Clear then cloudy.
66	146	−21.0686	23.2769	1239	1239	1333	1335		120	Clear.
67	146	−21.0709	23.2757			1338	1340	1346	110	Clear.
68	146	−21.0735	23.2741			1349	1352		130	Clear.
69	146	−21.0761	23.2725			1357	1359		145	Clear.
70	147	−21.8722	27.0508	1301	1301	1339	1342		155	Clear with thin cirrus.
71	147	−21.8741	27.0505			1349	1352	1354	155	Clear with thin cirrus.
72	147	−21.8759	27.0505			1405	1407		165	Clear with thin cirrus.
73	147	−21.8775	27.0505			1415	1418		180	Clear with thin cirrus.

Table C1. (cont.) The SeaBOARR-99 LoCNESS Log with all times reported in GMT.

Cast		*Position*		*Darks*		*Cast*		*CCD*	*Depth*	*Sky Conditions*
No.	*SDY*	*Longitude*	*Latitude*	*Ref.*	*Pro.*	*Beg.*	*End*	*Pic.*	[m]	*Around the Sun*
74	147	−21.8813	27.0504			1425	1428		150	Clear with thin cirrus.
75	147	−21.8835	27.0504			1432	1435		130	Clear with thin cirrus.
76	148	−21.4981	30.9547	1334	1334	1409	1412	1407	160	Overcast.
77	148	−21.4998	30.9542			1418	1421		155	Overcast with brightening at end.
78	148	−21.5008	30.9538			1425	1428		155	Overcast with slow brightening.
79	149	−20.6916	34.5498	1236	1236	1306	1308		155	Clear, cloud edges in middle of cast.
80	149	−20.6921	34.5504			1314	1316		90	Clear, cloud in middle of cast.
81	149	−20.6923	34.5503			1320	1323		140	Clear.
82	149	−20.6924	34.5503			1326	1329		175	Clear.
83	150	−20.0042	38.6417	1350	1350	1405	1408		155	Overcast with slow brightening.
84	150	−20.0060	38.6423			1413	1415	1419	155	Overcast with slow brightening.
85	150	−20.0072	38.6435			1425	1429		165	Clear with thin cumulus.
86	150	−20.0075	38.6442			1434	1437		175	Clear with thin cumulus.
87	152	−20.0039	46.3761	1302	1302	1333	1335		110	Clear with thin cirrus.
88	152	−20.0030	46.3740			1342	1345		95	Clear with cirrus.
89	152	−20.0025	46.3728			1348	1350		115	Cirrus and thin cumulus.
90	152	−20.0027	46.3709			1356	1357		100	Cloudy with brightening.
91	153	−15.6636	47.4543	1000	1000	1039	1041	1045	130	Overcast with slow brightening.
92	153	−15.6652	47.4552			1049	1051		110	Overcast.
93	153	−15.6661	47.4555			1054	1056		120	Overcast.
94	153	−15.6670	47.4561			1100	1102		120	Overcast.
95	153	−15.6685	47.4566			1107	1109		115	Overcast.
96	153	−15.6700	47.4574			1116	1118		100	Overcast.
97	154	−9.6645	48.1486	1022	1022	1051	1053		115	Clear.
98	154	−9.6647	48.1487			1103	1105		115	Clear.
99	154	−9.6648	48.1488			1108	1110	1111	100	Clear.
100	154	−9.6652	48.1487			1117	1118		75	Clear, cloud at end of cast.
101	154	−9.4086	48.2132		1232	1249	1249		75	Clear.
102	154	−9.4120	48.2132			1253	1254	1255	75	Clear.
103	154	−9.4143	48.2128			1258	1259		75	Clear.
104	154	−9.4156	48.2124			1302	1304		135	Clear.
105	154	−9.2356	48.2542		1451	1506	1508		65	Clear with thin cirrus.
106	154	−9.2366	48.2546			1510	1511		60	Clear with thin cirrus.
107	154	−9.2376	48.2552			1514	1515		55	Clear with thin cirrus.
108	154	−9.2382	48.2553			1517	1518	1519	65	Clear with thin cirrus.
109	154	−9.2391	48.2555			1521	1522		60	Clear with thin cirrus.
110	154	−9.2398	48.2556			1524	1525		55	Clear with thin cirrus.
111	154	−9.2417	48.2564			1532	1534		65	Clear with thin cirrus.
112	154	−9.2429	48.2569			1536	1537		70	Clear with thin cirrus.
113	154	−9.2446	48.2576			1540	1541		65	Clear with thin cirrus, cloud at end.
114 [2]	155	−9.2503	48.9774	1029	1029	1052	1055		100	Cirrus.
115 [2]	155	−9.2506	48.9760			1059	1102	1105	100	Cirrus.
116 [2]	155	−9.2508	48.9749			1106	1107		90	Cirrus, cloud edges at end of cast.
117 [2]	155	−9.2531	48.9721			1116	1118		90	Cirrus.
118 [2]	155	−9.2535	48.9708			1121	1123		100	Cirrus.
119 [2]	155	−9.1804	48.9836		1239	1254	1256		100	Overcast.
120 [2]	155	−9.1830	48.9833			1307	1309	1310	100	Overcast with brightening.
121 [2]	155	−9.1848	48.9831			1312	1313		75	Overcast with darkening.
122 [2]	155	−9.1860	48.9832			1315	1317		100	Overcast.
123 [2]	155	−9.1890	48.9824			1321	1322		100	Overcast; very small amount of rain.

[2] Indicates sampling in a coccolithophore bloom.
[3] Indicates the E_d and E_u heads were inadvertently switched.

Table D1. The SeaBOARR-99 SeaSAS Log with all times reported in GMT.

Cast		Position		Darks		Cast		CCD	L_i	Stability			Sky Conditions
No.	SDY	Longitude	Latitude	Ref.	Rad.	Beg.	End	Pic.	Views	L_i	L_T	E_d^+	Around the Sun
1	128	−29.5651	−24.5547	1425	1425	1513	1516		Cloud	0	1	1	Clear.
2	128	−29.5668	−24.5540			1521	1524		Sky/Cloud	0	1	1	Clear.
3	128	−29.5686	−24.5537			1530	1533		Sky/Cloud	1	0	1	Clear.
4	129	−25.8171	−22.2290	1334	1334	1402	1402		No Data			0	Clear.
5	129	−25.8178	−22.2280			1407	1410		No Data			0	Clear.
6	129	−25.8182	−22.2277			1410	1413		No Data			0	Clear.
7	129	−25.8191	−22.2272			1416	1419		No Data			1	Clear.
8	129	−25.8201	−22.2267			1420	1423		No Data			0	Clear.
9	129	−25.8211	−22.2263			1423	1426		No Data			0	Clear.
10	129	−25.8267	−22.2244			1443	1446		Sky/Cloud	1	0	0	Clear, some cirrus.
11	129	−25.8276	−22.2244			1447	1450		Sky	1	1	0	Clear.
12	129	−25.8285	−22.2245			1453	1456	1458	Sky/Cloud	2	0	0	Clear.
13	129	−25.8289	−22.2245			1456	1459		Sky/Cloud	0	1	0	Clear.
14	129	−25.8294	−22.2247			1500	1503		Cloud	2	2	1	Clear.
15	129	−25.8300	−22.2246			1504	1507		Sky/Cloud	1	1	1	Clear.
16	130	−23.2209	−19.2100	1124	1124	1145	1148		Sky	0	1	0	Clear.
17	130	−23.2211	−19.2096			1149	1152		Sky	2	1	1	Clear.
18	130	−23.2212	−19.2093			1153	1156		Sky	2	1	0	Clear.
19	130	−23.2216	−19.2090			1202	1205		Sky	1	1	0	Clear.
20	130	−23.2219	−19.2084			1208	1211		Bad Data	1	1	0	Clear (ship moved).
21	130	−23.2232	−19.2062			1213	1216		Sky	0	1	0	Clear.
22	130	−23.2248	−19.2042			1218	1221	1219	Sky	0	1	1	Clear.
23	130	−23.0388	−18.9923			1413	1413		Sky	0	1	0	Clear.
24	130	−23.0398	−18.9921			1417	1420		Sky/Cloud	1	2	2	Clear, cloud at end.
25	130	−23.0420	−18.9915			1427	1430		Sky	0	1	0	Clear.
26	130	−23.0437	−18.9909			1435	1438		Sky	1	1	0	Clear.
27	130	−23.0467	−18.9903			1449	1452		Sky	1	1	0	Clear.
28	130	−23.0477	−18.9902			1454	1458		Sky	0	1	1	Clear.
29	130	−23.0484	−18.9900			1459	1502		Sky/Cloud	1	1	1	Clear.
30	130	−23.0491	−18.9898			1503	1506		Cloud	2	1	1	Clear.
31	130	−23.0508	−18.9891			1513	1516		Sky	0	0	1	Clear.
32	130	−23.0514	−18.9889			1517	1520		Sky/Cloud	1	1	1	Clear.
33	130	−23.0543	−18.9885			1535	1538	1539	Sky	0	1	0	Clear.
34	130	−23.0555	−18.9880			1544	1547		Sky	0	1	0	Clear.
35	130	−23.0567	−18.9876			1550	1553		Sky	0	0	0	Clear.
36	130	−23.0577	−18.9876			1555	1558		Sky/Cloud	2	1	0	Clear.
37	130	−23.0590	−18.9872			1602	1605		Sky/Cloud	2	1	1	Clear, cloud at end.
38	131	−20.5361	−16.0447	1151	1151	1215	1218		Sky/Cloud	2	1	2	Clear.
39	131	−20.5365	−16.0446			1219	1222		Sky/Cloud	2	1	2	Clear, small cloud at end.
40	131	−20.5370	−16.0444			1223	1226		Sky/Cloud	2	1	1	Cloudy, sun at end.
41	131	−20.5371	−16.0446			1227	1227		Cloud	2	1	1	Clear.
42	131	−20.3917	−15.8630			1417	1420		Sky	0	1	1	Cloudy, sun at end.
43	131	−20.3923	−15.8622			1422	1425		Sky	0	1	0	Clear.
44	131	−20.3929	−15.8617			1426	1429		Sky	0	0	0	Clear.
45	131	−20.3933	−15.8614			1431	1434		Sky	0	0	0	Clear.
46	131	−20.3937	−15.8614			1435	1438	1436	Sky	0	0	0	Clear.
47	131	−20.3960	−15.8576			1500	1503		Sky	0	1	1	Clear.
48	131	−20.3965	−15.8568			1504	1507		Sky	0	0	0	Clear.
49	131	−20.3995	−15.8540			1526	1529		Sky	0	0	0	Clear.
50	131	−20.4001	−15.8536			1531	1534		Sky	0	1	1	Clear, cloud at end.
51	131	−20.4010	−15.8527			1538	1541		Sky	1	0	1	Clear.
52	131	−20.4014	−15.8523			1542	1545		Sky	1	0	0	Clear.
53	132	−18.1270	−13.1682	1000	1000	1055	1058		Sky/Cloud	1	1	1	Clear.
54	132	−18.1273	−13.1679			1059	1102		Sky	0	0	0	Clear.
55	132	−18.1283	−13.1661			1105	1108		Sky	1	1	0	Clear.
56	132	−18.1294	−13.1648			1109	1112	1110	Sky	0	1	0	Clear.

Table D1. (cont.) The SeaBOARR-99 SeaSAS Log with all times reported in GMT.

Cast		*Position*		*Darks*		*Cast*		*CCD*	L_i	*Stability*			*Sky Conditions*
No.	*SDY*	*Longitude*	*Latitude*	*Ref.*	*Rad.*	*Beg.*	*End*	*Pic.*	*Views*	L_i	L_T	E_d^+	*Around the Sun*
57	132	−18.1337	−13.1615			1124	1127		Sky	0	0	0	Clear.
58	132	−18.1355	−13.1604			1131	1134		Sky	0	1	1	Clear.
59	132	−17.9123	−12.8890			1338	1341		Sky	0	1	0	Clear.
60	132	−17.9132	−12.8886			1341	1344		Sky	0	1	0	Clear.
61	132	−17.9147	−12.8882			1347	1350		Sky	0	1	0	Clear.
62	132	−17.9154	−12.8879			1350	1353	1352	Sky	0	1	0	Clear.
63	132	−17.9223	−12.8847			1409	1412		Sky/Cloud	2	2	1	Cloudy, then clear.
64	133	−15.4025	−9.8587	0954	0954	1042	1045		Sky/Cloud	1	1	1	Clear, cloud at end.
65	133	−15.4032	−9.8588			1047	1050		Sky	1	2	2	Clear, then cloudy.
66	133	−15.4042	−9.8585			1053	1056	1058	Sky	1	1	1	Clear, cloud edge at end.
67	133	−15.4049	−9.8582			1057	1100		Sky	0	0	0	Clear, cloud edge at end.
68	133	−15.4065	−9.8574			1104	1107		Sky	1	1	0	Clear.
69	133	−15.4076	−9.8564			1108	1111		Sky/Cloud	1	2	1	Clear, small cloud in middle.
70	133	−15.2138	−9.6052			1306	1309		Sky	0	1	0	Clear.
71	133	−15.2156	−9.6041			1310	1313		Sky	0	1	0	Clear.
72	133	−15.2173	−9.6036			1315	1318		Sky	1	1	1	Clear.
73	133	−15.2188	−9.6034			1320	1323	1322	Sky	0	1	0	Clear.
74	133	−15.2200	−9.6030			1324	1327		Sky	1	1	0	Clear, small cloud in middle.
75	133	−15.2210	−9.6027			1327	1330		Sky/Cloud	1	1	0	Clear.
76[4]	133	−15.2313	−9.5920			1345	1348		Sky	0	1	1	Clear.
77[4]	133	−15.2339	−9.5871			1349	1352		Sky/Cloud	2	2	1	Clear.
78[4]	133	−15.2370	−9.5678			1402	1405		Sky	0	0	1	Clear.
79[4]	133	−15.2394	−9.5643			1405	1408		Sky	1	1	0	Clear.
80[4]	133	−15.2427	−9.5594			1409	1412		Sky	0	1	0	Clear.
81[4]	133	−15.2452	−9.5557			1412	1415		Sky	0	1	0	Clear.
82	139	−15.5310	−4.1195	1013	1013	1039	1042		Sky/Cloud	1	2	1	High haze.
83	139	−15.5314	−4.1197			1043	1046		Sky/Cloud	2	1	2	High haze, small clouds.
84	139	−15.5310	−4.1208			1050	1053		Sky/Cloud	2	2	1	High haze, cloud edges at start.
85	139	−15.5308	−4.1209			1054	1057		Cloud	1	1	1	High haze.
86	139	−15.5309	−4.1209			1057	1100	1102	Sky/Cloud	2	1	1	High haze.
87	139	−15.6181	−3.8713			1320	1323		Sky/Cloud	1	2	1	Cirrus clouds.
88	139	−15.6199	−3.8728			1327	1330	1330	Sky	1	2	1	Cirrus clouds.
89	139	−15.6212	−3.8739			1332	1335		Sky	0	2	2	Cirrus clouds.
90	140	−16.7110	−0.0753	0950	0950	1037	1040		Cloud	2	2	2	Thin cumulus, cloud in middle.
91	140	−16.7097	−0.0740			1048	1051		Sky/Cloud	2	2	1	Thin cumulus.
92	140	−16.7087	−0.0735			1056	1059		Cloud	2	2	1	Thin cumulus, cloud in middle.
93	140	−16.7068	−0.0724			1109	1111	1118	Sky/Cloud	2	2	1	Thin cumulus, cloud at end.
94	140	−16.7995	0.2318			1311	1314		Sky/Cloud	1	2	0	Thin cirrus.
95	140	−16.7995	0.2328			1315	1318	1319	Sky/Cloud	1	0	0	Thin cirrus.
96	140	−16.7998	0.2348			1322	1325		Sky/Cloud	1	1	1	Thin cirrus, cloud at end.
97	140	−16.8000	0.2360			1326	1329		Sky/Cloud	2	1	2	Thin cirrus, cloud at end.
98	140	−16.8018	0.2417			1343	1346		Sky/Cloud	1	1	1	Thin cirrus.
99	140	−16.8046	0.2440			1350	1353		Cloud	1	1	1	Thin cirrus, cloud in middle.
100	141	−17.8834	3.8994	0946	0946	1037	1040		Sky/Cloud	2	1	1	Thin cirrus.
101	141	−17.8834	3.8996			1041	1044		Sky/Cloud	1	0	0	Thin cirrus.
102	141	−17.8833	3.9001			1047	1050		Sky/Haze	0	1	0	Thin cirrus.
103	141	−17.8833	3.9003			1051	1054		Sky/Haze	0	0	0	Thin cirrus.
104	141	−17.8835	3.9006			1055	1058		Sky/Haze	0	1	1	Thin cirrus.
105	141	−17.8836	3.9012			1059	1102	1108	Sky/Cloud	0	0	1	Thin cirrus clouds.
106	141	−17.8839	3.9022			1108	1111		Sky/Cloud	2	1	1	Cloudy, brightening in middle.
107[5]	141	−17.8839	3.9026			1115	1118		Sky/Cloud	1	1	0	Thin cirrus.
108[5]	141	−17.8838	3.9027			1118	1121		Sky	0	0	0	Thin cirrus.
109[5]	141	−17.8838	3.9028			1121	1124		Sky/Cloud	1	1	0	Thin cirrus.
110[5]	141	−17.8838	3.9030			1125	1128		Sky/Cloud	1	1	0	Thin cirrus.
111[5]	141	−17.8837	3.9032			1129	1132		Sky/Cloud	1	1	0	Thin cirrus.
112[5]	141	−17.8837	3.9034			1132	1135		Sky/Haze	1	2	1	Thin cirrus.

Table D1. (cont.) The SeaBOARR-99 SeaSAS Log with all times reported in GMT.

Cast No.	SDY	Position Longitude	Latitude	Darks Ref.	Rad.	Cast Beg.	End	CCD Pic.	L_i Views	Stability L_i	L_T	E_d^+	Sky Conditions Around the Sun
113[5]	141	−17.8837	3.9038			1136	1139		Sky/Cloud	0	2	0	Thin cirrus.
114[5]	141	−18.0119	4.3128			1403	1406		Sky	0	0	1	Thin cirrus.
115[5]	141	−18.0121	4.3126			1406	1409		Sky	0	0	0	Thin cirrus.
116[5]	141	−18.0124	4.3126			1409	1412		Sky	0	1	0	Thin cirrus.
117[5]	141	−18.0128	4.3125			1413	1416		Sky	0	1	1	Thin cirrus.
118[5]	141	−18.0133	4.3123			1417	1420		Sky	0	1	1	Thin cirrus.
119[5]	141	−18.0137	4.3121			1420	1423		Sky	0	1	1	Thin cirrus.
120[5]	141	−18.0143	4.3119			1424	1427		Sky	0	0	1	Thin cirrus.
121[5]	141	−18.0148	4.3116			1428	1431		Sky/Haze	0	1	1	Thin cirrus.
122[5]	141	−18.0152	4.3114			1432	1435	1433	Sky/Haze	0	0	1	Thin cirrus.
123[5]	141	−18.0152	4.3110			1436	1439		Sky/Haze	0	0	0	Thin cirrus.
124[4]	141	−18.0188	4.3112			1446	1449		Sky/Haze	0	1	1	Thin cirrus.
125[4]	141	−18.0242	4.3126			1450	1453		Sky/Haze	1	0	0	Thin cirrus.
126[4]	141	−18.0283	4.3137			1453	1456		Sky/Haze	1	0	1	Thin cirrus.
127	142	−18.9875	7.6207	0947	0947	1038	1041		Haze	0	0	0	High haze.
128	142	−18.9871	7.6209			1042	1045		Haze	0	0	1	High haze.
129	142	−18.9870	7.6210			1046	1049		Haze/Cloud	1	1	0	High haze; cloud edge at end.
130	142	−18.9870	7.6210			1049	1052		Haze/Cloud	1	0	1	High haze.
131	142	−18.9868	7.6210			1053	1056	1054	Haze/Cloud	0	0	0	High haze.
132	142	−18.9864	7.6211			1056	1059		Haze/Cloud	0	0	0	High haze.
133[5]	142	−18.9856	7.6216			1103	1106		Haze	0	0	0	High haze.
134[5]	142	−18.9855	7.6219			1107	1110		Haze	0	1	0	High haze.
135[5]	142	−18.9853	7.6220			1110	1113		Haze	0	1	1	High haze.
136[5]	142	−18.9853	7.6220			1113	1116		Haze	1	1	1	High haze.
137[5]	142	−18.9852	7.6222			1118	1121		Haze/Cloud	2	2	0	High haze.
138[5]	142	−18.9850	7.6222			1121	1124		Haze/Cloud	1	2	0	High haze.
139[5]	142	−18.9848	7.6222			1124	1127		Haze	2	2	0	High haze.
140	142	−19.0524	7.8400			1250	1253		Haze	0	0	0	High haze.
141	142	−19.0516	7.8409			1254	1257		Haze	0	0	0	High haze.
142	142	−19.0510	7.8413			1257	1300		Haze	0	0	0	High haze.
143	142	−19.0500	7.8419			1301	1304		Haze	0	1	0	High haze.
144	142	−19.0493	7.8421			1304	1307		Haze/Cloud	0	0	0	High haze.
145	142	−19.0483	7.8426			1308	1311	1308	Haze/Cloud	0	0	0	High haze.
146[6]	142	−19.0459	7.8440			1318	1321		Haze	2	2	0	High haze.
147[6]	142	−19.0448	7.8442			1322	1325		Haze	1	1	0	High haze.
148[6]	142	−19.0437	7.8445			1326	1329		Haze	1	0	0	High haze.
149[6]	142	−19.0425	7.8448			1330	1333		Haze	1	0	0	High haze.
150[6]	142	−19.0416	7.8450			1334	1337		Cloud	0	1	0	High haze.
151[6]	142	−19.0413	7.8453			1338	1341		Haze/Cloud	1	0	0	High haze.
152[6]	142	−19.0415	7.8454			1342	1345		Haze/Cloud	0	1	1	High haze.
153	143	−20.1479	11.5645	0954	0954	1042	1045		Haze	1	0	1	High haze.
154	143	−20.1476	11.5646			1045	1048		Haze	1	1	1	High haze, cloudy at end.
155[4]	143	−20.2542	11.8745			1302	1305		Haze	2	2	1	High haze, cloudy at end.
156[4]	143	−20.2526	11.8839			1309	1312		Sky/Haze	1	0	1	High haze, cloud edge in middle.
157[4]	143	−20.2515	11.8907			1314	1317		Haze/Cloud	2	1	1	High haze, cloud edges in middle.
158[4]	143	−20.2559	11.9078			1324	1327		Haze/Cloud	2	2	2	High haze, cloudy at end.
159	143	−20.2589	11.9183			1352	1355		Haze/Cloud	1	0	1	High haze; cloud edges at end of.
160	143	−20.2593	11.9178			1405	1408		Haze/Cloud	2	1	2	Cloud edges for entire cast.
161	143	−20.2595	11.9177			1410	1413		Haze/Cloud	1	1	1	High haze.
162	143	−20.2597	11.9175			1413	1416	1415	Haze	0	0	1	High haze.
163	143	−20.2598	11.9171			1418	1421		Haze/Cloud	1	1	1	High haze.
164	143	−20.2601	11.9170			1422	1425		Haze	0	0	0	High haze.
165	144	−20.9986	15.1502	1001	1001	1053	1056		Sky/Haze	0	1	0	High haze.
166	144	−20.9984	15.1502			1056	1059		Sky/Haze	0	2	0	High haze.
167	144	−20.9986	15.1501			1101	1104		Sky/Haze	1	1	0	High haze.
168	144	−20.9986	15.1501			1104	1107		Sky/Haze	0	1	0	High haze.

Table D1. (cont.) The SeaBOARR-99 SeaSAS Log with all times reported in GMT.

Cast No.	SDY	Position Longitude	Latitude	Darks Ref.	Rad.	Cast Beg.	End	CCD Pic.	L_i Views	Stability L_i	L_T	E_d^+	Sky Conditions Around the Sun
169	144	−20.9984	15.1502			1107	1110	1109	Sky/Haze	0	1	0	High haze.
170	144	−20.9980	15.1503			1111	1114		Sky/Haze	0	1	0	High haze.
171	144	−20.9979	15.1502			1115	1118		Sky/Haze	0	1	0	High haze.
172	144	−20.9978	15.1501			1118	1121		Sky/Haze	0	1	0	High haze.
173	144	−20.9977	15.1502			1122	1124		Sky/Haze	0	2	0	High haze.
174	144	−20.9977	15.1496			1126	1129		Sky/Haze	0	2	0	High haze.
175[5]	144	−20.9997	15.1502			1231	1234		Sky/Haze	1	2	0	High haze.
176[5]	144	−20.9994	15.1507			1234	1237		Sky/Haze	0	2	0	High haze.
177[5]	144	−20.9996	15.1513			1238	1241		Sky/Haze	1	1	0	High haze.
178[5]	144	−20.9997	15.1515			1242	1245		Sky/Haze	0	1	0	High haze.
179[5]	144	−20.9996	15.1514			1246	1249		Sky/Haze	0	1	0	High haze.
180[5]	144	−20.9994	15.1510			1249	1252		Sky/Haze	0	2	0	High haze.
181[5]	144	−20.9992	15.1510			1253	1256	1254	Sky/Haze	0	2	0	High haze.
182	144	−20.9998	15.1508			1314	1317		Sky/Haze	0	1	0	High haze.
183	144	−20.9997	15.1509			1320	1323		Sky/Haze	0	1	0	High haze.
184	144	−20.9995	15.1510			1325	1328		Sky/Haze	0	1	0	High haze.
185	144	−20.9999	15.1511			1337	1340		Sky/Haze	0	1	0	High haze.
186	144	−21.0001	15.1510			1340	1343		Sky/Haze	1	1	0	High haze.
187	144	−21.0003	15.1511			1343	1346		Sky/Haze	0	1	0	High haze.
188	144	−21.0006	15.1510			1347	1350		Sky/Haze	0	2	0	High haze.
189[4]	144	−21.0008	15.1546			1354	1357		Sky/Haze	0	2	0	High haze.
190[4]	144	−21.0006	15.1601			1358	1401		Sky/Haze	0	2	0	High haze.
191[4]	144	−21.0004	15.1642			1401	1404		Sky/Haze	0	2	0	High haze.
192	145	−20.9996	18.8022	0945	0945	1035	1038		Sky/Cloud	2	1	1	Cloudy.
193	145	−20.9992	18.8024			1039	1042		Cloud	2	1	1	Cloudy, brightening.
194	145	−20.9991	18.8026			1043	1046		Cloud	2	0	1	Cloudy.
195	145	−20.9989	18.8025			1047	1050	1051	Cloud	2	2	2	Cloudy, brightening.
196	145	−20.9982	18.8039			1059	1102		Sky/Cloud	1	2	1	Clear then cloudy.
197	145	−20.9979	18.8046			1103	1105		Sky/Cloud	2	2	1	Clear, cloudy, clear, cloudy.
198	145	−20.9973	18.8057			1113	1116		Sky/Cloud	1	1	1	Clear then cloudy.
199	145	−20.9970	18.8066			1117	1120		Cloud	1	2	2	Clear then cloudy.
200	145	−20.9970	19.3093			1407	1410		Cloud	2	1	1	Cloudy, a little brightening.
201	145	−20.9966	19.3099			1410	1413		Cloud	2	2	2	Cloudy, brightening.
202	145	−20.9955	19.3107			1422	1425	1427	Cloud	2	1	1	Clear then cloudy.
203	145	−20.9943	19.3124			1428	1431		Cloud	2	0	1	Clear, some brightening.
204	145	−20.9940	19.3129			1432	1435		Cloud	1	1	1	Cloudy, a little brightening.
205	145	−20.9938	19.3133			1436	1439		Cloud	2	0	1	Cloudy, a little brightening.
206	145	−20.9935	19.3136			1440	1443		Cloud	2	1	1	Cloudy then brightening at end.
207	145	−20.9918	19.3154			1449	1452		Sky/Cloud	1	2	2	Clear then cloudy at end.
208	146	−21.0071	22.9116	0954	0954	1044	1047		Sky/Cloud	1	1	1	Thin cirrus, cloud at end.
209	146	−21.0075	22.9122			1058	1101		Sky/Cloud	1	1	1	Thin cirrus.
210	146	−21.0077	22.9122			1101	1104	1103	Sky/Cloud	0	1	1	Thin cirrus.
211	146	−21.0079	22.9124			1106	1109		Sky/Cloud	0	1	1	Thin cirrus; cloud edge in middle.
212	146	−21.0080	22.9127			1111	1114		Sky/Cloud	1	1	1	Thin cirrus; cloud edge at end.
213	146	−21.0081	22.9129			1114	1117		Sky/Cloud	1	1	1	Thin cirrus.
214	146	−21.0684	23.2770			1332	1335		Sky	0	1	1	Clear.
215	146	−21.0711	23.2756			1338	1341	1346	Sky/Cloud	2	1	1	Clear.
216	146	−21.0735	23.2741			1349	1352		Sky	0	1	0	Clear.
217	146	−21.0748	23.2733			1353	1356		Sky	0	1	0	Clear.
218	146	−21.0759	23.2726			1356	1359		Sky	0	1	0	Clear.
219	146	−21.0776	23.2717			1400	1403		Sky	1	1	0	Clear.
220[4]	146	−21.0860	23.2701			1409	1412		Sky	0	1	0	Clear.
221[4]	146	−21.0924	23.2699			1412	1415		Sky	0	1	0	Clear.
222[4]	146	−21.0987	23.2697			1415	1418		Sky	0	1	0	Clear.
223[4]	146	−21.1116	23.2696			1422	1425		Sky	0	1	0	Clear.
224[4]	146	−21.1176	23.2694			1426	1429		Sky	0	1	0	Clear.

Table D1. (cont.) The SeaBOARR-99 SeaSAS Log with all times reported in GMT.

Cast No.	SDY	Position Longitude	Latitude	Darks Ref.	Rad.	Cast Beg.	End	CCD Pic.	L_i Views	Stability L_i	L_T	E_d^+	Sky Conditions Around the Sun
225[4]	146	−21.1221	23.2693			1429	1432		Sky	0	1	0	Clear.
226[4]	146	−21.1423	23.2707			1438	1441		Sky	0	1	0	Clear.
227[4]	146	−21.1504	23.2714			1441	1444		Sky	0	1	0	Clear.
228[4]	146	−21.1585	23.2722			1444	1447		Sky	0	1	0	Clear.
229[4]	146	−21.1760	23.2740			1450	1453		Sky	0	2	0	Clear.
230[4]	146	−21.1858	23.2751			1453	1456		Sky	0	2	0	Clear.
231[4]	146	−21.1990	23.2767			1457	1500		Sky	1	2	1	Clear, cloud edges at end.
232	147	−21.8057	26.6931	0928	0928	1045	1048		Sky/Cloud	2	0	0	Clear.
233	147	−21.8050	26.6935			1049	1052		Sky	0	0	0	Clear.
234	147	−21.8046	26.6939			1053	1056		Sky	0	0	1	Clear, cloud edge at end.
235	147	−21.8042	26.6939			1057	1100	1058	Sky/Cloud	1	0	1	Clear.
236	147	−21.8032	26.6942			1103	1106		Sky/Cloud	2	1	0	Clear.
237	147	−21.8021	26.6951			1112	1115		Sky/Cloud	1	0	1	Clear.
238	147	−21.8720	27.0508			1338	1341		Sky	1	0	0	Thin cirrus.
239	147	−21.8725	27.0507			1342	1345		Sky/Cloud	1	0	0	Thin cirrus.
240	147	−21.8741	27.0505			1349	1352		Sky/Cloud	1	0	0	Thin cirrus.
241	147	−21.8749	27.0505			1352	1355	1354	Sky/Cloud	1	0	1	Thin cirrus.
242[7]	147	−21.8758	27.0505			1404	1407		Sky/Cloud	2	0	1	Thin cirrus.
243[7]	147	−21.8762	27.0505			1409	1412		Sky/Cloud	2	1	1	Thin cirrus.
244[7]	147	−21.8772	27.0505			1414	1417		Sky/Cloud	1	1	1	Thin cirrus.
245[7]	147	−21.8813	27.0504			1425	1428		Sky	2	1	1	Thin cirrus.
246[7]	147	−21.8824	27.0504			1428	1431		Sky/Cloud	1	0	1	Thin cirrus.
247[7]	147	−21.8835	27.0504			1432	1435		Sky/Cloud	1	0	1	Thin cirrus.
248	147	−21.8860	27.0503			1442	1445		Sky/Cloud	1	0	0	Thin cirrus.
249	148	−21.5607	30.4764	0955	0955	1033	1036		Cloud	2	1	1	Overcast, slow brightening.
250	148	−21.5608	30.4768			1037	1040		Cloud	2	2	1	Overcast, some brightening.
251	148	−21.5606	30.4769			1041	1044		Cloud	2	1	1	Overcast, a little brightening.
252	148	−21.5608	30.4776			1046	1049		Cloud	1	2	1	Overcast, brightening.
253	148	−21.5605	30.4781			1050	1053	1051	Cloud	1	1	1	Overcast.
254	148	−21.5601	30.4805			1101	1104		Cloud	1	1	0	Overcast.
255	148	−21.5602	30.4812			1104	1107		Cloud	1	1	1	Overcast.
256	148	−21.5602	30.4820			1108	1111		Cloud	1	1	1	Overcast.
257	148	−21.5601	30.4826			1112	1115		Cloud	1	0	0	Overcast.
258[4]	148	−21.5586	30.4963			1124	1127		Cloud	1	2	1	Overcast.
259[4]	148	−21.5579	30.5039			1127	1130		Cloud	1	2	1	Overcast.
260[4]	148	−21.5570	30.5140			1131	1134		Cloud	1	2	1	Overcast, brightening.
261[4]	148	−21.5005	30.9293			1350	1353		Cloud	1	1	1	Overcast, darkening.
262[4]	148	−21.4995	30.9351			1353	1356		Cloud	1	2	2	Overcast, darkening.
263[4]	148	−21.4984	30.9409			1356	1359		Cloud	1	1	1	Overcast.
264[4]	148	−21.4971	30.9486			1400	1403	1407	Cloud	1	0	1	Overcast.
265	148	−21.4981	30.9547			1409	1412		Cloud	1	0	0	Overcast.
266	148	−21.4992	30.9544			1414	1417		Cloud	2	1	1	Overcast, brightening.
267	148	−21.4998	30.9542			1418	1421		Cloud	1	1	1	Overcast, brightening at end.
268	148	−21.5003	30.9540			1421	1424		Cloud	1	1	1	Overcast, slow brightening.
269	148	−21.5008	30.9538			1425	1428		Cloud	1	1	1	Overcast, slow brightening.
270	148	−21.5013	30.9535			1429	1432		Cloud	1	2	2	Overcast, darkening.
271[4]	148	−21.5086	30.9531			1439	1442		Cloud	1	0	0	Overcast.
272[4]	148	−21.5135	30.9531			1442	1445		Cloud	1	1	1	Overcast.
273[4]	148	−21.5199	30.9530			1446	1449		Cloud	2	1	1	Overcast.
274	149	−20.7876	34.3650	1010	1010	1050	1053		Sky	0	2	0	Clear.
275	149	−20.7877	34.3643			1054	1057	1055	Sky	0	2	0	Clear.
276	149	−20.7873	34.3635			1100	1103		Sky	1	2	1	Clear, cloud edge in middle.
277	149	−20.7877	34.3634			1104	1107		Sky	0	2	0	Clear.
278	149	−20.7883	34.3630			1112	1115		Sky/Cloud	2	2	2	Clear, cloud in middle.
279	149	−20.7886	34.3629			1115	1118		Sky/Cloud	1	2	1	Clear, cloud at end.
280	149	−20.6917	34.5497			1305	1308	1313	Sky/Cloud	2	2	1	Clear, cloud edges in middle.

Table D1. (cont.) The SeaBOARR-99 SeaSAS Log with all times reported in GMT.

Cast		*Position*		*Darks*		*Cast*		*CCD*	*L_i*	*Stability*			*Sky Conditions*
No.	*SDY*	*Longitude*	*Latitude*	*Ref.*	*Rad.*	*Beg.*	*End*	*Pic.*	*Views*	L_i	L_T	E_d^+	*Around the Sun*
281	149	−20.6922	34.5504			1314	1317		Sky/Cloud	1	1	1	Clear, cloud in middle.
282	149	−20.6923	34.5503			1320	1323		Sky/Cloud	1	1	1	Clear.
283	149	−20.6924	34.5503			1326	1329		Sky	0	1	0	Clear.
284	149	−20.6924	34.5502			1330	1333		Sky	0	1	1	Clear, cloud in middle.
285	150	−20.0143	38.1779			1010	1010	1037	Sky	1	1	1	Clear.
286	150	−20.0148	38.1773			1038	1041	1039	Sky/Cloud	2	1	1	Clear, small cloud in middle.
287	150	−20.0163	38.1753			1053	1056		Sky	0	1	1	Clear.
288	150	−20.0165	38.1747			1056	1059		Sky/Cloud	2	2	2	Clear.
289	150	−20.0177	38.1742			1103	1106		Cloud	1	1	1	Overcast, light rain.
290	150	−20.0042	38.6417			1405	1408		Sky/Cloud	2	1	1	Overcast, slow brightening.
291	150	−20.0048	38.6418			1408	1411		Sky/Cloud	1	1	1	Overcast, slow brightening.
292	150	−20.0061	38.6424			1413	1416	1419	Sky/Cloud	0	2	2	Overcast, slow brightening.
293	150	−20.0071	38.6435			1425	1428		Sky	0	1	0	Thin cumulus.
294	150	−20.0072	38.6438			1429	1432		Sky	0	1	0	Thin cumulus.
295	150	−20.0075	38.6442			1434	1437		Sky	0	1	0	Thin cumulus.
296	150	−20.0084	38.6452			1438	1441		Sky/Cloud	0	1	0	Thin cumulus.
297	151	−20.0001	42.0019	1011	1011	1042	1045		Cloud	2	1	1	Overcast.
298	151	−20.0000	42.0021			1045	1048		Cloud	2	1	1	Overcast.
299	151	−20.0000	42.0026			1049	1052	1051	Cloud	1	1	1	Overcast, slow brightening.
300	151	−20.0000	42.0026			1049	1052		Cloud	2	1	1	Overcast, slow brightening.
301	151	−19.9962	42.0076			1121	1124		Sky/Cloud	2	2	2	Clear then cloudy.
302	151	−20.0079	42.2642			1304	1307		Sky/Cloud	1	2	1	Clear, small cloud at end.
303	151	−20.0076	42.2643			1308	1311	1309	Sky/Cloud	1	2	1	Clear.
304	151	−20.0064	42.2664			1315	1318		Sky	1	2	1	Clear, small cloud in middle.
305	151	−20.0058	42.2672			1318	1321		Sky	1	2	1	Clear.
306	152	−19.9783	45.9438	0942	0942	1014	1017		Sky/Cloud	1	0	0	Thin cirrus.
307	152	−19.9784	45.9437			1018	1021		Sky/Cloud	1	0	0	Thin cirrus.
308	152	−19.9788	45.9440			1024	1027	1025	Sky/Cloud	0	0	1	Thin cirrus.
309	152	−19.9794	45.9442			1028	1031		Sky/Cloud	1	0	1	Thin cirrus.
310	152	−19.9798	45.9445			1031	1034		Sky/Cloud	1	0	0	Thin cirrus.
311	152	−19.9800	45.9450			1035	1038		Sky/Cloud	1	0	1	Thin cirrus.
312	152	−19.9803	45.9453			1039	1042		Sky/Cloud	1	1	0	Thin cirrus.
313	152	−19.9812	45.9459			1045	1048		Sky/Cloud	1	1	0	Thin cirrus.
314	152	−19.9818	45.9463			1054	1057		Cloud	1	1	0	Thin cirrus (a little prop wash).
315	152	−19.9814	45.9470			1058	1101		Cloud	1	1	1	Thin cirrus (prop wash at end).
316	152	−20.0039	46.3760			1333	1336		Sky/Cloud	1	1	1	Thin cirrus.
317	152	−20.0036	46.3752			1336	1339	1338	Sky/Cloud	2	1	2	Clear with cirrus.
318	152	−20.0030	46.3740			1342	1345		Cloud	1	1	1	Clear with cirrus.
319	152	−20.0025	46.3727			1348	1351		Cloud	2	1	2	Cirrus and thin cumulus.
320	152	−20.0027	46.3709			1355	1358		Sky/Cloud	2	2	1	Cloudy, brightening.
321	153	−15.6636	47.4542	1000	1000	1038	1041		Cloud	1	1	1	Overcast, slow brightening.
322	153	−15.6645	47.4546			1043	1046	1045	Cloud	1	1	1	Overcast, some brightening.
323	153	−15.6653	47.4552			1049	1052		Sky/Cloud	1	1	2	Overcast.
324	153	−15.6660	47.4555			1053	1056		Cloud	1	1	1	Overcast.
325	153	−15.6665	47.4558			1056	1059		Cloud	1	0	1	Overcast.
326	153	−15.6671	47.4561			1100	1103		Cloud	1	1	1	Overcast.
327	153	−15.6678	47.4563			1103	1106		Cloud	1	1	0	Overcast.
328	153	−15.6686	47.4566			1107	1110		Cloud	1	0	1	Overcast.
329	153	−15.6691	47.4569			1110	1113		Cloud	1	1	1	Overcast, slow brightening.
330	153	−15.6697	47.4572			1114	1117		Cloud	1	0	1	Overcast.
331	153	−14.7766	47.5429			1524	1527		Cloud	2	1	1	Cloudy, bright, cloudy, bright.
332	153	−14.7784	47.5429			1535	1535		Cloud	1	2	2	Cloudy.
333	153	−14.7801	47.5427			1541	1544		Cloud	2	1	1	Cloudy.
334	153	−14.7808	47.5424			1550	1553		Cloud	1	1	1	Cloudy (prop wash after 90 s).
335	154	−9.6645	48.1486	0909	1029	1051	1054		Sky	0	1	0	Clear.
336	154	−9.6647	48.1487			1102	1105		Sky/Cloud	1	1	1	Clear.

Table D1. (cont.) The SeaBOARR-99 SeaSAS Log with all times reported in GMT.

Cast No.	SDY	Position Longitude	Latitude	Darks Ref.	Rad.	Cast Beg.	End	CCD Pic.	L_i Views	Stability L_i	L_T	E_d^+	Sky Conditions Around the Sun
337	154	−9.6648	48.1488			1106	1109	1111	Sky	0	1	0	Clear.
338	154	−9.6650	48.1488			1113	1116		Cloud	2	1	2	Clear, cloud at end.
339	154	−9.6653	48.1487			1117	1120		Cloud	2	2	2	Clear, cloud at end.
340	154	−9.4098	48.2132			1249	1252		Sky/Cloud	0	1	1	Clear.
341	154	−9.4120	48.2132			1252	1255	1255	Sky	1	1	1	Clear.
342	154	−9.4147	48.2127			1258	1301		Sky/Cloud	1	2	1	Clear.
343	154	−9.4156	48.2125			1301	1304		Sky/Cloud	1	1	0	Clear.
344	154	−9.4165	48.2120			1305	1308		Sky	0	1	0	Clear.
345	154	−9.4181	48.2118			1309	1312		Sky	0	1	0	Clear.
346	154	−9.4233	48.2121			1325	1328		Sky/Cloud	2	2	1	Clear, cloud at end.
347	154	−9.4270	48.2122			1334	1337		Sky/Cloud	1	1	1	Clear, cloud at end.
348	154	−9.4284	48.2121			1337	1340		Sky/Cloud	1	1	0	Clear.
349	154	−9.4303	48.2123			1342	1345		Sky	0	2	0	Clear.
350	154	−9.4310	48.2122			1345	1348		Sky/Cloud	1	2	1	Clear, cloud edge in middle.
351	154	−9.4335	48.2115			1352	1355		Sky/Cloud	1	1	0	Clear.
352	154	−9.4347	48.2113			1356	1359		Sky	1	2	1	Clear.
353	154	−9.2358	48.2543			1506	1509		Sky	0	2	1	Thin cirrus.
354	154	−9.2366	48.2547			1509	1512		Sky	0	2	0	Thin cirrus.
355	154	−9.2375	48.2551			1513	1516		Sky	1	0	1	Thin cirrus.
356	154	−9.2385	48.2554			1517	1520	1519	Sky	1	0	0	Thin cirrus.
357	154	−9.2392	48.2555			1520	1523		Sky/Cloud	1	1	0	Thin cirrus.
358	154	−9.2400	48.2557			1524	1527		Sky/Cloud	1	1	1	Thin cirrus.
359	154	−9.2406	48.2560			1528	1531		Sky	1	0	1	Thin cirrus.
360	154	−9.2419	48.2565			1532	1535		Sky/Cloud	0	1	1	Thin cirrus.
361	154	−9.2433	48.2571			1536	1539		Sky	0	1	1	Thin cirrus.
362	154	−9.2446	48.2576			1539	1542		Sky/Cloud	1	1	2	Thin cirrus, cloud at end.
363[8]	155	−9.2503	48.9774	1021	1021	1052	1055		Cloud	1	2	2	Cirrus, cloud edges at end.
364[8]	155	−9.2506	48.9760			1059	1102	1105	Cloud	2	2	2	Cirrus, cloud edges in middle.
365[2]	155	−9.2509	48.9749			1105	1108		Cloud	2	2	2	Cirrus, cloud at end.
366[2]	155	−9.2531	48.9720			1116	1119		Cloud	2	2	2	Cirrus.
367[2]	155	−9.2534	48.9709			1120	1123		Cloud	1	2	1	Cirrus, a little brightening.
368[2]	155	−9.2539	48.9702			1123	1126		Cloud	1	2	2	Cirrus, a little darkening.
369[2]	155	−9.1805	48.9836			1254	1257		Cloud	1	2	2	Overcast.
370[2]	155	−9.1830	48.9833			1307	1309	1310	Cloud	1	1	1	Overcast, brightening.
371[2]	155	−9.1848	48.9831			1311	1314		Cloud	1	2	1	Overcast, darkening.
372[2]	155	−9.1860	48.9832			1315	1317		Cloud	2	1	1	Overcast.
373[2]	155	−9.1890	48.9824			1321	1322		Cloud	2	1	1	Overcast (very light rain).
374[2]	155	−9.1963	48.9802			1333	1336		Cloud	1	2	1	Overcast (prop wash after 90 s).
375[2]	155	−8.8705	49.0310			1509	1512	1506	Cloud	2	1	1	Overcast, slow darkening.
376[2]	155	−8.8712	49.0310			1512	1515		Cloud	1	1	1	Overcast, slow brightening.
377[2]	155	−8.8723	49.0311			1517	1520		Cloud	1	1	1	Overcast, darkening, very light rain.
378	156	−4.4464	49.7001	0913	0913	0935	0938		Cloud	1	0	1	Overcast.
379	156	−4.4443	49.6993			0939	0942		Cloud	2	1	1	Overcast.
380	156	−4.4428	49.6989			0942	0945	0945	Sky	2	1	1	Overcast.
381	156	−4.4344	49.6973			1004	1004		Sky/Cloud	0	1	1	Clear, cloud in middle.
382	156	−4.4326	49.6966			1008	1011		Sky/Cloud	1	1	1	Clear, cloud at end.
383	156	−4.4299	49.6955			1016	1019		Sky/Cloud	2	1	1	Clear, cloud in middle and end.
384	156	−4.4286	49.6950			1022	1022		Cloud	2	1	1	Overcast, brightening.
385	156	−4.4259	49.6940			1030	1030		Cloud	1	1	1	Overcast, darkening.

[2] Indicates sampling in a coccolithophore bloom.
[4] Indicates SeaSAS and SUnSAS underway experiments.
[5] Indicates SeaSAS azimuth pointing experiments.
[6] Indicates SeaSAS nadir- and zenith-viewing angle experiments.
[7] Indicates SeaSAS and SUnSAS nadir- and zenith-viewing angle experiments.
[8] Indicates SUnSAS underway experiments with T69 (L_i sensor) in place of T28 (L_p/L_T sensor).

Table E1. The SeaBOARR-99 SUnSAS Log with all times reported in GMT.

Cast		Position		Darks		Cast		CCD	L_i	L_T	Stability			Sky Conditions
No.	SDY	Longitude	Latitude	Ref.	Rad.	Beg.	End	Pic.	Views	Views	L_i	L_T	E_d^+	Around the Sun
1	129	−25.8173	−22.2287	1334	1329	1402	1405		Sky/Cloud	Water	1	1	0	Clear.
2	129	−25.8178	−22.2280			1407	1410		Sky/Cloud	Gray	1	0	0	Clear.
3	129	−25.8182	−22.2277			1410	1413		Sky/Cloud	Water	0	1	0	Clear.
4	129	−25.8191	−22.2272			1416	1419		Sky/Cloud	Gray	1	0	1	Clear.
5	129	−25.8201	−22.2267			1420	1423		Sky/Cloud	Water	1	1	0	Clear.
6	129	−25.8211	−22.2263			1423	1426		Sky/Cloud	Gray	1	0	0	Clear.
7	130	−23.2209	−19.2100	1124	1140	1145	1148		Sky/Cloud	Water	1	1	0	Clear.
8	130	−23.2211	−19.2096			1149	1152		Sky/Cloud	Gray	1	1	1	Clear.
9	130	−23.2212	−19.2093			1153	1156		Sky/Cloud	Water	1	1	0	Clear.
10	130	−23.2216	−19.2090			1202	1205		Sky/Cloud	Gray	2	1	1	Clear.
11	130	−23.2219	−19.2084			1208	1211		Bad Data	Water	2	2	0	Clear (ship moved).
12	130	−23.2232	−19.2062			1213	1216		Sky/Cloud	Water	0	1	0	Clear.
13	130	−23.2248	−19.2042			1218	1221	1219	Sky	Gray	0	0	1	Clear.
14	130	−23.0467	−18.9903			1449	1452		Sky/Cloud	Water	0	1	0	Clear.
15	130	−23.0476	−18.9902			1454	1457		Sky	Gray	1	0	1	Clear.
16	130	−23.0484	−18.9900			1459	1502		Sky	Water	0	1	1	Clear.
17	130	−23.0491	−18.9898			1503	1506		Sky	Gray	2	1	1	Clear.
18	130	−23.0508	−18.9891			1513	1516		Sky	Water	0	1	1	Clear.
19	130	−23.0514	−18.9889			1517	1520	1539	Sky	Gray	1	1	1	Clear.
20	131	−20.3960	−15.8576	1151	1442	1500	1503	1436	Sky	Water	0	1	1	Clear.
21	131	−20.3965	−15.8568			1504	1507		Sky	Gray	0	0	0	Clear.
22	131	−20.3995	−15.8540			1526	1529		Sky	Water	0	1	0	Clear.
23	131	−20.4001	−15.8536			1531	1534		Sky	Gray	1	1	1	Clear, cloud at end.
24	131	−20.4010	−15.8527			1538	1541		Sky	Water	1	1	1	Clear.
25	131	−20.4014	−15.8523			1542	1545		Sky/Cloud	Gray	1	1	0	Clear.
26	132	−18.1270	−13.1682	1000	1000	1055	1058		Sky/Cloud	Water	1	1	1	Clear.
27	132	−18.1273	−13.1679			1059	1102		Sky	Gray	1	0	0	Clear.
28	132	−18.1283	−13.1661			1105	1108		Sky	Water	1	0	0	Clear.
29	132	−18.1294	−13.1648			1109	1112	1110	Sky	Gray	0	1	0	Clear.
30	132	−18.1337	−13.1615			1124	1127		Sky/Cloud	Water	0	0	0	Clear.
31	132	−18.1355	−13.1604			1131	1134		Sky/Cloud	Gray	1	1	1	Clear.
32	133	−15.4025	−9.8587	0954	0954	1042	1045		Sky	Water	1	1	1	Clear, cloud at end.
33	133	−15.4032	−9.8588			1047	1050		Sky/Cloud	Gray	1	1	2	Clear, cloudy at end.
34	133	−15.4042	−9.8585			1053	1056		Sky/Cloud	Water	1	1	1	Clear, cloud edge at end.
35	133	−15.4049	−9.8582			1057	1100	1058	Sky	Gray	0	0	0	Clear, cloud edge at end.
36	133	−15.4065	−9.8574			1104	1107		Sky	Water	1	1	0	Clear.
37	133	−15.4076	−9.8564			1108	1111		Sky	Gray	1	1	1	Clear, small cloud in middle.
38[4]	133	−15.2313	−9.5920		1342	1345	1348		Sky/Cloud	Water	2	2	1	Clear.
39[4]	133	−15.2339	−9.5871			1349	1352		Sky/Cloud	Gray	2	0	1	Clear.
40[4]	133	−15.2370	−9.5678			1402	1405		Sky	Water	2	2	1	Clear.
41[4]	133	−15.2394	−9.5643			1405	1408		Sky	Gray	1	0	0	Clear.
42[4]	133	−15.2427	−9.5594			1409	1412		Sky	Water	0	2	0	Clear.
43[4]	133	−15.2452	−9.5557			1412	1415		Sky	Gray	1	0	0	Clear.
44	139	−15.5310	−4.1195	1012	1012	1039	1042		Cloud	Water	1	2	1	High haze.
45	139	−15.5314	−4.1197			1043	1046		Cloud	Water	2	1	2	High haze, small clouds.
46	139	−15.5310	−4.1208			1050	1053		Sky/Cloud	Water	2	1	1	High haze, cloud edges.
47	139	−15.5308	−4.1209			1054	1057		Sky/Cloud	Water	2	2	1	High haze.
48	139	−15.5309	−4.1210			1058	1101	1102	Cloud	Water	2	1	1	High haze.
49	140	−16.7068	−0.0724	0950	1104	1109	1111	1118	Sky/Cloud	Water	2	1	1	Thin cumulus, cloud at end.
50	140	−16.7995	0.2318			1311	1314		Sky	Water	1	2	0	Thin cirrus.
51	140	−16.7995	0.2328			1315	1318	1319	Sky	Gray	1	0	0	Thin cirrus.
52	140	−16.7998	0.2348			1322	1325		Sky	Water	1	2	1	Thin cirrus, cloud at end.
53	140	−16.8000	0.2360			1326	1329		Sky/Cloud	Gray	1	1	2	Thin cirrus, cloud at end.
54	141	−17.8834	3.8994	0946	0946	1037	1040		Sky/Cloud	Water	2	0	1	Thin cirrus.
55	141	−17.8834	3.8996			1041	1044		Sky	Gray	1	0	0	Thin cirrus.
56	141	−17.8833	3.9001			1047	1050		Sky/Cloud	Water	0	0	0	Thin cirrus.

Table E1. (cont.) The SeaBOARR-99 SUnSAS Log with all times reported in GMT.

Cast No.	SDY	Position Longitude	Latitude	Darks Ref.	Rad.	Cast Beg.	End	CCD Pic.	L_i Views	L_T Views	Stability L_i	L_T	E_d^+	Sky Conditions Around the Sun
57	141	−17.8833	3.9003			1051	1054		Sky/Haze	Gray	0	0	0	Thin cirrus.
58	141	−17.8835	3.9006			1055	1058		Sky	Water	0	0	1	Thin cirrus.
59	141	−17.8836	3.9012			1059	1102		Sky/Cloud	Gray	0	1	1	Thin cirrus.
60	141	−17.8839	3.9022			1108	1111	1108	Sky/Cloud	Water	1	1	1	Cloudy, brightening.
61[5]	141	−17.8839	3.9026			1115	1118		Sky	Water	0	0	0	Thin cirrus.
62[5]	141	−17.8838	3.9027			1118	1121		Sky	Water	0	0	0	Thin cirrus.
63[5]	141	−17.8838	3.9028			1121	1124		Sky	Water	0	0	0	Thin cirrus.
64[5]	141	−17.8838	3.9030			1125	1128		Sky	Water	0	0	0	Thin cirrus.
65[5]	141	−17.8837	3.9032			1129	1132		Sky	Water	2	1	0	Thin cirrus.
66[5]	141	−17.8837	3.9034			1132	1135		Sky/Cloud	Water	1	0	1	Thin cirrus.
67[5]	141	−17.8837	3.9038			1136	1139		Sky/Cloud	Water	2	0	0	Thin cirrus.
68[5]	141	−18.0119	4.3128			1403	1406		Sky/Haze	Water	2	0	1	Thin cirrus.
69[5]	141	−18.0121	4.3126			1406	1409		Sky/Haze	Water	1	0	0	Thin cirrus.
70[5]	141	−18.0124	4.3126			1409	1412		Sky/Haze	Water	1	0	0	Thin cirrus.
71[5]	141	−18.0128	4.3125			1413	1416		Sky/Haze	Water	1	0	1	Thin cirrus.
72[5]	141	−18.0133	4.3123			1417	1420		Sky/Haze	Water	1	0	1	Thin cirrus.
73[5]	141	−18.0137	4.3121			1420	1423		Sky/Haze	Water	1	1	1	Thin cirrus.
74[5]	141	−18.0143	4.3119			1424	1427		Sky/Haze	Water	1	0	1	Thin cirrus.
75[5]	141	−18.0148	4.3116			1428	1431		Sky/Haze	Water	1	0	1	Thin cirrus.
76[5]	141	−18.0152	4.3114			1432	1435	1433	Sky/Haze	Water	1	0	1	Thin cirrus.
77[5]	141	−18.0152	4.3110			1436	1439		Sky/Haze	Water	1	0	0	Thin cirrus.
78[4]	141	−18.0188	4.3112			1446	1449		Sky/Cloud	Water	1	0	1	Thin cirrus.
79[4]	141	−18.0242	4.3126			1450	1453		Sky/Cloud	Water	1	0	0	Thin cirrus.
80[4]	141	−18.0324	4.3148			1456	1459		Sky/Cloud	Water	2	0	1	Thin cirrus.
81	142	−18.9875	7.6207	0947	0947	1038	1041		Sky/Haze	Water	0	0	0	High haze.
82	142	−18.9871	7.6209			1042	1045		Sky/Cloud	Gray	1	1	1	High haze.
83	142	−18.9870	7.6210			1046	1049		Sky/Cloud	Water	1	0	0	High haze, cloud at end.
84	142	−18.9870	7.6210			1049	1052		Sky/Haze	Gray	1	1	1	High haze.
85	142	−18.9868	7.6210			1053	1056	1054	Sky/Cloud	Water	1	0	0	High haze.
86	142	−18.9864	7.6211			1056	1059		Sky/Cloud	Gray	1	0	0	High haze.
87[5]	142	−18.9856	7.6216			1103	1106		Sky	Water	1	0	0	High haze.
88[5]	142	−18.9855	7.6219			1107	1110		Sky/Haze	Water	0	0	0	High haze.
89[5]	142	−18.9853	7.6220			1110	1113		Sky/Haze	Water	0	1	1	High haze.
90[5]	142	−18.9853	7.6220			1113	1116		Sky/Haze	Water	1	1	1	High haze.
91[5]	142	−18.9852	7.6222			1118	1121		Sky/Haze	Water	1	1	0	High haze.
92[5]	142	−18.9850	7.6222			1121	1124		Haze/Cloud	Water	2	1	0	High haze.
93[5]	142	−18.9848	7.6222			1124	1127		Sky	Water	1	1	0	High haze.
94	142	−19.0524	7.8400			1250	1253		Haze/Cloud	Water	0	1	0	High haze.
95	142	−19.0516	7.8409			1254	1257		Haze/Cloud	Gray	0	0	0	High haze.
96	142	−19.0510	7.8413			1257	1300		Haze/Cloud	Water	1	0	0	High haze.
97	142	−19.0500	7.8419			1301	1304		Haze/Cloud	Gray	1	0	0	High haze.
98	142	−19.0493	7.8421			1304	1307		Sky/Haze	Water	1	0	0	High haze.
99	142	−19.0483	7.8426			1308	1311	1308	Sky/Haze	Gray	0	0	0	High haze.
100[6]	142	−19.0459	7.8440			1318	1321		Sky/Haze	Water	0	0	0	High haze.
101[6]	142	−19.0448	7.8442			1322	1325		Sky/Haze	Water	0	1	0	High haze.
102[6]	142	−19.0437	7.8445			1326	1329		Sky/Haze	Water	1	1	0	High haze.
103[6]	142	−19.0425	7.8448			1330	1333		Sky/Haze	Water	1	0	0	High haze.
104[6]	142	−19.0416	7.8450			1334	1337		Sky/Haze	Water	1	0	0	High haze.
105[6]	142	−19.0413	7.8453			1338	1341		Sky/Haze	Water	1	0	0	High haze.
106[6]	142	−19.0415	7.8454			1342	1345		Haze/Cloud	Water	0	0	1	High haze.
107	143	−20.1479	11.5645	0954	0954	1042	1045		Sky/Haze	Water	1	1	1	High haze.
108	143	−20.1476	11.5646			1045	1048		Haze/Cloud	Gray	2	2	1	High haze.
109[4]	143	−20.2542	11.8745			1302	1305		Sky/Cloud	Water	2	2	1	High haze, cloudy at end.
110[4]	143	−20.2526	11.8839			1309	1312		Sky/Cloud	Water	2	2	1	High haze, edges in middle.
111[4]	143	−20.2515	11.8907			1314	1317		Sky/Cloud	Water	1	1	1	High haze, edges in middle.
112[4]	143	−20.2559	11.9078			1324	1327		Sky/Cloud	Water	2	1	2	High haze, cloudy at end.

Table E1. (cont.) The SeaBOARR-99 SUnSAS Log with all times reported in GMT.

Cast		Position		Darks		Cast		CCD	L_i	L_T	Stability			Sky Conditions
No.	SDY	Longitude	Latitude	Ref.	Rad.	Beg.	End	Pic.	Views	Views	L_i	L_T	E_d^+	Around the Sun
113	143	−20.2589	11.9183			1352	1355		Sky/Cloud	Water	1	0	1	High haze, edges at end.
114	143	−20.2593	11.9178			1405	1408		Haze/Cloud	Water	1	1	2	Cloud edges for entire cast.
115	143	−20.2595	11.9177			1410	1413		Sky/Haze	Water	1	0	1	High haze.
116	143	−20.2597	11.9175			1413	1416	1415	Haze/Cloud	Gray	1	1	1	High haze.
117	143	−20.2598	11.9171			1418	1421		Sky/Haze	Water	1	1	1	High haze.
118	143	−20.2601	11.9170			1422	1425		Haze/Cloud	Gray	1	0	0	High haze.
119	144	−20.9986	15.1502	1001	1001	1053	1056		Sky/Haze	Water	0	1	0	High haze.
120	144	−20.9984	15.1502			1056	1059		Sky/Haze	Gray	0	0	0	High haze.
121	144	−20.9986	15.1501			1101	1104		Sky/Haze	Water	1	1	0	High haze.
122	144	−20.9986	15.1501			1104	1107		Sky/Haze	Gray	0	0	0	High haze.
123	144	−20.9984	15.1502			1107	1110	1109	Sky/Haze	Water	0	1	0	High haze.
124	144	−20.9980	15.1503			1111	1114		Sky/Haze	Gray	0	0	0	High haze.
125	144	−20.9979	15.1502			1115	1118		Sky/Haze	Water	0	1	0	High haze.
126	144	−20.9978	15.1501			1118	1121		Sky/Haze	Gray	0	0	0	High haze.
127	144	−20.9977	15.1501			1122	1125		Sky/Haze	Water	0	1	0	High haze.
128	144	−20.9977	15.1496			1126	1129		Sky/Haze	Gray	0	0	0	High haze.
129[5]	144	−20.9997	15.1502			1231	1234		Sky/Haze	Water	1	2	0	High haze.
130[5]	144	−20.9994	15.1507			1234	1237		Sky/Haze	Water	0	2	0	High haze.
131[5]	144	−20.9996	15.1513			1238	1241		Sky/Haze	Water	1	2	0	High haze.
132[5]	144	−20.9997	15.1515			1242	1245		Sky/Haze	Water	0	2	0	High haze.
133[5]	144	−20.9996	15.1514			1246	1249		Sky/Haze	Water	0	2	0	High haze.
134[5]	144	−20.9994	15.1510			1249	1252		Sky/Haze	Water	0	2	0	High haze.
135[5]	144	−20.9992	15.1510			1253	1256	1254	Sky/Haze	Water	0	2	0	High haze.
136	144	−20.9999	15.1511			1337	1340		Sky/Haze	Water	0	2	0	High haze.
137	144	−21.0001	15.1510			1340	1343		Sky/Haze	Water	1	2	0	High haze.
138	144	−21.0003	15.1511			1343	1346		Sky/Haze	Water	0	2	0	High haze.
139	144	−21.0006	15.1510			1347	1350		Sky/Haze	Water	0	2	0	High haze.
140[4]	144	−21.0008	15.1546			1354	1357		Sky/Haze	Water	0	2	0	High haze.
141[4]	144	−21.0006	15.1601			1358	1401		Sky/Haze	Water	1	2	0	High haze.
142[4]	144	−21.0004	15.1642			1401	1404		Sky/Haze	Water	0	2	0	High haze.
143	145	−20.9996	18.8022	0945	0945	1035	1038		Sky/Cloud	Water	2	1	1	Cloudy.
144	145	−20.9992	18.8024			1039	1042		Cloud	Gray	1	1	1	Cloudy, brightening.
145	145	−20.9991	18.8026			1043	1046		Cloud	White	2	1	1	Cloudy.
146	145	−20.9989	18.8025			1047	1050	1051	Sky/Cloud	Water	1	1	2	Cloudy, brightening.
147	145	−20.9982	18.8039			1059	1102		Sky/Cloud	Water	2	1	1	Clear then cloudy.
148	145	−20.9979	18.8046			1103	1105		Sky/Cloud	Water	2	2	1	Clear, cloudy, clear, cloudy.
149	145	−20.9973	18.8057			1113	1116		Sky/Cloud	Water	1	1	1	Clear and cloudy.
150	145	−20.9970	18.8066			1117	1120		Sky/Cloud	Water	1	2	2	Clear then cloudy.
151	145	−20.9970	19.3093			1407	1410		Cloud	Water	1	0	1	Cloudy, some brightening.
152	145	−20.9966	19.3099			1410	1413		Cloud	Gray	1	2	2	Cloudy, brightening.
153	145	−20.9955	19.3107			1422	1425	1427	Cloud	Water	1	2	1	Clear then cloudy.
154	145	−20.9943	19.3124			1428	1431		Cloud	Water	1	0	1	Clear, some brightening.
155	145	−20.9940	19.3129			1432	1435		Cloud	Gray	1	1	1	Cloudy, some brightening.
156	145	−20.9938	19.3133			1436	1439		Cloud	Water	1	1	1	Cloudy, some brightening.
157	145	−20.9935	19.3136			1440	1443		Sky/Cloud	Gray	1	1	1	Cloudy, brightening at end.
158	145	−20.9918	19.3154			1449	1452		Sky	Water	1	1	2	Clear, cloudy towards end.
159	146	−21.0071	22.9116	0954	0954	1044	1047		Sky/Cloud	Water	2	1	1	Thin cirrus, cloud at end.
160	146	−21.0075	22.9122			1058	1101		Sky/Cloud	Water	1	1	1	Thin cirrus.
161	146	−21.0077	22.9122			1101	1104	1103	Sky/Cloud	Gray	2	1	1	Thin cirrus.
162	146	−21.0079	22.9124			1106	1109		Sky/Cloud	Water	1	0	1	Thin cirrus, edge in middle.
163	146	−21.0080	22.9127			1111	1114		Sky/Cloud	Gray	2	1	1	Thin cirrus, edge at end.
164	146	−21.0081	22.9129			1114	1117		Sky/Cloud	Water	1	1	1	Thin cirrus.
165	146	−21.0684	23.2770			1332	1335		Sky	Water	0	2	1	Clear.
166	146	−21.0711	23.2756			1338	1341	1346	Sky	Water	1	2	1	Clear.
167	146	−21.0735	23.2741			1349	1352		Sky/Cloud	Water	0	1	0	Clear.
168	146	−21.0748	23.2733			1353	1356		Sky/Cloud	Gray	0	0	0	Clear.

Table E1. (cont.) The SeaBOARR-99 SUnSAS Log with all times reported in GMT.

Cast		Position		Darks		Cast		CCD	L_i	L_T	Stability			Sky Conditions
No.	SDY	Longitude	Latitude	Ref.	Rad.	Beg.	End	Pic.	Views	Views	L_i	L_T	E_d^+	Around the Sun
169	146	−21.0759	23.2726			1356	1359		Sky/Cloud	Water	0	2	0	Clear.
170	146	−21.0776	23.2717			1400	1403		Sky	Gray	1	0	0	Clear.
171[4]	146	−21.0860	23.2701			1409	1412		Sky	Water	1	1	0	Clear.
172[4]	146	−21.0924	23.2699			1412	1415		Sky	Water	0	2	0	Clear.
173[4]	146	−21.0987	23.2697			1415	1418		Sky	Water	0	2	0	Clear.
174[4]	146	−21.1116	23.2696			1422	1425		Sky	Water	0	1	0	Clear.
175[4]	146	−21.1176	23.2694			1426	1429		Sky	Water	0	1	0	Clear.
176[4]	146	−21.1221	23.2693			1429	1432		Sky	Water	0	1	0	Clear.
177[4]	146	−21.1423	23.2707			1438	1441		Sky	Water	0	1	0	Clear.
178[4]	146	−21.1504	23.2714			1441	1444		Sky	Water	0	1	0	Clear.
179[4]	146	−21.1585	23.2722			1444	1447		Sky	Water	0	1	0	Clear.
180[4]	146	−21.1760	23.2740			1450	1453		Sky	Water	0	1	0	Clear.
181[4]	146	−21.1858	23.2751			1453	1456		Sky	Water	1	1	0	Clear.
182[4]	146	−21.1990	23.2767			1457	1500		Sky/Cloud	Water	1	1	1	Clear, edges at end.
183	147	−21.8032	26.6580	1006	1006	1015	1018		Sky	Water	0	0	0	Clear.
184	147	−21.8046	26.6671			1018	1021		Sky	Water	0	0	0	Clear.
185	147	−21.8060	26.6761			1021	1024		Sky	Water	0	0	0	Clear.
186	147	−21.8057	26.6931			1045	1048		Sky	Water	0	0	0	Clear.
187	147	−21.8050	26.6935			1049	1052		Sky	Gray	1	0	0	Clear.
188	147	−21.8046	26.6939			1053	1056		Sky	Water	0	0	1	Clear, edge at end.
189	147	−21.8042	26.6939			1057	1100	1058	Sky	Gray	0	1	1	Clear.
190	147	−21.8032	26.6942			1103	1106		Sky/Cloud	Water	1	0	0	Clear.
191	147	−21.8021	26.6951			1112	1115		Sky	Water	0	0	1	Clear.
192	147	−21.8588	27.0176			1312	1315		Sky	Water	0	0	0	Thin cirrus.
193	147	−21.8612	27.0296			1316	1319		Sky	Water	0	0	0	Thin cirrus.
194	147	−21.8630	27.0386			1319	1322		Sky	Water	0	0	0	Thin cirrus.
195	147	−21.8720	27.0508			1338	1341		Sky/Cloud	Water	1	0	0	Thin cirrus.
196	147	−21.8725	27.0507			1342	1345		Sky/Cloud	Gray	0	0	0	Thin cirrus.
197	147	−21.8741	27.0505			1349	1352		Sky/Cloud	Water	0	0	0	Thin cirrus.
198	147	−21.8749	27.0505			1352	1355	1354	Sky/Cloud	Gray	1	0	1	Thin cirrus.
199[7]	147	−21.8758	27.0505			1404	1407		Sky/Cloud	Water	1	0	1	Thin cirrus.
200[7]	147	−21.8762	27.0505			1409	1412		Sky/Cloud	Water	1	0	1	Thin cirrus.
201[7]	147	−21.8772	27.0505			1414	1417		Sky/Cloud	Water	1	0	1	Thin cirrus.
202[7]	147	−21.8813	27.0504			1425	1428		Sky/Cloud	Water	1	0	1	Thin cirrus.
203[7]	147	−21.8824	27.0504			1428	1431		Sky/Cloud	Water	1	0	1	Thin cirrus.
204[7]	147	−21.8835	27.0504			1432	1435		Sky/Cloud	Water	1	0	1	Thin cirrus.
205	147	−21.8860	27.0503			1442	1445		Sky/Cloud	Water	1	0	0	Thin cirrus.
206	148	−21.5705	30.4339	0955	0955	1002	1005		Cloud	Water	1	0		Overcast.
207	148	−21.5705	30.4339			1002	1005		Cloud	Water	1	0		Overcast.
208	148	−21.5705	30.4339			1002	1005		Cloud	Water	0	0		Overcast.
209	148	−21.5607	30.4764			1033	1036		Cloud	Water	1	0	1	Overcast, slow brightening.
210	148	−21.5608	30.4768			1037	1040		Cloud	Gray	1	1	1	Overcast, some brightening.
211	148	−21.5606	30.4769			1041	1044		Cloud	White	1	1	1	Overcast, a little brightening.
212	148	−21.5608	30.4776			1046	1049		Cloud	Water	1	0	1	Overcast, brightening.
213	148	−21.5605	30.4781			1050	1053	1051	Cloud	Gray	1	1	1	Overcast.
214	148	−21.5601	30.4805			1101	1104		Cloud	White	1	1	0	Overcast.
215	148	−21.5602	30.4812			1104	1107		Cloud	Water	1	0	1	Overcast.
216	148	−21.5602	30.4820			1108	1111		Cloud	White	1	1	1	Overcast.
217	148	−21.5601	30.4826			1112	1115		Cloud	Gray	1	0	0	Overcast.
218[4]	148	−21.5586	30.4963			1124	1127		Cloud	Water	1	0	1	Overcast.
219[4]	148	−21.5579	30.5039			1127	1130		Cloud	Water	1	0	1	Overcast.
220[4]	148	−21.5570	30.5140			1131	1134		Cloud	Water	1	0	1	Overcast, brightening.
221[4]	148	−21.5005	30.9293			1350	1353		Cloud	Water	1	1	2	Overcast, darkening.
222[4]	148	−21.4995	30.9351			1353	1356		Cloud	Water	1	1	1	Overcast, darkening.
223[4]	148	−21.4984	30.9409			1356	1359		Cloud	Water	2	1	1	Overcast.
224[4]	148	−21.4971	30.9486			1400	1403	1407	Cloud	Water	1	0	0	Overcast.

Table E1. (cont.) The SeaBOARR-99 SUnSAS Log with all times reported in GMT.

Cast		Position		Darks		Cast		CCD	L_i	L_T	Stability			Sky Conditions
No.	SDY	Longitude	Latitude	Ref.	Rad.	Beg.	End	Pic.	Views	Views	L_i	L_T	E_d^+	Around the Sun
225	148	−21.4981	30.9547			1409	1412		Cloud	Water	1	0	0	Overcast.
226	148	−21.4992	30.9544			1414	1417		Cloud	Gray	1	1	1	Overcast, brightening.
227	148	−21.4998	30.9542			1418	1421		Cloud	Water	1	0	1	Overcast, brightening at end.
228	148	−21.5003	30.9540			1421	1424		Cloud	Gray	0	1	1	Overcast, slow brightening.
229	148	−21.5008	30.9538			1425	1428		Cloud	Water	1	1	1	Overcast, slow brightening.
230	148	−21.5013	30.9535			1429	1432		Cloud	Gray	1	2	2	Overcast, darkening.
231 [4]	148	−21.5086	30.9531			1439	1442		Cloud	Water	1	0	0	Overcast.
232 [4]	148	−21.5135	30.9531			1442	1445		Cloud	Water	1	1	1	Overcast.
233 [4]	148	−21.5199	30.9530			1446	1449		Cloud	Water	1	1	1	Overcast.
234	148	−21.5273	30.9661			1455	1458		Cloud	Water	1	0	1	Overcast, some brightening.
235	148	−21.5256	30.9781			1459	1502		Cloud	Water	1	0	1	Overcast, brightening at end.
236	149	−20.7876	34.3650	1010	1010	1050	1053		Sky	Water	0	1	0	Clear.
237	149	−20.7877	34.3643			1054	1057	1055	Sky	Gray	0	0	0	Clear.
238	149	−20.7873	34.3635			1100	1103		Sky	Water	1	1	1	Clear, cloud edge in middle.
239	149	−20.7877	34.3634			1104	1107		Sky	Gray	1	0	0	Clear.
240	149	−20.7883	34.3630			1112	1115		Sky	Water	2	2	2	Clear, cloud in middle.
241	149	−20.7886	34.3629			1115	1118		Sky/Cloud	Gray	2	1	1	Clear, cloud at the end.
242	149	−20.6996	34.5362			1247	1250		Sky/Cloud	Water	1	2	0	Clear.
243	149	−20.6971	34.5399			1250	1253		Sky/Cloud	Water	2	2	1	Clear, edges middle and end.
244	149	−20.6940	34.5448			1254	1257		Sky	Water	1	1	1	Overcast, brightening, clear.
245	149	−20.6917	34.5497			1305	1308	1313	Sky/Cloud	Water	1	2	1	Clear, edges in middle.
246	149	−20.6922	34.5504			1314	1317		Sky	Water	1	1	1	Clear, cloud in middle.
247	149	−20.6923	34.5503			1320	1323		Sky/Cloud	Water	0	1	1	Clear.
248	149	−20.6924	34.5503			1326	1329		Sky	Water	0	1	0	Clear.
249	149	−20.6924	34.5502			1330	1333		Sky	Water	0	2	1	Clear, cloud in middle.
250	150	−20.0143	38.1779	1010	1010	1034	1037		Water	Water	1	1	1	Clear.
251	150	−20.0148	38.1773			1038	1041	1039	Sky/Cloud	Gray	2	1	1	Clear, cloud in middle.
252	150	−20.0163	38.1753			1053	1056		Sky/Cloud	Water	1	1	1	Clear.
253	150	−20.0165	38.1747			1056	1059		Cloud	Water	2	1	2	Clear.
254	150	−20.0177	38.1742			1103	1106		Cloud	Water	2	1	1	Overcast, light rain.
255	150	−20.0042	38.6417			1405	1408		Sky	Water	2	1	1	Overcast, slow brightening.
256	150	−20.0048	38.6418			1408	1411		Sky	Gray	1	1	1	Overcast, slow brightening.
257	150	−20.0061	38.6424			1413	1416	1419	Sky	Gray	0	1	2	Overcast, slow brightening.
258	150	−20.0071	38.6435			1425	1428		Sky	Water	0	1	0	Thin cumulus.
259	150	−20.0072	38.6438			1429	1432		Sky	Gray	1	0	0	Thin cumulus.
260	150	−20.0075	38.6442			1434	1437		Sky	Water	0	1	0	Thin cumulus.
261	150	−20.0084	38.6452			1438	1441		Sky	Gray	1	0	0	Thin cumulus.
262	150	−20.0142	38.6506			1450	1453		Sky/Cloud	Water	2	2	1	Cloudy then clear.
263	150	−20.0196	38.6544			1454	1457		Sky	Water	1	2	0	Clear.
264	150	−20.0235	38.6572			1457	1500		Sky	Water	1	2	1	Clear, clouds in middle.
265	151	−20.0001	42.0019	1011	1011	1042	1045		Cloud	Water	2	1	1	Overcast.
266	151	−20.0000	42.0021			1045	1048		Cloud	Water	2	1	1	Overcast.
267	151	−20.0000	42.0026			1049	1052	1051	Cloud	White	2	2	1	Overcast, slow brightening.
268	151	−20.0000	42.0026			1049	1052		Cloud	Gray	2	1	1	Overcast, slow brightening.
269	151	−19.9962	42.0076			1121	1124		Sky/Cloud	Water	1	2	2	Clear then cloudy.
270	151	−20.0079	42.2642			1304	1307		Sky	Water	1	2	1	Clear, small cloud at end.
271	151	−20.0076	42.2643			1308	1311	1309	Sky	Gray	1	1	1	Clear.
272	151	−20.0064	42.2664			1315	1318		Sky	Water	1	2	1	Clear, cloud in middle.
273	151	−20.0058	42.2672			1318	1321		Sky	Gray	1	1	1	Clear.
274	152	−19.9863	45.9088	0940	0940	0949	0952		Sky/Cloud	Water	1	0	0	Clear.
275	152	−19.9826	45.9177			0952	0955		Sky/Cloud	Water	0	0	0	Clear.
276	152	−19.9789	45.9266			0955	0958		Sky/Cloud	Water	0	0	0	Very thin cirrus.
277	152	−19.9783	45.9438			1014	1017		Sky/Cloud	Water	1	0	0	Thin cirrus.
278	152	−19.9784	45.9437			1018	1021		Sky/Cloud	Gray	1	0	0	Thin cirrus.
279	152	−19.9788	45.9440			1024	1027	1025	Sky	Water	0	0	1	Thin cirrus.
280	152	−19.9794	45.9442			1028	1031		Sky	Gray	0	0	1	Thin cirrus.

Table E1. (cont.) The SeaBOARR-99 SUnSAS Log with all times reported in GMT.

Cast No.	SDY	Position Longitude	Latitude	Darks Ref.	Rad.	Cast Beg.	End	CCD Pic.	L_i Views	L_T Views	Stability L_i	L_T	E_d^+	Sky Conditions Around the Sun
281	152	−19.9798	45.9445			1031	1034		Sky/Cloud	Water	1	0	0	Thin cirrus.
282	152	−19.9800	45.9450			1035	1038		Sky/Cloud	Gray	1	1	1	Thin cirrus.
283	152	−19.9803	45.9453			1039	1042		Sky/Cloud	Water	1	0	0	Thin cirrus.
284	152	−19.9812	45.9459			1045	1048		Sky/Cloud	Water	1	0	0	Thin cirrus.
285	152	−19.9818	45.9463			1054	1057		Sky/Cloud	Water	1	0	0	Thin cirrus, prop wash.
286	152	−19.9814	45.9470			1058	1101		Sky/Cloud	Water	0	0	1	Thin cirrus, wash at end.
287	152	−20.0039	46.3760			1333	1336		Sky/Cloud	Water	1	2	1	Thin cirrus.
288	152	−20.0036	46.3752			1336	1339	1338	Sky/Cloud	Gray	1	1	2	Clear with cirrus.
289	152	−20.0030	46.3740			1342	1345		Sky/Cloud	Water	2	2	1	Clear with cirrus.
290	152	−20.0025	46.3727			1348	1351		Sky/Cloud	Water	1	2	2	Cirrus and thin cumulus.
291	152	−20.0027	46.3709			1355	1358		Cloud	Water	1	2	1	Cloudy, brightening.
292	153	−15.7106	47.4500	1000	1000	1013	1016		Cloud	Water	1	1	1	Overcast.
293	153	−15.6973	47.4516			1016	1019		Cloud	Water	1	1	1	Overcast, brightening at end.
294	153	−15.6749	47.4544			1021	1024		Cloud	Water	1	1	1	Overcast.
295	153	−15.6636	47.4542			1038	1041		Cloud	Water	1	1	1	Overcast, slow brightening.
296	153	−15.6645	47.4546			1043	1046	1045	Cloud	Gray	1	1	1	Overcast, some brightening.
297	153	−15.6653	47.4552			1049	1052		Cloud	Water	1	1	2	Overcast.
298	153	−15.6660	47.4555			1053	1056		Cloud	White	1	0	1	Overcast.
299	153	−15.6665	47.4558			1056	1059		Cloud	Gray	1	0	1	Overcast.
300	153	−15.6671	47.4561			1100	1103		Cloud	Water	1	0	1	Overcast.
301	153	−15.6678	47.4563			1103	1106		Cloud	White	2	0	0	Overcast.
302	153	−15.6686	47.4566			1107	1110		Cloud	Gray	1	1	1	Overcast.
303	153	−15.6691	47.4569			1110	1113		Cloud	Water	1	1	1	Overcast, slow brightening.
304	153	−15.6697	47.4572			1114	1117		Cloud	Water	1	0	1	Overcast.
305	153	−14.7766	47.5429			1524	1527		Cloud	Water	1	1	1	Cloudy, bright, cloudy.
306	153	−14.7784	47.5429			1535	1535		Cloud	Water	1	2	2	Cloudy.
307	153	−14.7801	47.5427			1541	1544		Cloud	Water	1	1	1	Cloudy.
308[8]	154	−9.9580	48.0692	0909	0909	0914	0917		Sky	[Gray]	1	0	1	Clear.
309[8]	154	−9.9430	48.0728			0919	0922		Sky	[White]	0	1	1	Clear.
310[8]	154	−9.9255	48.0772			0923	0926		Sky	[Gray]	1	1	0	Clear.
311[8]	154	−9.9079	48.0818			0927	0930		Sky	[White]	1	1	0	Clear, cloud edges in middle.
312[8]	154	−9.8947	48.0855			0930	0933		Sky	[Gray]	0	1	0	Clear.
313[8]	154	−9.8773	48.0903			0934	0937		Sky	[White]	0	1	0	Clear.
314[8]	154	−9.8600	48.0949			0938	0941		Sky	[Gray]	0	1	0	Clear.
315[8]	154	−9.8466	48.0983			0941	0944		Sky	[White]	0	1	1	Clear.
316[8]	154	−9.8158	48.1063			0948	0951		Sky	Water	0	1	0	Clear.
317[8]	154	−9.8023	48.1098			0951	0954		Sky	Gray	0	0	0	Clear.
318[8]	154	−9.7844	48.1145			0955	0958		Sky	White	0	0	0	Clear.
319[8]	154	−9.7669	48.1191			0959	1002		Sky	Water	0	1	0	Clear.
320[8]	154	−9.7537	48.1226			1002	1005		Sky	Gray	0	0	1	Clear.
321[8]	154	−9.7360	48.1273			1006	1009		Sky	White	0	0	1	Clear.
322[8]	154	−9.7229	48.1308			1009	1012		Sky	Water	0	1	1	Clear.
323[8]	154	−9.7052	48.1356			1013	1016		Sky	Gray	0	0	0	Clear.
324[8]	154	−9.6925	48.1391			1016	1019		Sky	White	1	0	0	Clear.
325	154	−9.4098	48.2132			1249	1252		Sky	Water	1	2	1	Clear.
326	154	−9.4120	48.2132			1252	1255	1255	Sky	Gray	2	1	1	Clear.
327	154	−9.4147	48.2127			1258	1301		Sky/Cloud	Water	1	2	1	Clear.
328	154	−9.4156	48.2125			1301	1304		Sky	Gray	1	0	0	Clear.
329	154	−9.4165	48.2120			1305	1308		Sky	Water	0	1	0	Clear.
330	154	−9.4181	48.2118			1309	1312		Sky/Cloud	Gray	1	0	0	Clear.
331	154	−9.4233	48.2121			1325	1328		Sky/Cloud	Water	1	2	1	Clear, cloud at end.
332	154	−9.4270	48.2122			1334	1337		Sky/Cloud	Water	1	2	1	Clear, cloud at end.
333	154	−9.4284	48.2121			1337	1340		Sky	Water	0	2	0	Clear.
334	154	−9.4303	48.2123			1342	1345		Sky	Water	1	1	0	Clear.
335	154	−9.4310	48.2122			1345	1348		Sky	Gray	1	1	1	Clear, cloud edge in middle.
336	154	−9.4335	48.2115			1352	1355		Sky	Water	1	2	0	Clear.

Table E1. (cont.) The SeaBOARR-99 SUnSAS Log with all times reported in GMT.

Cast		*Position*		*Darks*		*Cast*		*CCD*	L_i	L_T	*Stability*			*Sky Conditions*
No.	*SDY*	*Longitude*	*Latitude*	*Ref.*	*Rad.*	*Beg.*	*End*	*Pic.*	*Views*	*Views*	L_i	L_T	E_d^+	*Around the Sun*
337	154	−9.4347	48.2113			1356	1359		Sky/Cloud	Gray	1	1	1	Clear.
338 [2]	155	−9.2503	48.9774	1021	1048	1052	1055		Cloud	Water	1	2	2	Cirrus, cloud edges at end.
339 [2]	155	−9.2506	48.9760			1059	1102	1105	Cloud	Water	1	2	1	Cirrus, edges in middle.
340 [2]	155	−9.2509	48.9749			1105	1108		Cloud	Water	1	2	2	Cirrus, cloud at end.
341 [2]	155	−9.2531	48.9720			1116	1119		Cloud	Water	1	2	2	Cirrus.
342 [2]	155	−9.2534	48.9709			1120	1123		Cloud	Water	1	2	1	Cirrus, a little brightening.
343 [2]	155	−9.2539	48.9702			1123	1126		Cloud	Water	1	2	2	Cirrus, a little darkening.
344 [2]	155	−9.1805	48.9836			1254	1257		Cloud	Water	1	2	2	Overcast.
345 [2]	155	−9.1830	48.9833			1307	1309	1310	Cloud	Water	1	2	1	Overcast, brightening.
346 [2]	155	−9.1848	48.9831			1311	1314		Cloud	Water	1	2	1	Overcast, darkening.
347 [2]	155	−9.1860	48.9832			1315	1317		Cloud	Water	1	2	1	Overcast.
348 [2]	155	−9.1890	48.9824			1321	1322		Cloud	Water	1	2	1	Overcast (very little rain).
349	156	−4.4464	49.7001	0913	0913	0935	0938		Sky/Cloud	Water	1	1	1	Overcast.
350	156	−4.4443	49.6993			0939	0942		Sky/Cloud	Water	2	2	1	Overcast.
351	156	−4.4428	49.6989			0942	0945	0945	Sky/Cloud	Water	1	1	1	Overcast.
352	156	−4.4344	49.6973			1004	1004		Sky/Cloud	Water	1	2	1	Clear, cloud in middle.
353	156	−4.4326	49.6966			1008	1011		Sky/Cloud	Water	2	1	1	Clear, cloud at end.
354	156	−4.4299	49.6955			1016	1019		Cloud	Water	1	2	1	Clear, then cloud.
355	156	−4.4286	49.6950			1022	1022		Cloud	Water	1	1	1	Overcast, brightening.
356	156	−4.4259	49.6940			1030	1030		Cloud	Water	1	1	1	Overcast, darkening.

[2] Indicates sampling in a coccolithophore bloom.
[4] Indicates SeaSAS and SUnSAS underway experiments.
[5] Indicates SeaSAS azimuth pointing experiments.
[6] Indicates SeaSAS nadir- and zenith-viewing angle experiments.
[7] Indicates SeaSAS and SUnSAS nadir- and zenith-viewing angle experiments.
[8] Indicates SUnSAS underway experiments with T69 (L_i sensor) in place of T28 (L_p/L_T sensor).
[White] Indicates sea- then (white) plaque-viewing in the same file (about 90 s each).
[Gray] Indicates sea- then (gray) plaque-viewing in the same file (about 90 s each).

Table F1. A summary of the SQM and SQM-II Deployment Log for SeaBOARR-99. All times are in GMT, and the low and medium levels correspond to the 1 A and 2 A being used for illumination, respectively.

Session	SDY	*Level*	SQM	SQM-II	Q16	Q33	R36	H23	I48	I50	M30	N46	N48	T28	T68	T69	T75	M35	M95
1	97	Low	×	×	×	×	×	×	×	×	×	×	×	×	×	×	×	×	×
2	128	Low	×		×		×	×	×	×	×	×							
3	129	Low	×			×							×	×	×	×	×		
4	130	Low	×		×		×	×	×	×	×	×							
5	131	Low	×			×							×	×	×	×	×	×	×
6	132	Low	×		×		×	×	×	×	×	×							
7	133	Med.	×			×							×	×	×	×	×	×	×
8	134	Med.	×		×		×	×	×	×	×	×							
9	137	Low	×		×		×	×	×	×	×	×							
10	138	Low	×			×							×	×	×	×	×	×	×
11	139	Med.	×		×		×	×	×	×	×	×							
12	140	Med.	×			×							×	×	×	×	×	×	×
13	141	Low	×	×	×		×	×	×	×	×	×							
14	142	Low	×	×		×							×	×	×	×	×	×	×
15	143	Med.	×	×	×		×	×	×	×	×	×							
16	144	Med.	×	×		×							×	×	×	×	×	×	×
17	145	Low	×	×	×		×	×	×	×	×	×							
18	146	Low	×	×		×							×	×	×	×	×	×	×
19	147	Med.	×	×	×		×	×	×	×	×	×							
20	148	Med.	×	×		×							×	×	×	×	×	×	×

Table F1. (cont.) A summary of the SQM and SQM-II Deployment Log for SeaBOARR-99.

Session	SDY	*Level*	SQM	SQM-II	Q16	Q33	R36	H23	I48	I50	M30	N46	N48	T28	T68	T69	T75	M35	M95
21	149	Low	×	×	×		×	×	×	×	×	×							
22	150	Low	×	×		×							×	×	×	×	×	×	×
23	151	Med.	×	×	×		×	×	×	×	×	×							
24	152	Med.	×	×		×							×	×	×	×	×	×	×
25	153	Low	×	×	×		×	×	×	×	×	×							
26	154	Low	×	×		×							×	×	×	×	×	×	×
27	155	Med.	×	×	×		×	×	×	×	×	×							
28	156	Med.	×	×		×							×	×	×	×	×	×	×

Glossary

A/D Analog-to-Digital
AC Alternating Current
AMT Atlantic Meridional Transect
AMT-1 The First AMT Cruise
AMT-2 The Second AMT Cruise
AMT-5 The Fifth AMT Cruise
AMT-8 The Eighth AMT Cruise
ASCII American Standard Code for Information Interchange
CCD Charge-Coupled Device
CERT Calibration Evaluation and Radiometric Testing
CT Conductivity and Temperature (probe)
CTD Conductivity, Temperature, and Depth (instrument)
CVE Calibration and Validation Element
DalBOSS Dalhousie Buoyant Optical Surface Sensor
DAS Data Acquisition Sequence
DATA Not an acronym, but a designator for the series of power and telemetry units from Satlantic, Inc.
DC Direct Current
DIR Not an acronym, but a designator for the Satlantic, Inc., series of directional units.
DUT Device Under Test
DVM Digital Voltmeter
GMT Greenwich Mean Time
GSFC Goddard Space Flight Center
HPLC High Performance Liquid Chromatography
JCR (Royal Research Ship) *James Clark Ross*
LoCNESS Low-Cost NASA Environmental Sampling System
NASA National Aeronautics and Space Administration
NIR Near-Infrared
NIST National Institute of Standards and Technology
NRSR Normalized Remote Sensing Reflectance
OCI Ocean Color Irradiance
OCR Ocean Color Radiance
PC Personal Computer
RMSD Root Mean Square Difference
RSMAS Rosenstiel School for Marine and Atmospheric Science
S/N Serial Number
SAS Surface Acquisition System
SeaBOARR SeaWiFS Bio-Optical Algorithm Round-Robin
SeaBOARR-98 The First SeaBOARR (held in 1998)
SeaBOARR-99 The Second SeaBOARR (held in 1999)
SeaBOSS SeaWiFS Buoyant Optical Surface Sensor
SeaFALLS SeaWiFS Free-Falling Advanced Light Level Sensors
SeaOPS SeaWiFS Optical Profiling System
SeaSAS SeaWiFS Surface Acquisition System
SeaSHADE SeaWiFS Shadow Band (radiometer)
SeaSURF SeaWiFS Square Underwater Reference Frame
SeaWiFS Sea-viewing Wide Field-of-view Sensor
SDY Sequential Day of the Year
SMSR SeaWiFS Multichannel Surface Reference
SOOP SeaWiFS Ocean Optics Protocols
SPMR SeaWiFS Profiling Multichannel Radiometer
SQM SeaWiFS Quality Monitor
SQM-II The Second Generation SQM
SUnSAS SeaWiFS Underway Surface Acquisition System
THOR Three-Headed Optical Recorder
UIC Underway Instrumentation and Control (a room)
UPS Uninterruptable Power Supply

Symbols

C Chlorophyll concentration.
e A regression coefficient.
E_d Downwelled irradiance.
E_i Indirect (diffuse) irradiance.
E_p Plaque downwelling total irradiance.
E_u Upwelled irradiance.
i A given point.
j Reference observation.
K_u The diffuse attenuation coefficient calculated from $L_u(z)$ data.
L_i Indirect (sky) radiance.
L_p Plaque radiance.
L_T Total radiance (for $z = 0^+$, right above the sea surface).
L_u Upwelled radiance.
L_W Water-leaving radiance.
L_W^L Water-leaving radiance derived from LoCNESS data.
L_W^S Water-leaving radiance derived from SeaFALLS data.

m Slope of the reduced major axis linear regression.
M Number of wavelengths.
n_w The refractive index of seawater.
N The number of measurements.
R^2 Coefficient of determination.
R_{rs} Remote sensing reflectance.
S Salinity.
T Temperature.
x The abscissa.
X Variable under consideration.
y The ordinate.
z The vertical coordinate.
z_0 Center depth.
$\delta(\lambda)$ The percent difference between two variables.
$\overline{\delta}$ The total mean percent difference.
$\overline{\delta}_\lambda$ The mean percent difference over a range of wavelengths.
$\delta^i(\lambda)$ An individual percent difference between two variables within a time series of observations.
Δz The integration half interval ($\Delta z \approx 4$–10 m).
ΔL A correction factor for the specular reflection of sky light and the residual reflection of downwelling radiation from wave facets.
θ The solar zenith angle.
ϑ The nadir angle.
ϑ' $\pi - \vartheta$.
λ Wavelength (the spectral coordinate).
λ_7 Seven spectral channels.
λ_{13} Thirteen spectral channels.
λ_r A wavelength in the near infrared part of the spectrum.
ρ The Fresnel reflectance of seawater.
ϕ The solar azimuth angle.
ϕ' $\phi \pm \frac{\pi}{2}$ (90° away from the sun in either direction, i.e., ϕ^+ or ϕ^-).
ϕ^- $\phi - \frac{\pi}{2}$.
ϕ^+ $\phi + \frac{\pi}{2}$.
φ The perturbations (or tilts) in alignment away from z.
χ_c A regression coefficient.
$\psi(\lambda)$ The RMSD for a particular wavelength.
$\overline{\psi}_\lambda$ The mean RMSD over a range of wavelengths.

References

Aiken, J., D.G. Cummings, S.W. Gibb, N.W. Rees, R. Woodd-Walker, E.M.S. Woodward, J. Woolfenden, S.B. Hooker, J-F. Berthon, C.D. Dempsey, D.J. Suggett, P. Wood, C. Donlon, N. González-Benítez, I. Huskin, M. Quevedo, R. Barciela-Fernandez, C. de Vargas, and C. McKee, 1998: AMT-5 Cruise Report. *NASA Tech. Memo. 1998-206892, Vol. 2,* S.B. Hooker and E.R. Firestone, Eds., NASA Goddard Space Flight Center, Greenbelt, Maryland, 113 pp.

Austin, R.W., 1974: The Remote Sensing of Spectral Radiance from Below the Ocean Surface. In: *Optical Aspects of Oceanography,* N.G. Jerlov and E.S. Nielsen, Eds., Academic Press, London, 317–344.

——, and T.J. Petzold, 1981: The determination of diffuse attenuation coefficient of sea water using the Coastal Zone Color Scanner. In: *Oceanography from Space,* J.F.R. Gower, Ed., Plenum Press, 239–256.

Bukata, R.P., J.H. Jerome, and J.E. Bruton, 1988: Particulate concentrations in Lake St. Clair as recorded by shipborne multispectral optical monitoring system. *Remote Sens. Envir.,* **25,** 201–229.

Carder, K.L., and R.G. Steward, 1985: A remote sensing reflectance model of a red tide dinoflagellate off West Florida. *Limnol. Oceanogr.,* **30,** 286–298.

Gordon, H.R., 1981: A preliminary assessment of the Nimbus-7 CZCS atmospheric correction algorithm in a horizontally inhomogeneous atmosphere. In: *Oceanography from Space,* J.F.R. Gower, Ed., Plenum Press, 257–266.

Hooker, S.B., W.E. Esaias, G.C. Feldman, W.W. Gregg, and C.R. McClain, 1992: An Overview of SeaWiFS and Ocean Color. *NASA Tech. Memo. 104566, Vol. 1,* S.B. Hooker and E.R. Firestone, Eds., NASA Goddard Space Flight Center, Greenbelt, Maryland, 24 pp., plus color plates.

——, and ——, 1993: An overview of the SeaWiFS project. *Eos, Trans., Amer. Geophys. Union,* **74,** 241–246

——, and J. Aiken, 1998: Calibration evaluation and radiometric testing of field radiometers with the SeaWiFS Quality Monitor (SQM). *J. Atmos. Oceanic Tech.,* **15,** 995–1,007.

——, G. Zibordi, G. Lazin, and S. McLean, 1999: The SeaBOARR-98 Field Campaign. *NASA Tech. Memo. 1999-206892, Vol. 3,* S.B. Hooker and E.R. Firestone, Eds., NASA Goddard Space Flight Center, Greenbelt, Maryland, 40 pp.

——, and C.R. McClain, 2000: A comprehensive plan for the calibration and validation of SeaWiFS data. *Prog. Oceanogr.,* (in press).

——, and S. Maritorena, 2000: An evaluation of oceanographic radiometers and deployment methodologies. *J. Atmos. Oceanic Technol.,* (in press).

Johnson, B.C., P-S. Shaw, S.B. Hooker, and D. Lynch, 1998: Radiometric and engineering performance of the SeaWiFS Quality Monitor (SQM): A portable light source for field radiometers. *J. Atmos. Oceanic Tech.,* **15,** 1,008–1,022.

Lazin, G., 1998: Correction Methods for Low-Altitude Remote Sensing of Ocean Color. *M. Sc. Thesis,* Dalhousie University, 98 pp.

Lee, Z.P., K.L. Carder, R.G. Steward, T.G. Peacock, C.O. Davis, and J.L. Mueller, 1996: Remote sensing reflectance and inherent optical properties of oceanic waters derived from above-water measurements. *Proc. SPIE,* **2963,** 160–166.

McClain, C.R., W.E. Esaias, W. Barnes, B. Guenther, D. Endres, S.B. Hooker, G. Mitchell, and R. Barnes, 1992: Calibration and Validation Plan for SeaWiFS, *NASA Tech. Memo. 104566, Vol. 3,* S.B. Hooker and E.R. Firestone, Eds., NASA Goddard Space Flight Center, Greenbelt, Maryland, 41 pp.

Morel, A., 1980: In-water and remote measurements of ocean color. *Bound.-Layer Meteorol.,* **18,** 177–201.

——, 1988: Optical modeling of the upper ocean in relation to its biogenous matter content (Case I waters). *J. Geophys. Res.*, **93,** 10,749–10,768.

Mueller, J.L., and R.W. Austin, 1995: Ocean Optics Protocols for SeaWiFS Validation, Revision 1. *NASA Tech. Memo. 104566, Vol. 25,* S.B. Hooker, E.R. Firestone, and J.G. Acker, Eds., NASA Goddard Space Flight Center, Greenbelt, Maryland, 66 pp.

Press, W.H., and S.A. Teukolsky, 1992: Fitting straight line data with errors in both coordinates. *Computers in Phys.*, **6,** 274–276.

Ricker, W.E., 1973: Linear regressions in fishery research. *J. Fish. Res. Board Canada,* **30,** 409–434.

Robins, D.B., A.J. Bale, G.F. Moore, N.W. Rees, S.B. Hooker, C.P. Gallienne, A.G. Westbrook, E. Marañón, W.H. Spooner, and S.R. Laney, 1996: AMT-1 Cruise Report and Preliminary Results. *NASA Tech. Memo. 104566, Vol. 35,* S.B. Hooker and E.R. Firestone, Eds., NASA Goddard Space Flight Center, Greenbelt, Maryland, 87 pp.

Smith, R.C., and K.S. Baker, 1984: The analysis of ocean optical data. *Ocean Optics VII, SPIE,* M. Blizard, Ed., **478,** 119–126.

Waters, K.J., R.C. Smith, and M.R. Lewis, 1990: Avoiding ship induced light-field perturbation in the determination of oceanic optical properties. *Oceanogr.*, **3,** 18–21.

The SeaWiFS Postlaunch Technical Report Series

Vol. 1

Johnson, B.C., J.B. Fowler, and C.L. Cromer, 1998: The SeaWiFS Transfer Radiometer (SXR). *NASA Tech. Memo. 1998-206892, Vol. 1,* S.B. Hooker and E.R. Firestone, Eds., NASA Goddard Space Flight Center, Greenbelt, Maryland, 58 pp.

Vol. 2

Aiken, J., D.G. Cummings, S.W. Gibb, N.W. Rees, R. Woodd-Walker, E.M.S. Woodward, J. Woolfenden, S.B. Hooker, J-F. Berthon, C.D. Dempsey, D.J. Suggett, P. Wood, C. Donlon, N. González-Benítez, I. Huskin, M. Quevedo, R. Barciela-Fernandez, C. de Vargas, and C. McKee, 1998: AMT-5 Cruise Report. *NASA Tech. Memo. 1998-206892, Vol. 2,* S.B. Hooker and E.R. Firestone, Eds., NASA Goddard Space Flight Center, Greenbelt, Maryland, 113 pp.

Vol. 3

Hooker, S.B., G. Zibordi, G. Lazin, and S. McLean, 1999: The SeaBOARR-98 Field Campaign. *NASA Tech. Memo. 1999-206892, Vol. 3,* S.B. Hooker and E.R. Firestone, Eds., NASA Goddard Space Flight Center, Greenbelt, Maryland, 40 pp.

Vol. 4

Johnson, B.C., E.A. Early, R.E. Eplee, Jr., R.A. Barnes, and R.T. Caffrey, 1999: The 1997 Prelaunch Radiometric Calibration of SeaWiFS. *NASA Tech. Memo. 1999-206892, Vol. 4,* S.B. Hooker and E.R. Firestone, Eds., NASA Goddard Space Flight Center, Greenbelt, Maryland, 51 pp.

Vol. 5

Barnes, R.A., R.E. Eplee, Jr., S.F. Biggar, K.J. Thome, E.F. Zalewski, P.N. Slater, and A.W. Holmes 1999: The SeaWiFS Solar Radiation-Based Calibration and the Transfer-to-Orbit Experiment. *NASA Tech. Memo. 1999-206892, Vol. 5,* S.B. Hooker and E.R. Firestone, Eds., NASA Goddard Space Flight Center, 28 pp.

Vol. 6

Firestone, E.R., and S.B. Hooker, 1999: SeaWiFS Postlaunch Technical Report Series Cumulative Index: Volumes 1–5. *NASA Tech. Memo. 1999-206892, Vol. 6,* S.B. Hooker and E.R. Firestone, Eds., NASA Goddard Space Flight Center, Greenbelt, Maryland, (in preparation).

Vol. 7

Johnson, B.C., H.W. Yoon, S.S. Bruce, P-S. Shaw, A. Thompson, S.B. Hooker, R.E. Eplee, Jr., R.A. Barnes, S. Maritorena, and J.L. Mueller, 1999: The Fifth SeaWiFS Intercalibration Round-Robin Experiment (SIRREX-5), July 1996. *NASA Tech. Memo. 1999-206892, Vol. 7,* S.B. Hooker and E.R. Firestone, Eds., NASA Goddard Space Flight Center, 75 pp.

Vol. 8

Hooker, S.B., and G. Lazin, 2000: The SeaBOARR-99 Field Campaign. *NASA Tech. Memo. 2000-206892, Vol. 8,* S.B. Hooker and E.R. Firestone, Eds., NASA Goddard Space Flight Center, 46 pp.

REPORT DOCUMENTATION PAGE

Form Approved
OMB No. 0704-0188

1. AGENCY USE ONLY *(Leave blank)*	2. REPORT DATE	3. REPORT TYPE AND DATES COVERED
	January 2000	Technical Memorandum

4. TITLE AND SUBTITLE
SeaWiFS Postlaunch Technical Report Series
Volume 8: The SeaBOARR–99 Field Campaign

5. FUNDING NUMBERS
Code 970.2

6. AUTHOR(S)
Stanford B. Hooker and Gordana Lazin

Series Editors: Stanford B. Hooker and Elaine R. Firestone

7. PERFORMING ORGANIZATION NAME(S) AND ADDRESS(ES)
Laboratory for Hydrospheric Processes
Goddard Space Flight Center
Greenbelt, Maryland 20771

8. PERFORMING ORGANIZATION REPORT NUMBER
2000-01143-0

9. SPONSORING/MONITORING AGENCY NAME(S) AND ADDRESS(ES)
National Aeronautics and Space Administration
Washington, D.C. 20546–0001

10. SPONSORING/MONITORING AGENCY REPORT NUMBER
TM—2000–206892, Vol. 8

11. SUPPLEMENTARY NOTES
E.R. Firestone: SAIC General Sciences Corporation, Beltsville, Maryland; G. Lazin: Satlantic, Inc., Halifax, Nova Scotia

12a. DISTRIBUTION/AVAILABILITY STATEMENT
Unclassified–Unlimited
Subject Category 48
Report available from the NASA Center for AeroSpace Information,
7121 Standard Drive, Hanover, MD 21076-1320, (301) 621-0390.

12b. DISTRIBUTION CODE

13. ABSTRACT *(Maximum 200 words)*

This report documents the scientific activities during the second Sea-viewing Wide Field-of-view Sensor (SeaWiFS) Bio-Optical Algorithm Round-Robin (SeaBOARR-99) field campaign, which took place from 2 May to 7 June 1999 on board the Royal Research Ship *James Clark Ross* during the eighth Atlantic Meridional Transect cruise (AMT-8). The ultimate objective of the SeaBOARR activity is to evaluate the effect of different measurement protocols on bio-optical algorithms using data from a variety of field campaigns. The SeaBOARR-99 field campaign was concerned with collecting a high quality data set of simultaneous in-water and above-water radiometric measurements. The deployment goals documented in this report were to: a) use four different surface glint correction methods to compute water-leaving radiances, $L_w(\lambda)$, from above-water data; b) use two different in-water profiling systems and three different methods to compute $L_w(\lambda)$ from in-water data; c) use instruments with a common calibration history to minimize intercalibration uncertainties; d) monitor the calibration stability of the instruments in the field with the original SeaWiFS Quality Monitor (SQM) and a commercial, second-generation device called the SQM-II, thereby allowing a distinction between differences in methods from changes in instrument performance; and e) compare the $L_w(\lambda)$ values estimated from the above-water and in-water measurements. In addition to describing the instruments deployed and the data collected, a preliminary analysis of part of the SeaBOARR-99 data set is presented (using only the data collected during clear sky, calm sea, and Case-1 waters).

14. SUBJECT TERMS
SeaWiFS, Oceanography, Bio-Optical Algorithm, Round-Robin, SeaBOARR, Field Campaign

15. NUMBER OF PAGES
46

16. PRICE CODE

17. SECURITY CLASSIFICATION OF REPORT	18. SECURITY CLASSIFICATION OF THIS PAGE	19. SECURITY CLASSIFICATION OF ABSTRACT	20. LIMITATION OF ABSTRACT
Unclassified	Unclassified	Unclassified	Unlimited